CIRCADIAN RHYTHMS IN LATE PREGNANCY:
A ROLE IN THE REPRODUCTIVE AXIS, UTERINE CONTRACTIONS AND PRETERM LABOR

By

Thu Van Quynh Duong

A DISSERTATION

Submitted to
Michigan State University
in partial fulfillment of the requirements
for the degree of

Biochemistry and Molecular Biology—Doctor of Philosophy

2022

ABSTRACT

CIRCADIAN RHYTHMS IN LATE PREGNANCY:
A ROLE IN THE REPRODUCTIVE AXIS, UTERINE CONTRACTIONS AND PRETERM LABOR

By

Thu Van Quynh Duong

What drives labor onset remains largely unknown. Understanding the molecular mechanisms defining pregnancy duration and preparing the uterus for labor onset can help improve current treatment strategies to promote or halt labor. Biological processes with a ~24-hour cycle called circadian rhythms are generated by endogenous “clock” transcription factors referred to as the molecular clock, which drives daily changes in cellular functions. To understand the role of circadian rhythms in pregnancy, we first characterized how the molecular clock of the reproductive axis adapts to pregnancy and found the molecular clock is upregulated. Next, to understand if the molecular clock helps define pregnancy duration, we analyzed gene expression data from pregnant women. We found that low maternal levels of two clock genes increased the risk of preterm birth 5 fold. As preterm birth is driven by a premature increase in uterine contractions, we then asked how time of day impacted uterine contractile response to oxytocin, a hormone that increases uterine contractions and is widely used to induce labor. As model for human pregnancy, mice presented with daily time windows of increased uterine sensitivity to oxytocin. To determine if the molecular clock drives this daily change in sensitivity to oxytocin, we used conditional knockout mice which had the molecular clock ablated in uterine smooth muscle. These mice lost the daily change in sensitivity to oxytocin-induced contractions and presented stronger spontaneous uterine contractions than controls. In conclusion, we show that circadian rhythms have an important role in regulating pregnancy duration and uterine function, where the uterine molecular clock defines daily time windows of enhanced uterine sensitivity to oxytocin.

ACKNOWLEDGEMENTS

The author thanks Drs. Hanne Hoffmann, Amy Ralston, Erik Martinez-Hackert, Stephanie Watts and Timothy Zacharewski for mentorship and advice over the course of the PhD training. The author also thanks Ms. Duong Nguyen, Ms. Nicky Ly, Mr. Aneesh Cherukuri, Ms. Brooke Devries, Dr. Alexandra Yaw and Dr. Guoli Zhou for their companionship and assistance with various aspects of laboratory experiments. The author is indebted to the DO/PhD Program – especially Dr. Justin J. McCormick, Ms. Bethany Heinlen, Dr. Brian Schutte, Dr. John Goudreau and Ms. Michelle Volker – for the training opportunity and their ongoing support. The author is grateful for Dr. David Arnosti and Ms. Jessica Lawrence from the Department of Biochemistry and Molecular Biology for helping the author navigate the administrative complexity of being a dual-degree student during the PhD training.

Special thanks go to the author's loved ones for their unconditional love and support. The author's significant other, Mr. Aiden Quang H. Nguyen, offered many late-night snacks, phone calls, a great listening ear and cheerful spirits for when things were challenging. The author's family, especially her mom, Ms. Diep N. Le and her sisters, Dr. Quynh Van Duong and Ms. Phuc V. Duong, are always anchors of mental strength.

This research was made possible by the Eunice Kennedy Shriver National Institute of Child Health & Human Development of the National Institutes of Health under Award Number R00 HD084759 (H.M.H.), the USDA National Institute of Food and Agriculture Hatch project MICL1018024 (H.M.H.) and by the March of Dimes Grant no 5-FY19-111 (H.M.H.).

PREFACE

In this dissertation, the role of the circadian rhythms in uterine contractions in late pregnancy is explored. The studies demonstrate for the first time how the circadian rhythms can be used as biomarkers for spontaneous preterm birth and potentially targets for development of drugs to modulate uterine contractions. Each chapter in the dissertation is dedicated to an aspect crucial to the work and is briefly summarized below.

Chapter one first established changes in circadian rhythms in normal pregnancy, both at the tissue levels and the behavior levels. Chapter two then explored the role of circadian rhythms in spontaneous preterm birth. Lastly, chapter three looked at how circadian rhythms of the uterus regulated uterine contractile functions in late pregnancy, as the first step in determining uterine circadian rhythms as a potential direction for future drug development for mistimed labor onset.

Even though more work is needed to translate the findings of this dissertation to clinical practice, my work identified for the first time circadian rhythms as potential biomarkers for spontaneous preterm birth and established the important role of circadian rhythms in uterine contractile functions in late pregnancy, opening a new direction to develop treatments for preterm labor and postterm labor.

TABLE OF CONTENTS

LIST OF TABLES

LIST OF FIGURES

KEY TO ABBREVIATIONS

bHLH	basic helix-loop-helix
Bmal1	brain and muscle ARNT-like protein 1
CCG	“clock” controlled gene
Clock	circadian locomotor output cycles kaput
Cry	cryptochrome
h	hour
Luc	firefly luciferase
Oxtr	oxytocin receptor
PAS	Per-ARNT-SIM
Per	period
PER2::LUC	PER2::LUCIFERASE
Rev-ERB	reverse orientation c-erb
ROR	retinoic acid receptor-related orphan receptor
RORE	RevErbA/ROR-binding element
SCN	suprachiasmatic nucleus
sPTB	spontaneous preterm birth

CHAPTER 1 – CIRCADIAN RHYTHMS IN LATE PREGNANCY

SIGNIFICANCE

Disruptions in timing of labor and birth often result in Caesarian section (C-section). Almost 4 million births occur each year in the United States[1–3]. About 30% of these are from C-sections[4]. C-section not only costs 50% more than vaginal birth[4], but is also associated with increased risk of long-term maternal and neonatal complications and therefore should be avoided unless medically required[5]. One way to avoid unnecessary C-sections is to efficiently induce labor. Unfortunately, labor induction drugs (uterotonics) have variable efficacies and approximately 25% of induced labors still result in C-section[6,7]. Understanding what drives labor onset will help develop strategies to efficiently induce labor and reduce C-sections.

THE NATURAL TIMING OF LABOR AND BIRTH

Sixty percent of labor inductions occur at times of the day drastically different than natural labor and birth. Across species, labor onset primarily occurs during the inactive (rest) phase of the day[8,9]. Evolutionarily speaking, this timing of labor and birth provides protection from predators for both the mother and the newborn thanks to the presence of herd members, and is timed to the rest phase of the day, where little to no ambulatory activity is needed[8–10]. In humans labor onset and birth remains circadian timed, where the pregnant uterus is physiologically primed to increase contractions at night and most spontaneous births occur around 4.30AM[10].What allows this timing of labor and birth to the rest phase of the day is poorly understood, but one possibility is that factors that modulate uterine contractions may be more effective at night than during the day. The current clinical practice of labor induction, however, does not take this nocturnal aspect of natural birth into account as labor inductions are scheduled in the morning or early afternoon for the convenience of hospital staffing[11–13]. We propose that the timing difference between labor induction and natural labor onset is a contributing factor to the high rate of unsuccessful labor

inductions, as we speculate the uterus is less responsive to labor-inducing drugs during the day than the night period.

THE UTERUS AND UTERINE CONTRACTIONS

The uterus is the organ that protects the developing fetus until birth. The myometrium is the smooth muscle layer that generates uterine contractions for labor and delivery (Figure 1.1). Pregnant women that deliver at term have a nocturnal increase in uterine contractions in the third trimester. Interestingly, a small cohort study showed that women that experienced preterm birth lost this nocturnal increase in uterine contractions in the third trimester, suggesting a disruption to the circadian rhythms of uterine contractions might be associated with disruptions of pregnancy length. One mechanism that drives the nocturnal increase in uterine contractions is increased uterine sensitivity to oxytocin at night. Oxytocin, a major hormone in pregnancy known to increase uterine contractions[14,15] and widely used to clinically induce labor in the form of Pitocin, its synthetic version. A small study in late-pregnant *Rhesus* monkeys (n=5) shows that oxytocin given at night is more efficient at inducing uterine contractions, than when given during the daytime[16–18]. It remains unknown what drives this daily change in uterine sensitivity to oxytocin, where I propose it is driven by the molecular clock within the myometrium.

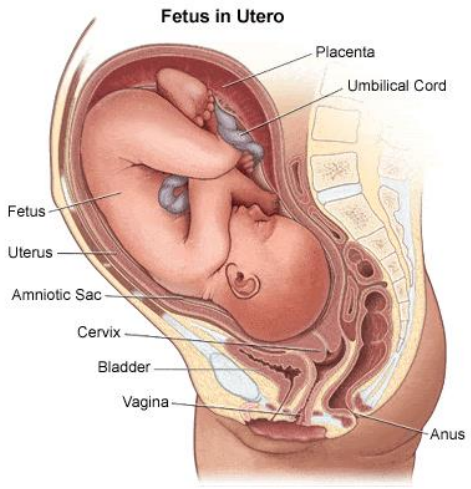

Figure 1.1. Diagram of a uterus in pregnancy. The uterus consists of the endometrium and the smooth muscle myometrium, which generates uterine contractions.

CIRCADIAN RHYTHMS AND THE MOLECULAR CLOCK

Circadian rhythms are biological processes with a ~24h cycle that are autonomous and persist without environmental cues[19–21]. Circadian rhythms exist at the behavioral, tissue and cellular levels. At the behavior level, circadian rhythms take many forms, the most common of which is sleep-wake cycles[22]. Circadian rhythms at the tissue level are reflected in for example hormonal release patterns and changes in metabolisms[23].

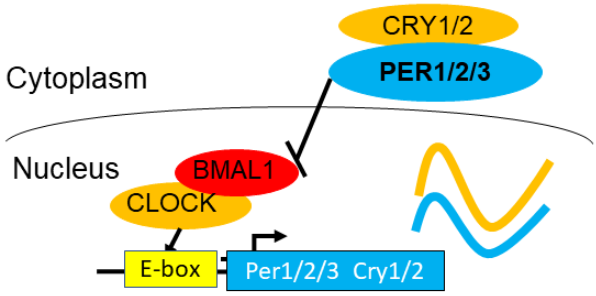

Figure 1.2. A transcriptional feed-back loop within each cell generates circadian rhythms. Simplified view of how cellular circadian rhythms are generated. The transcription factors BMAL1 and CLOCK drive expression of *Per* and *Cry,* which after translation repress BMAL1/CLOCK driven transcription by binding to the BMAL1/CLOCK complex. This feed-back loop generates a

Figure 1.2. (cont'd)

~24h rhythm within each cell. The capacity of BMAL1 to regulate tissue specific genes allows a set of genes to acquire a circadian expression which drives optimal tissue function.

At the cellular level, circadian rhythms are an inherent property of almost all nucleated cells. Circadian rhythms are generated by "clock" transcription factors, which are conserved across species (Figure 1.2). Each cell contains an autonomous circadian clock allowing time-of-day specific functions of cellular processes. The mammalian core molecular clock consists of the transcription factors brain and muscle ARNT-like protein 1 (BMAL1 or MOP3), cryptochrome (CRY1/2), circadian locomotor output cycles kaput (CLOCK) and period (PER1/2/3)[21]. BMAL1 and CLOCK are members of the basic helix-loop-helix/Per-ARNT-SIM (bHLH/PAS) proteins (REF?). BMAL1 and CLOCK heterodimerize and initiate the transcription of CRYs and PERs by directly binding to E-box (5'-CACGTG-3') or E'-box (5'-CACGTT-3') *cis*-regulatory elements (DNA sequence) of these genes[24–28]. E-box and E'-box sequences can be located in the proximal or distal promoter region, or even within the coding region of the target gebe[25,28–31], and there can be more than one E-box or E'-box sequences per gene[25,32,33]. CRYs and PERs in turn dimerize and inhibit their own transcription by binding to the BMAL1/CLOCK complex[33], generating a ~24h oscillation in gene expression. The BMAL1/CLOCK heterodimer remains bound on the DNA throughout the circadian oscillation, and inhibition of transcription occurs through the interaction between DNA bound BMAL1/CLOCK with negative regulators such as PERs and CRYs[33]. Beside the core clock transcription factors exists complex accessory regulatory loops that add additional layers of control to the cellular circadian rhythms. One such loop is via the reverse orientation c-Erb α and β (Rev-ERB α and β) and retinoic acid receptor-related orphan receptors (RORs) α, β and γ. These nuclear receptors bind to the RevErbs/ROR-binding elements (ROREs) in the *Bmal1* promoter region. RORs activate the transcription of *Bmal1* while RevErbs inhibit it[21,34–38].

Interestingly, the expression of *Rev-Erbs* and *Rors* are regulated by CLOCK/BMAL1 binding to E-boxes in their promoter regions[39].

Beside generating cell's endogenous circadian rhythms, "clock" transcription factors are also involved in the transcription of about 25% of all genes in the cells. These genes are called "clock-controlled genes" (CCGs). The "clock" transcription factors regulate the expression of CCGs by binding to E-box or E'-box *cis*-regulatory elements, giving these genes a circadian pattern of expression[21,40]. The circadian expressions of CCGs are responsible for daily functional changes in cells and tissues and have been utilized to improve drug efficacy as they allow for tissue level circadian changes in response to treatments[41]. This field of science is called chronopharmacology.

THE MOLECULAR CLOCK IN PREGNANCY

It is becoming evident that clock genes play an important role in a healthy pregnancy. Different tissues have daily changes in clock gene expression during pregnancy [42,43]. In mice, knock-outs of clock genes resulted in pregnancy complications. Disruptions to the clock genes *Clock* (the negative dominant *ClockΔ19* mutant) and *Bmal1* (the myometrium-specific *Bmal1* knock-out) resulted in dystocia and mistiming of labor onset, respectively[44,45]. *Bmal1* null-mutants displayed an even more severe phenotype as they could not sustain pregnancy due to low serum progesterone levels[46]. Interestingly, in humans, clock genes are also involved in pregnancy complications. Specifically, *Per2* is associated with implantation failure[47], *Rev-Erb* α is involved in spontaneous abortion[48], *Clock* plays a role in preeclampsia and miscarriage[49,50], and certain polymorphisms of the clock gene *BMAL1* are associated with an increased risk of in miscarriage[51].

One unique characteristic of BMAL1 is its essential role in generating circadian rhythms, where its deletion results in loss of circadian rhythms at both the behavioral level and the cellular level[52–54]. Even though deletion of the other clock genes results in disruption to circadian rhythms, circadian rhythms still exist at the behavior and cellular levels[21,55–57]. Deletion of *Bmal1*, on the

other hand, completely abolishes the circadian rhythm of locomotor activity and clock gene expression[40,56,57]. Interestingly, the involvement of the molecular clock in the timing of labor and birth is supported by studies in conditional knock-out mice, where BMAL1 is deleted in the myometrium by crossing Bmal1$^{flox/flox}$ mice with mice carrying the Telokin^{Cre} allele, an allele targeting the myometrium and the smooth muscle of the bladder[58]. These mice will be referred to as cKO mice. Even though otherwise healthy, 35% of cKO mice have mistimed labor onset: they give birth either too early or too late compared to wild type mice[58].

VALUE OF THE MOUSE MODEL IN CIRCADIAN RHYTHM AND PREGNANCY RESEARCH

Much of our knowledge about circadian rhythms in mammals comes from the mouse model. The smallest mammalian species available for studies, the mouse offers numerous transgenic models, allowing us to study the function of a specific gene within a defined cell type. With regards to circadian rhythms, while knock-outs of clock genes allow us to study the role of each clock gene on the cellular or behavioral level, the knock-in PER2::LUCIFERASE (PER2::LUC) reporter mice allow for real time detection of the circadian rhythms as evaluated by PER2 levels at the cellular and tissue levels[59]. PER2::LUC expression reflects the expression of *Per2,* as well as the other clock genes due to their inter-regulation of each other (Figure 2). The PER2::LUC knock-in mice contain the firefly luciferase (*Luc*) gene attached to the endogenous *Per2* gene. Incubating tissues from PER2::LUC mice in tissue culture media containing luciferin, a substrate for luciferase, provides a semi-quantitative evaluation of PER2 through the measure of luciferase, which is detected by a light signal generated by luciferase cleaving luciferin[59–63]. Attaching *Luciferase* after genes of interest to detect their expression levels have been a commonly used method to detect real-time gene expressions thanks to the short half-life of luciferase (~10 minutes)[64].

The mouse model hence is a valid model to study the role of circadian rhythms in uterine functions. The mouse, despite being a nocturnal organism (active at night) vs human (diurnal-

active during the day), exhibits a time-of-day-dependent timing of labor and birth: most mice give birth around the transition between the dark phase and light phase[58]. The molecular clock is conserved between human and mouse, and the mouse uterus also shows an increase in uterine contractions in response to oxytocin[65–67], a primary hormone promoting labor and commonly used in labor induction in humans[14,15]. The action of oxytocin through oxytocin receptor (OXTR) is greatly conserved between human and mouse. Furthermore, the mouse model offers greater experimental feasibility as pregnancy in the mouse is relatively short, ranging from 19 to 20 days, vs 9 months in human[68].

It is worth mentioning that most mouse models, especially C57B/6J, the most commonly used laboratory mouse strain and also the genetic background of PER2::LUC mice, do not have endogenous melatonin[59,69,70]. Melatonin is a peptide hormone produced by the pineal gland which synchronize circadian rhythms of cells and tissues in the body[10]. However, within the scope of our proposed studies focused on the role of circadian rhythms in uterine contractile functions and receptor expression, C57B/6J remains a valid model.

RATIONALE AND HYPOTHESIS

Despite the vast knowledge of clock genes and circadian rhythms in the non-pregnant state[71,72], little is known about clock genes and circadian rhythms in pregnancy, at both the tissue and the behavioral levels, and how they relate to labor onset. The goal of my studies is to fill in this gap of knowledge primarily using the mouse model. I hypothesized that circadian rhythms exist at the tissue and behavior levels in pregnancy and regulate tissue functions, especially uterine contractions in late pregnancy. In the first chapter, I determined how circadian rhythms in the reproductive axis (the suprachiasmatic nucleus, the ovary and the uterus) and the locomotor behavior adapted as pregnancy progressed. The second chapter explored the relationship between circadian rhythms and timing of labor onset by determining the associations of serum levels of clock genes and preterm birth (a type of mistiming of labor onset). Lastly, the third chapter

examined how uterine circadian rhythms, through the clock gene *Bmal1,* regulated uterine contractile functions in late pregnancy.

CHAPTER 2 – CIRCADIAN RHYTHMS IN THE MOUSE REPRODUCTIVE AXIS DURING THE ESTROUS CYCLE AND PREGNANCY

This chapter was adapted from the following previously published manuscript:

Yaw, AM,* **Duong, TV**,* Nguyen, D and Hoffmann, HM. *Circadian rhythms in the mouse reproductive axis during the estrous cycle and pregnancy*. J Neurosci Res. 2021 Jan;99(1):294-308. PMID: 32128870, PMCID: PMC7483169

* Authors contributed equally

ABSTRACT

Molecular and behavioral timekeeping is regulated by the circadian system which includes the brain's suprachiasmatic nucleus (SCN) that translates environmental light information into neuronal and endocrine signals aligning peripheral tissue rhythms to the time of day. Despite the critical role of circadian rhythms in fertility, it remains unexplored how circadian rhythms change within reproductive tissues during pregnancy. To determine how estrous cycle and pregnancy impact phase-relationships of reproductive tissues, we used PER2::Luciferase (PER2::LUC) circadian reporter mice and determined the time of day of PER2::LUC peak (phase) in the SCN, pituitary, uterus, and ovary. The relationships between reproductive tissue PER2::LUC phases changed throughout the estrous cycle and late pregnancy and were accompanied by changes to PER2::LUC period in the SCN, uterus, and ovary. To determine if the phase relationship adaptations were driven by sex steroids, we asked if progesterone, a hormone involved in estrous cyclicity and pregnancy, could regulate Per2-luciferase expression. Using an *in vitro* transfection assay, we found that progesterone increased Per2-luciferase expression in immortalized SCN (SCN2.2) and arcuate nucleus (KTAR) cells. In addition, progesterone shortened PER2::LUC period in *ex vivo* uterine tissue recordings collected during pregnancy. As progesterone dramatically increases during pregnancy, we evaluated wheel-running patterns in PER2::LUC mice. We confirmed that activity levels decrease during pregnancy and found that activity onset was delayed. Although SCN, but not arcuate nucleus, PER2::LUC period changed during late pregnancy, onset of locomotor activity did not correlate with SCN or arcuate nucleus PER2::LUC period.

INTRODUCTION

Circadian timekeeping plays an essential role in successful pregnancy, which requires the precise coordination of a number of essential processes to occur, including ovarian follicular development and maturation[73], ovulation[74,75], mating behavior initiation[74,75] and mature oocyte release[73,75]. Each of these processes are controlled by a fine-tuned feedback mechanism in which the timing of hormone release is synchronized with receptor expression throughout the female reproductive system to ensure pregnancy success[76,77]. On a cellular level, circadian rhythms are generated by an autoregulated transcription-translation feedback loop of molecular clock transcription factors, of which Period 1/2 (Per1/2), Brain and Muscle ARNT-Like 1 (Bmal1), Clock and Cryptochrome1/2/3, comprise the core mechanism, reviewed in[78]. To synchronize these cellular circadian rhythms to environmental conditions, a combined mechanism encompassing both neural and hormonal signals is coordinated by the brain's primary circadian pacemaker, the suprachiasmatic nucleus (SCN)[73,75,79]. The SCN's principal role is to translate environmental lighting information into neuronal and hormonal signals, allowing synchronization of behavioral activity, hormonal release, and tissue sensitivity[80]. Despite the well-established role of day-length and circadian rhythms in regulating reproductive status in seasonal breeders[81–84], the luteinizing hormone surge promoting ovulation[85–88], and the circadian timing of labor onset[89–92], little is known about how pregnancy impacts circadian rhythms and daily changes in behavior[93,94]. A significant step towards understanding behavioral and circadian changes in pregnancy was published by Martin-Fairey et al., 2019, who showed that pregnancy in both humans and mice was associated with a reduction in locomotor activity and a shift in the timing of activity onset[94], two behaviors known to be regulated by the SCN[95–97].

In addition to understanding the role of circadian changes in behavior during pregnancy, metabolic and hormonal changes during pregnancy may be influenced by circadian rhythms, although this remains largely unexplored. Pregnancy is associated with dramatic changes in metabolism[98] and hormone release patterns[99], both of which maintain strong ties to circadian

rhythmicity[100–105]. Progesterone is a sex steroid which increases towards late pregnancy, and peaks around gestation day (GD) 15-17 in mice[106–108]. The primary role of progesterone during pregnancy is to allow implantation[109–112] and to silence uterine contractions prior to labor onset. Progesterone performs these functions through activation of both nuclear receptors, progesterone receptor A and B (PRA and PRB, respectively), as well as membrane bound progesterone receptors[113–116]. During late pregnancy (beginning approximately at GD 17 in the mouse), a reduction in progesterone in combination with PRA and PRB function allows for the progression of parturition[117,118], initiation of lactation[119–122], and maternal behaviors[123,124]. It should be noted that the role of progesterone in labor initiation varies between species[125]. In addition to the aforementioned roles, progesterone also acts as a regulator of metabolic function[126]. Recent work indicates this metabolic action of progesterone might be regulated by the arcuate nucleus, a hypothalamic structure which express high levels of progesterone receptors[127–129].

While it is known that disrupted circadian rhythms can be detrimental to reproductive success[130,131], it remains largely unknown how they change from the non-pregnant state to pregnancy. Understanding the role of circadian rhythms in regulating both behavior and tissue specific circadian function during the estrous cycle and in pregnancy is an essential first step towards elucidating the underlying mechanisms associated with infertility and pregnancy complications, which are more prevalent in women with disrupted circadian rhythms[132–135]. We hypothesize that circadian timekeeping during late pregnancy influences mouse behavior and reproductive tissue circadian function in preparation for labor. Here, we confirm locomotor activity changes during pregnancy and describe the changes in molecular circadian time-keeping between the estrous cycle and pregnancy using the circadian knock-in reporter mouse, PER2::Luciferase (PER2::LUC). Finally, we explore the potential role of PRA/B in driving circadian rhythm changes.

MATERIALS AND METHODS

Mice

All methods described here have been approved by the Institutional Animal Care and Use Committee of Michigan State University and conducted in accordance with the Guide for the Care and Use of Laboratory Animals. Period2::Luciferase (PER2::LUC) mice were purchased from JAX (strain B6.129S6-Per2tm1Jt/J, #006852, https://www.jax.org/strain/006852). Mice were housed under a 12 h light-dark cycle, lights on at 6AM (Zeitgeber time 0, ZT 0), with food and water *ad libitum*. Mice were sacrificed by isoflurane or CO_2 overdose, followed by cervical dislocation. Experimental mice were 6-14 weeks of age at the start of experiments.

Timed mating

Two females and one male were housed together at ZT 10-11 and vaginal plug formation was checked at ZT 3-4 during the mating assay. On the day of vaginal plug identification, the female was separated from the male. If no vaginal plug was found, mating pairs remained co-housed for up to 5 days, and daily checks for vaginal plugs were continued. Following vaginal plug identification, pregnancy was confirmed by a significant increase in body weight, where a weight gain of >2 g from gestational day (GD) 1 to 10 was indicative of pregnancy [136]. Gestational stage was further confirmed the day of tissue collection, where embryo development was established using Theiler Stage (https://www.emouseatlas.org/emap/ema/theiler_stages/StageDefinition/stagedefinition.html; accessed January 2020). For wheel running behavior, timed mating was conducted as described above, except that one female was mated with one male.

Wheel-running behavior

During timed mating, female and male mice were housed in light and temperature controlled circadian cabinets (standard mouse circadian cabinet, Actimetrics, Wilmette, IL) within

polypropylene cages (33.2 × 15 × 13cm.2 cm) containing a metal running wheel (11 cm diameter). Males utilized for timed mating were individually housed in the same behavioral cabinet as the females. Females were allowed 2-5 days acclimatization to running wheels prior to experimental start. Female locomotor activity rhythms were monitored with a ClockLab data collection system (Version 3.603, Actimetrics, Wilmette, IL) through the number of electrical closures triggered by wheel rotations. Light intensity varied between 268-369 Lux inside the mouse cage with wheel. Cage changes were scheduled at 3-week intervals. Wheel-running activity was analyzed using ClockLab Analysis (Actimetrics Software) and complied into 5-minute bins by persons blind to experimental group. Activity data collected during timed mating were not included in statistical analyses. Daily onset of activity was defined as the first time when activity was counted for at least 1 h after at least 4 h of inactivity. Pregnant females were euthanized and gestation day assigned according to timed mating and Theiler Stage as described in “Timed Mating”. Following euthanasia, *ex vivo* tissue explants were monitored for PER2::LUC bioluminescence as described in “Monitoring of PER2::LUC bioluminescence”. To correlate locomotor activity onset with SCN and PER2::LUC period, only PER2::LUC females used in the running wheel locomotor activity set-up were used.

Determination of estrous stage

To assess estrous stage, vaginal smears were performed at the time of euthanasia between ZT 3-6 on female mice (3-6 months) by vaginal lavage[137]. Smears were collected on glass slides and counterstained with 0.1% methylene blue (Spectrum, Gardena, CA). Cell type was observed through bright field microscopy to determine the corresponding stage of the estrous cycle, by persons blind to experimental group.

Monitoring of PER2::LUC bioluminescence

Mice were euthanized at ZT 3-6 or ZT 15-17. Data from mice euthanized at ZT15-17 were not used in phase analyses. Following euthanasia, the uterus, ovary, pituitary and brain were removed and placed in a semi-frozen 1x Hank's buffered salt solution (HBSS, 14065-056, Gibco). Using a dissection scope the ovary and pituitary were isolated and the uterus dissected into pieces of ≈ 4 mm^2 (~2 mm x 2 mm). To prepare the uterine pieces the whole uterus was cleaned from fat, and the uterine segment surrounding the fetuses cut in the longitudinal direction of the uterine horn. The uterine horn was opened into a sheet and pinned down to a dissection dish. Using a ruler, 2 x 2 mm uterine strips were collected midway between the cervix and the ovary near the placental attachment and placed with the endometrium side down onto the MiliCell membrane (MilliCell, PICM0RG50; MilliporeSigma, Burlington, MA). Ice-cold brains were sliced coronally on a vibratome (Leica VT 1200S) at 300 µm. After sectioning on the vibratome, a dissection scope was used to identify the appropriate brain regions. The SCN and arcuate nucleus were identified through anatomical identification [138]. The SCN was dissected as previously described Figure 2.1A [139,140]. For the arcuate nucleus, the median eminence was removed, where after two bilateral scalpel incisions allowed to isolate the arcuate nuclei Figure 2.1B. Both arcuate nuclei were placed onto a MilliCell membrane. MiliCell membranes were placed in 35 mm dishes (Nunc, Thermo Fisher Scientific, Rochester, NY) containing 1.5 ml of 35.5 °C recording medium (Neurobasal, 1964475, Gibco) supplemented with 20 mM HEPES (pH 7.2), B27 supplement (2%; 12349-015, Gibco), 1 mM luciferin (luciferin sodium salt; 1-360242-200, Regis, Grove, IL), and antibiotics (8 U/ml penicillin, 0.2mg/ml streptomycin, 4mM L-glutamine; Sigma-Aldrich). Dishes were sealed using vacuum grease and placed into a LumiCycle (Actimetrics, Wilmette, IL) inside a light-tight 35.5 °C, 5% CO_2, non-humidified environmental chamber. Uterine tissue was treated with vehicle (1/50 dilution of diH_2O) or water-soluble progesterone (P4, Sigma Aldrich #P7556, 50 nM and 100 nM, data was pooled as no difference in effect was observed). The bioluminescence signal was counted every ten minutes for 1.11 min for 6 days (day 1- day 6 of

recording time). Data were normalized by subtraction of the 24 h running average from the raw data and then smoothed with a 1 h running average (Luminometer Analysis, Actimetrics) and analyzed blind to experimental group. During the initial ~24 h (day 0) in the LumiCycle, the PER2::LUC signal tends to decrease significantly prior to achieving a stable waveform. In our analysis of PER2::LUC period, we exclude the first 24 h of recording to account for this. Incomplete data sets, as caused by loss of data points, other technical problems, or explants failing to show two PER2::LUC peaks (deemed arrhythmic[141]) were not included in the analyses (Total of 6 SCN, 2 arcuate nucleus, 5 pituitary, 2 ovary and 1 uterine explants). PER2::LUC phase was determined as the time-of-day of first PER2::LUC peak. PER2::LUC period was analyzed by the Luminometer Analysis software (Actimetrics) as the time difference in hours between the two peaks, with LM fit (damped sin) as the mathematical model. To determine the phase of the tissue, we utilized the time peak activity on day 1 of recording (time of first peak). All phase data are reported in degrees and reference to zeitgeber time (ZT) with time of lights on at ZT 0 from the day of euthanasia.

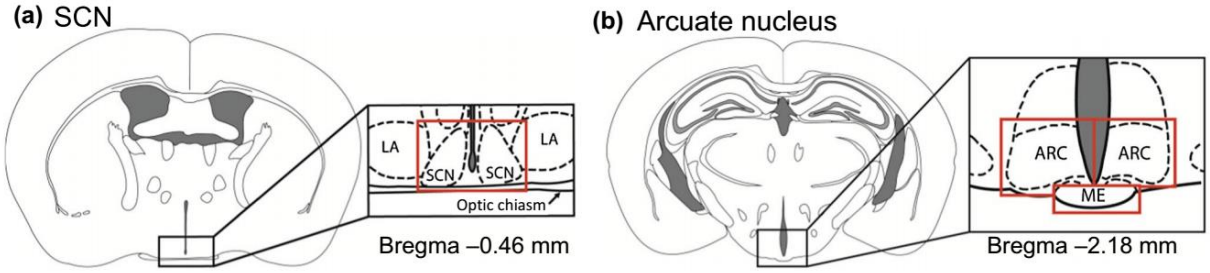

Figure 2.1. Diagram of SCN and arcuate nucleus dissections. Representative diagram of dissected A.) suprachiasmatic nucleus (SCN) and B.) arcuate nucleus (ARC) for monitoring of Per2::luciferase bioluminescence. Red lines indicate where individual cuts were made in the tissue slices. Abbreviations are as follows: LA- lateroanterior hypothalamic nucleus, SCN- suprachiasmatic nucleus, ME- median eminence, ARC-arcuate nucleus.

Cell culture, transfections, luciferase assays and hormone treatment

NIH3T3 (mouse embryonic fibroblasts, American Type Culture Collection), KTAR (female arcuate nucleus neurons, mouse)[142]; and SCN2.2 cells (immortalized rat suprachiasmatic nucleus neurons)[143], were cultured in a humidified 5% CO_2 environment in DMEM (Corning/Mediatech), with 1% penicillin-streptomycin (Sigma Aldrich) and 10% heat inactivated fetal bovine serum (Sigma Aldrich) or 10% charcoal stripped fetal bovine serum (Gibco Cat#A33821), as indicated in figures. NIH3T3, KTAR, and SCN2.2 cells were seeded into 24-well plates (Thermo Scientific) at $0.05x10^6$ (NIH3T3 and KTAR) and $0.3x10^6$ (SCN2.2) cells per well. Transfection of cells was performed 24 h after the cells were plated. Transient transfections were performed using PolyJet™ (SignaGen Laboratories, Rockville, MD), following a previously published protocol [144,145]. For luciferase assays, cells were transfected with 200 ng/well mouse -1128 to +2129 bp Per2-luciferase reporter plasmid (pGL6 plasmid, Addgene.org)[146] and 100 ng progesterone receptor A, B or pcDNA empty vector[147]. Five ng/well pGL4.74 Renilla luciferase reporter plasmid (hRluc, Promega) was added and served as an internal control. To equalize the amount of DNA transfected into cells, we systematically equalized plasmid concentrations by adding the corresponding plasmid empty vector. Twenty-four hours after transfection, culture medium was replaced with DMEM containing 0.1% Bovine Serum Albumin (BSA, Fisher Scientific) and progesterone (water soluble P4, 100 nM, Sigma Aldrich #P7556) or vehicle control (water 1/50 dilution). For luciferase assays, cells were harvested 48 h after transfection in 1x Passive lysis buffer (Promega Dual-Luciferase Reporter Assay System Kit). Dual-Luciferase assays were performed following manufacturers recommendations. Luciferase values are normalized to hRluc values to control for transfection efficiency. Values are normalized to pGL3 and are expressed as fold change as compared to control plasmid as indicated in the figure legends. Data represent the mean ± SEM of at least four independent experiments done in replicate.

Statistical analysis

Data were analysed using GraphPad Prism 8 (Graph Pad Software, La Jolla, CA). Significant differences were designated as $P < 0.05$. Wheel running activity (total wheel rotations) was analysed via a repeated measures mixed effects model. Correlation analyses were completed using Pearson r. Wheel running onset, PER2::LUC period, and transient transfection data were analyzed via one-way ANOVA. Post-hoc tests were completed using Tukey's multiple comparison test. PER2::LUC timing of first peak phase relationships were analyzed via a One Criterion Analysis of Variance for Circular Data, followed by pairwise comparisons, Watson's Two Sample Test of Homogeneity using Bonferroni's correction to accommodate familywise error rate, where appropriate. Phase data were reported in degrees and standard error (SE). All data passed normality testing. Statistical analyses for outliers (Grubbs' test) were conducted on all data sets, and no outliers were identified. Using G*Power software[148], we estimated the number of animals required for each experiment. Based on the literature, we expected that pregnancy would dramatically reduce locomotor activity[94]. Using the ANOVA repeated measures with an effect size of 0.5, alfa-probability of 0.05, with a power at 0.95, with 6 measurements (repeated measure of activity level) the experiment requires a total sample size of n = 8.

RESULTS

Late pregnancy impacts activity levels and activity onset independent of litter size

Pregnancy is associated with dramatic physiological changes, including great weight gain [149,150]. Recent work showed that pregnancy caused a reduction in activity levels of both humans and mice [94]. To determine if the reduction in activity levels was directly associated with litter size, we placed virgin female mice on running wheels for 15-20 days with light 12h:dark 12h (LD12:12) to establish their baseline activity level Figure 2.2A, B (non-pregnant; NP). A male was introduced to the chamber to allow pregnancy (timed mating). After positive identification of male mounting (as evidenced by a vaginal plug), the male was removed and female running-wheel activity

monitored till late gestation (Gestation day 18-19; GD 18-19) Figure 2A, B. In agreement with the previous study[94], wheel running activity decreased significantly during pregnancy, specifically during late gestation [GD 12-19, $F(2.20, 13.46) = 19.99$, n = 6-8/time point $p < 0.0001$], Figure 2.2B. This decrease in wheel running activity was not significantly correlated with the number of pups in each litter [$r(8) = 0.052$, n = 8, $p = 0.902$; $R^2 = 0.003$], Figure 2.2C, or significantly correlated with percentage of weight gain during pregnancy [$r(8) = 0.321$, n = 8, $p = 0.44$; $R^2 = 0.11$], Figure 2.2D. Interestingly, females displayed a delayed onset in activity during mid pregnancy [GD 8-13, $F(1.026, 7.182) = 6.182$, n = 8/time point, $p = 0.037$], Figure 2.2E. The changes to total activity and onset timing were not accompanied with changes in wheel running period, for non-pregnant (24.00 h ± 0.02), early (GD 2-7; 24.06 h ± 0.02), mid (GD 8-15; 24.06 h ± 0.06), or late (GD 16-19; 24.06 h ± 0.2) pregnancy [$F(1.09, 7.27) = 0.149$, n = 7-8/time point, $p = 0.15$]. Given the high variability in onset times during GD 14-19, we compared onset times from GD 14-15, GD 16-17, and GD 18-19; however there were no differences [$F(1.604, 9.625) = 0.766$, n = 7/time point, $p = 0.46$].

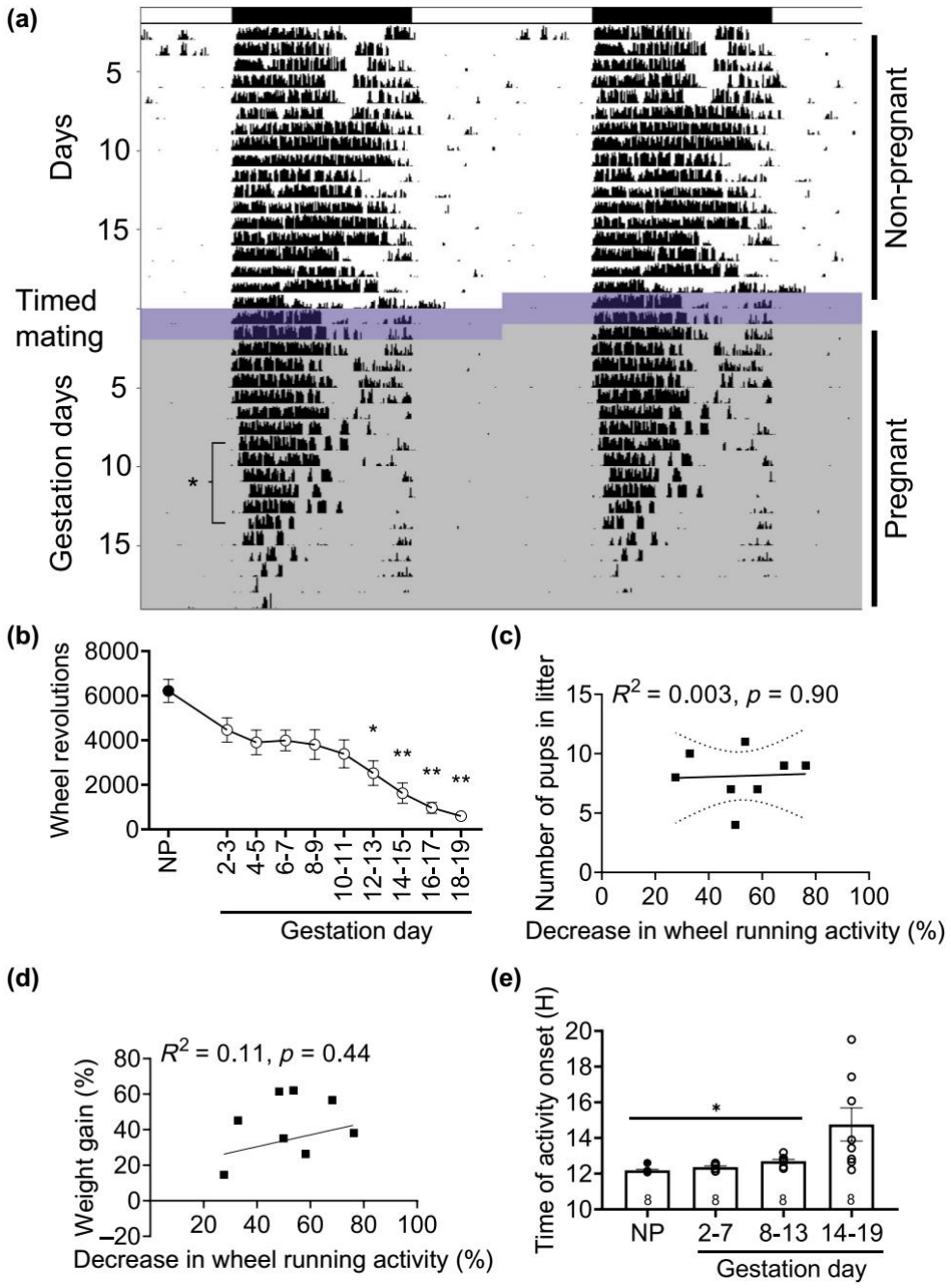

Figure 2.2. Pregnancy impacts activity levels and activity onset independent of litter size. (A) Representative double plotted actogram of wheel running in a female mouse before pregnancy (Day 1-20), during timed mating (Day 21-22; dark blue-purple shading), and during pregnancy [Gestation day (GD) 1-19; light gray shading]. (B) Total number of wheel revolutions decrease beginning GD 12-13 and continued to decrease through late pregnancy. Pearson

Figure 2.2. (cont'd)

correlation examining the relationship between the percentage decrease in wheel running activity from non-pregnant to late pregnant levels (GD 14-19) compared to the number of pups in each litter (C, n = 8, individual mice are shown as squares) and the percentage of weight gain during pregnancy (D, n = 8). R^2 and p values are indicated next to linear regression lines. Dashed curves indicate 95% confidence intervals. (E) Timing of activity onset is significantly delayed during mid pregnancy (GD 8-13), compared to non-pregnant (NP), early (GD 2-7), and late pregnancy (GD 14-19). Individual mice are shown as circles. Data were analyzed via repeated-measures one-way ANOVA followed by a Tukey post hoc. *, p<.05; **, p<.01.

PER2::LUC period in the SCN and arcuate nucleus does not correlate with locomotor activity onset in late pregnancy

To further understand the molecular mechanisms driving the changes in activity onset and locomotor activity patterns in late pregnancy Figure 2.2, we used the validated circadian reporter mouse, PER2::LUC to establish *ex vivo* tissue circadian rhythms in non-pregnant and pregnant females. It is well-established that PER2::LUC rhythms reliably recapitulate SCN function and reflect on behavioral wheel-running patterns[146]. We compared PER2::LUC period in the SCN from estrus (non-pregnant females), GD 14-15, GD 16-17 and GD 18-19 females. There was a significant decrease in PER2::LUC period between estrus and early (GD 14-15) and late (GD 18-19) pregnancy [$F(3, 33) = 5.61$, n = 6-14/group, $p = 0.003$], Figure 2.3A, B. This suggests that changes to SCN period may be involved in the delayed locomotor onset in pregnancy. However, due to the large behavioral variation in activity onset during late pregnancy Figure 2.2E, we established the correlation between SCN PER2::LUC period and time of day of wheel running onset Figure 2.3C. These correlation data [$r(7) = 0.072$, n = 7, $p = 0.80$; $R^2 = 0.014$], suggest the SCN probably does not contribute to the delayed activity onset in pregnancy. Recent work identified the arcuate nucleus as important in modulating metabolic status-driven locomotor

activity changes[151]. To determine if the molecular clock in the arcuate nucleus was involved in changing locomotor onset during pregnancy, we recorded arcuate nucleus circadian rhythms in our newly established arcuate nucleus slice preparation. The arcuate nucleus presents a circadian expression of PER2::LUC Figure 2.3D, E. There were no significant changes in PER2::LUC period between estrus and any of the studied gestation days [$F(3, 28) = 1.104$, n = 6-13/group, $p = 0.36$], nor a significant correlation between arcuate PER2::LUC period and time of day of wheel running onset [$r(6) = 0.739$, n = 6, $p = 0.44$; $R^2 = 0.16$], Figure 2.3F.

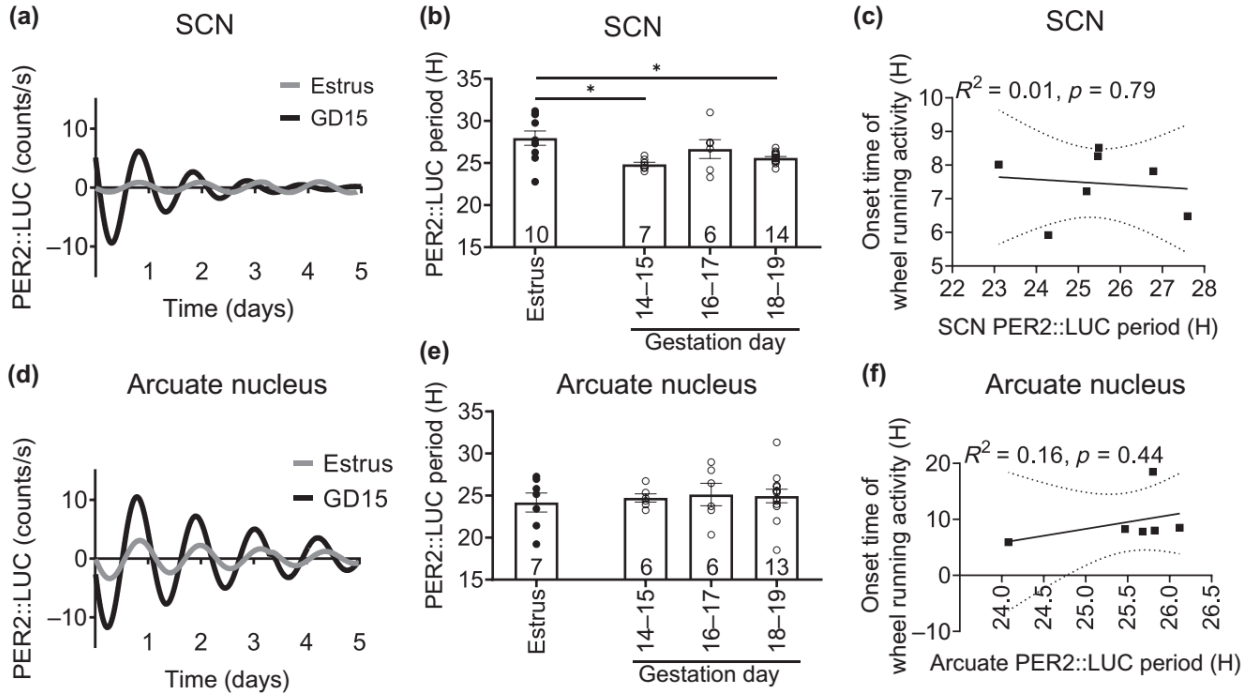

Figure 2.3. SCN, but not arcuate nucleus, PER2::LUC period correlates with locomotor activity onset during late pregnancy. (A) Example traces of representative SCN PER2::LUC recordings. (B) Histogram of PER2::LUC period in the SCN during pregnancy (n = 6-14/group). (C) Pearson correlation examining the relationship between the SCN PER2::LUC period and onset of wheel running activity on the day of euthanasia (GD 16-19), n = 7. (D) Example traces of representative arcuate nucleus PER2::LUC recordings, and (E) histogram of PER2::LUC period in the arcuate nucleus during pregnancy (n = 6-13/group). (F) Pearson correlation examining the relationship between the arcuate nucleus PER2::LUC period and onset of wheel running the day

Figure 2.3. (cont'd)

of euthanasia (GD 16-19), n = 6. Period data (B, E) were analyzed via one-way ANOVA followed by a Tukey post hoc. *, p<.05. Individual values are indicated by circles or squares, and n is indicated on the bars. R^2 values and p-values are indicated next to linear regression lines. Dashed curves indicate 95% confidence intervals.

Pregnancy alters reproductive tissue phase relationships

Changes in SCN output (as evidenced by changes in PER2::LUC period and behavioral changes, Figures 2.2 and 2.3), might impact phase relationships between peripheral tissues. No studies have, to our knowledge, addressed how phase relationships and circadian period changes in normal pregnancy. We compared phase-relationships between reproductive tissues during each stage of the estrous cycle and late pregnancy (GD 14-19) Figure 2.4A-C. There were significant differences in the timing of PER2::LUC peak expression between the different tissues during each stage of the estrous cycle [estrus: $F(3, 29) = 21.7$, n = 33, $p = 1.4e^{-07}$; proestrus: $F(3, 26) = 49.58$, n = 34, $p = 1.7e^{-10}$; diestrus I/II: $F(3, 36) = 20.17$, n = 40, $p = 7.7e^{-08}$]. Specifically, during proestrus, pituitary peak PER2::LUC expression (expressed in mean degrees ± standard deviation; 217.51 degrees ± 0.55, n = 10) was significantly different from peak timing in the ovary (327.77 degrees ± 0.48, n = 6; Watson's Two Sample Test of Homogeneity (referred to as Watson's) = 0.32, 0.001 < p < 0.01), uterus (47.30 degrees ± 0.89, n = 11; Watson's = 0.41, p < 0.001), and SCN (300.16 degrees ± 0.67, n = 7; Watson's = 0.21, 0.01 < p < 0.05). The ovary and SCN both exhibited a phase difference from the uterus (ovary: Watson's = 0.23, 0.01 < p < 0.05, and SCN: Watson's = 0.24, 0.01 < p < 0.05), but did not differ from each other (Watson's = 0.09, p > 0.10). During estrus, SCN (270.02 degrees ± 0.89, n = 10 ; Watson's = 0.34, 0.001 < p < 0.01) and pituitary (203.11 degrees ± 0.80, n = 8; Watson's = 0.30, 0.001 < p < 0.01), peak expression occurred ~2-8 h later than in the uterus (46.97 degrees ± 0.77, n = 8). The pituitary phase also significantly differed from the ovary (277.30 degrees ± 1.01, n = 7; Watson's = 0.22, 0.01 < p <

0.05) and uterus (Watson's = 0.24, 0.01 < p < 0.05), with no differences between ovarian peak expression and the SCN (Watson's = 0.11, p > 0.10). Diestrus I/II peak phase analyses revealed that SCN and pituitary time of peak expression did not differ (SCN,169.95 degrees ± 0.64, n = 11 vs pituitary, 300.29 degrees ± 1.29, n = 9; Watson's = 0.19, 0.01 < p < 0.05), and both the pituitary (Watson's = 0.36, 0.001 < p < 0.01) and SCN (Watson's = 0.39, p < 0.001) exhibited peaks later in the day than peak expression in the uterus (35.10 degrees ± 1.27, n = 8). DI/II ovary phase (301.69 degrees ± 0.37, n = 12) differed from the pituitary (Watson's = 0.26, 0.01 < p < 0.05) and uterus (Watson's = 0.26, 0.01 < p < 0.05) with no differences between the ovary and SCN (Watson's = 0.09, p > 0.10) Figure 2.4A-C. To understand phase relationships during late pregnancy, we next analyzed phase relationships across two-day periods from GD 14-19, Figure 2.4D. There were significant differences in the timing of PER2::LUC peak expression between the different tissues during each of the 2-day periods [GD 14-15: $F(3, 22) = 16.86$, n = 26, $p = 6.5e^{-06}$; GD 16-17: $F(3, 20) = 25.6$, n = 24, $p = 4.7e^{-07}$; GD 18-19: $F(3, 51) = 50.8$, n = 55, $p = 2.4e^{-15}$]. Specifically, during GD 14-15, SCN PER2::LUC peaked (169.95 degrees ± 0.64, n = 5) after peak timing in the uterus (35.10 degrees ± 1.27, n = 10; Watson's = 0.29, 0.001 < p < 0.01), and ovary (301.69 degrees ± 0.37, n = 5; Watson's = 0.23, 0.01 < p < 0.05), with no differences between the SCN and pituitary (pituitary: 300.29 degrees ± 1.29; n = 6; Watson's = 0.18, 0.5 < p < 0.10). GD 14-15 pituitary phase did not differ from peak phase in the uterus (Watson's = 0.13, p > 0.10) or ovary (Watson's = 0.07, p > 0.10), however, the ovary and uterus exhibited different phases (Watson's = 0.20, 0.01 < p < 0.05). For GD 16-17, the SCN (173.68 degrees ± 0.69, n = 6), again differed from the uterus (27.18 degrees ± 0.68, n = 8; Watson's = 0.30, 0.001 < p < 0.01) and ovary (306.16 degrees ± 0.70, n = 6; Watson's = 0.26, 0.01 < p < 0.05), with no differences between the SCN and pituitary (pituitary: 276.54 degrees ± 1.47, n = 4; Watson's = 0.15, 0.5 < p < 0.10). GD 16-17 pituitary phase differed from the phase in the uterus (Watson's = 0.24, 0.01< p < 0.05), but not the ovary (Watson's = 0.05, p > 0.10). During this time point, the ovary and uterus phases did not differ (Watson's = 0.14, p > 0.10). GD 18-19 peak phase analyses revealed

that SCN time of peak expression differed from all other tissues (185.36 degrees ± 0.79, n = 14; ovary: Watson's = $p < 0.001$, uterus: Watson's = 0.53, $p < 0.001$, pituitary: Watson's = 0.37, $0.001 < p < 0.01$). The ovary (310.97 degrees ± 1.08 n = 14) and uterus (33.73 degrees ± 0.89, n = 14) differed, Watson's = 0.30, $0.001 < p < 0.01$, and there were no differences between the pituitary (20.49 degrees ± 1.85, n = 13), compared to the ovary (Watson's = 0.14, $p < 0.10$) or uterus (Watson's = 0.15, $0.05 < p < 0.10$). There were no significant changes in PER2::LUC period in the pituitary [$F (3, 28) = 0.82$ n = 5-13/group, $p = 0.49$], Figure 2.4E, F. However the PER2::LUC period in the ovary was significantly different between estrus and GD 16-17 [$F (3, 28) = 3.10$, n = 6-13/group, $p = 0.042$]. Uterine PER2::LUC period revealed a significant change [$F(3, 36) = 4.97$, $p = 0.006$], with a lengthening of period from GD 16-17 to GD 18-19, Figure 2.4E, F. Correlation analyses between time of first peak and period revealed a significant correlation in the ovary [$r(50) = -0.324$, $p = 0.02$; $R^2 = 0.105$], whereas no significant correlations were seen in the pituitary [$r(50) = 0.062$, $p = 0.67$; $R^2 = 0.004$], or uterus [$r(59) = 0.073$, $p = 0.58$; $R^2 = 0.005$].

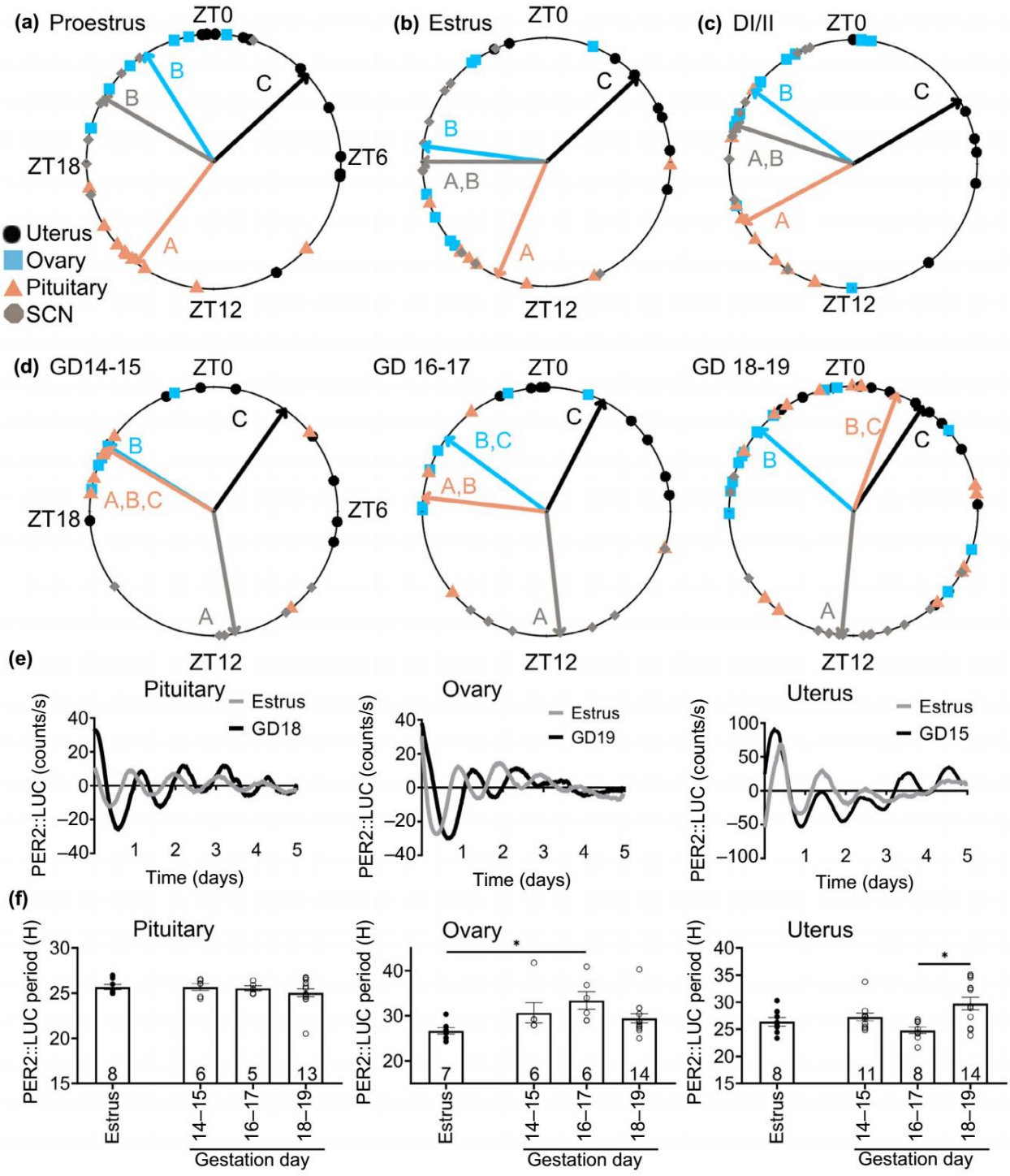

Figure 2.4. Reproductive tissue phase-relationships during estrous cycle and pregnancy. Time of day of first PER2::LUC peak was used to establish the phase of the studied tissues during the estrous cycle and during pregnancy. Phase-relationships during (A) estrus, n= 7-10/group, (B) proestrus, n= 6-11/group, (C) diestrus I and II (DI/II). n=8-12/group, and (D) late pregnancy

Figure 2.4. (cont'd)

[gestation day (GD) 14-19], n =5-15/group, except GD 16-17 pituitary, n=4. Mean time of first peak is indicated by the vector lines and symbols indicate individual data points. Data were analyzed via circular ANOVA where different letters indicate significantly different phases. (E) Representative PER2::LUC traces during estrus and GD 15-19 in the pituitary, ovary and uterus and (F) histogram of PER2::LUC period was compared between the indicated days in the pituitary, ovary, and uterus. Data were analyzed via one-way ANOVA followed by a Tukey post hoc. *, $p<.05$. For periods, individual values are shown as circles and n is as indicated.

Progesterone regulates PER2::LUC period in uterine tissue in late pregnancy

Given the important role of progesterone in uterine function in preparation for parturition[152,153], we examined the effect of progesterone on PER2::LUC period of uterine tissue by treating *ex vivo* GD 18-19 uterine tissue with either vehicle (water) or progesterone (50 and 100 nM) and following recorded the PER2::LUC period. We found that progesterone significantly shortened PER2::LUC period [Student's t-test, $t = 2.195$, $df = 20$, $n = 10$-12, $p = 0.040$], Figure 2.5A, B.

Progesterone receptors regulate Per2-luciferase expression in vitro

The potential role of PRs in the SCN remains elusive[154,155], whereas PRs in the arcuate nucleus are known to be important in regulating the negative feedback controlling the LH surge[156]. To determine if PRA and/or PRB can regulate the mouse Per2-luciferase promoter *in vitro*, we transiently transfected NIH3T3 cells (control cell line), SCN2.2 (rat SCN cell line) and KTAR cells (mouse arcuate nucleus cell line) with Per2-luciferase with and without PRA/B. As progesterone levels change dramatically during the estrous cycle and pregnancy, we compared the capacity of exogenous progesterone to regulate Per2-luciferase in NIH3T3, SCN2.2 and KTAR cells cultured in heat-inactivated FBS (contains progesterone), and charcoal stripped serum (depleted of

progesterone) (Figure 2.5C-E). In NIH3T3 cells, progesterone (100 nM), enhanced Per2-luciferase expression through PRA/B, independent of the type of media Figure 2.5C (NIH3T3). Interestingly, Per2-luciferase expression in SCN2.2 cells responded differently to progesterone depending on the type of culture media, where progesterone significantly enhanced Per2-luciferase expression in heat inactivated FBS (Figure 2.5D, left), which was not the case in charcoal stripped media (Figure 2.5D, right). In addition, in SCN2.2 cells Per2-luciferase expression increased in cells transfected with PRB in absence of progesterone, suggesting this receptor might acquire constitutive activity in this cell line (Figure 2.5D). In the arcuate nucleus kisspeptin cell line (KTAR), progesterone enhanced Per2-lucefase expression through PRA in charcoal stripped buffer (Figure 2.5E, right), but had no effect in heat-inactivated FBS (Figure 2.5E, left).

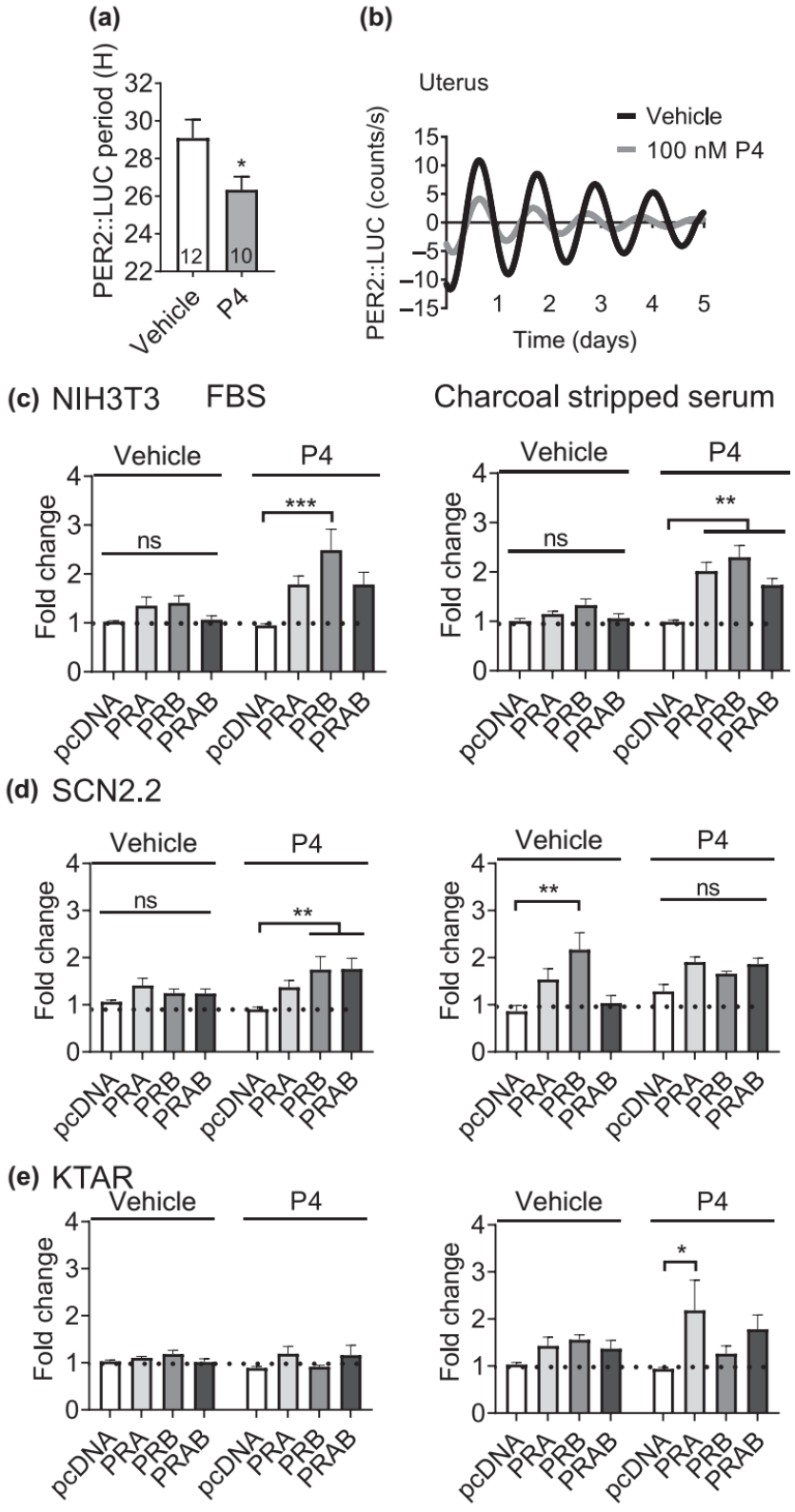

Figure 2.5. Progesterone regulates Per2-luciferase expression. (A) Histogram and (B) example trace of PER2::LUC period in the GD 18-19 uterus in response to progesterone (P4 50-

Figure 2.5. (cont'd)

100 nM) or vehicle control. (C-E) Transient transfections of NIH3T3 (mouse fibroblasts), SCN2.2 (rat SCN cells), and KTAR (mouse arcuate nucleus kisspeptin neurons) with Per2-luciferase, PRA, PRB or empty vector (pcDNA), cultured in in heat inactive heat inactivated FBS (FBS, left side) or charcoal stripped serum (right side). The capacity of progesterone (100 nM) or vehicle to drive Per2-luciferase expression was evaluated. Data is expressed as fold change as compared to control (pcDNA, vehicle). N=3-6 in duplicate. Statistical analysis by two-way ANOVA, followed by a Tukey post hoc. *, $p<0.05$; **, $p<.01$; ***, $p<.001$, ns: non-significant.

DISCUSSION

The precise timing of hormone release and downstream signaling is central to optimal functioning of the reproductive axis[157,158]. The SCN, pituitary, ovary, and uterus are all important components of female reproductive function, where each of these tissues exhibit circadian rhythms which are necessary for female fertility, including, but not limited to, ovulation [159,160] and embryo implantation[161–163]. Measures of circadian-alignment between reproductive tissues can be obtained using the validated circadian reporter mouse, PER2::LUC, PCR, or western blot studies. Such experiments have determined that phase of reproductive tissues changes throughout the estrous cycle[164,165]. During the estrous cycle, the changes in circadian rhythms and tissue phase, are in part driven by steroid hormone signaling, including progesterone[164,166], a central hormone in estrous cycling and pregnancy[167–169]. To further these studies, we assessed PER2::LUC period and phase relationships between the SCN, pituitary, ovary, and uterus during the estrous cycle and GD 14-19. Throughout all stages of the estrous cycle, the uterus and pituitary displayed different phases, ~10-12h apart, of peak timing in PER2::LUC expression. Interestingly, the SCN exhibited phase relationships during proestrus that were different from estrus or DI/II, which suggests a possible role of progesterone on the phase of the SCN, due to the peak of progesterone in proestrus, the estrous stage preceding estrus[157]. Specifically, during proestrus,

the SCN exhibited a similar PER2::LUC peak to the uterus and ovary. During both estrus and DI/II, the SCN was in phase with the pituitary and ovary, while the uterine PER2::LUC peak occurred earlier in the day than the SCN and pituitary. The fact that the SCN displays different phase relationships within estrous cycle stages supports its sensitivity to estrogen and/or progesterone, a mechanism supported in the work presented here, where we found progesterone can regulate Per2-luciferase expression *in vitro* in SCN cells. However, more work, including studies directly examining hormone application to tissue explants, is needed to further understand the impact of estrogen and progesterone on the circadian timing of these tissues. In pregnancy, progesterone and estrogen levels also change dramatically, and, as such, these hormones could also change circadian rhythms throughout the reproductive axis at this time of life. Indeed, we found that progesterone can shorten PER2::LUC period in the *ex vivo* uterus during late gestation. Further, during late gestation (GD 14-15, GD 16-17, and GD 18-19), we observed significant differences between the phases of reproductive tissues at each studied timepoint. Perhaps the most striking changes involve the relationships surrounding the pituitary. During both GD 14-15 and GD 16-17, the pituitary is in phase with the SCN, however, during GD 18-19, the pituitary exhibits an approximate 13 h delay following SCN peak phase. It is possible that these different relationships could be occurring in preparation for parturition, potentially driven by the hormonal changes involved in the transition to labor, including changes in oxytocin release, however more work is necessary to investigate this hypothesis. It is important to note that while we examined phase relationships within each stage of estrous and late pregnancy, we did not perform any statistical analysis of the phase relationships of individual tissues between stages of estrous and pregnancy. We chose not to run such statistical tests, as doing so would have greatly reduced our statistical power, given the necessary additional p-value corrections required to examine the tissue phase across the six time points. Nonetheless, given the dramatic changes in phase relationships within each stage of estrous cycle and during late pregnancy, we believe these adaptations reflect upon a combined effect of changes in hormone release and tissue sensitivity.

This hypothesis is supported by our finding that progesterone, a central sex steroid released from the corpus luteum after ovulation, increases Per2-luciferase expression in SCN and kisspeptin cells *in vitro*, and shortens PER2::LUC period in uterine tissue in late gestation. Others have explored similar ideas and demonstrated that individual changes in tissue phase occur between proestrus and diestrus, and that such circadian changes can be regulated by sex steroids and gonadotropins[164,170–172]. Examining the contribution of hormones involved in reproductive function and metabolism in adapting these relationships through the estrous cycle and pregnancy will be of interest.

With the multitude of hormonal and physiological changes occurring during late pregnancy, it is no surprise that behavioral activity patterns are altered during this time period. Others have indicated a decrease in locomotor activity during pregnancy in a number of species, including humans[94], non-human primates[173], and rodents[94,174–176]. The work presented here confirms this decrease in locomotor activity during pregnancy and suggests that this decline in activity occurs independently from litter size and may be only modestly caused by weight gain. Importantly, others have found that pseudopregnancy, which is associated with increased progesterone[177], causes decreased locomotor activity[175]. This suggests that a hormonal mechanism, and not metabolic changes or fetal signaling, is a plausible candidate driving the decrease in activity observed in pregnancy. In addition to decreases in locomotor activity, the onset timing of locomotor activity is altered during pregnancy[94,176]. Both our study and work by Martin-Fairey *et al* (2019) observed a change in activity onset time during mid-pregnancy; however, their results differ from ours in direction, where we observed a significant delay in onset of wheel running activity, while they observed an advanced onset. These differences could be attributed to several factors, including mouse strain, which has recently been shown to influence circadian wheel running activity between C57BL6/N and C57BL6/J males under constant light[178], as well as differences in locomotor activity analysis (5-min bins in our work versus 6-min bins), and/or rodent housing, where we maintained males within the behavioral chamber where the

females were housed throughout the experiment. Even given these differences, it is evident that circadian locomotor rhythms are highly influenced by pregnancy. As several aspects of circadian rhythms, including period, timing onset, and length of activity combine to produce specific rhythmic behavior patterns, it is important to consider how circadian variables influence each other. One such relationship is an established correlation between increased locomotor activity with advanced activity onset, whereas reduced locomotor activity delayed activity onset in constant conditions[179]. This is supported by our findings, where pregnancy dramatically decreased overall locomotor activity and delayed activity onset. To further our understanding of the underlying mechanisms driving the changes in onset timing and overall locomotor activity during pregnancy, we focused on the known role of the SCN in regulating wheel running behaviors[180–182]. Using *ex vivo* SCN explants, we found that PER2::LUC period was significant shortened during two timepoints during late gestation, as compared to estrus. However, this change in PER2::LUC period did not correlate with activity onset, suggesting the SCN is not a strong driver of this behavioral change. That said, light can mask the effects of SCN function on locomotor activity [183], and, as such, future studies done in constant darkness are required to understand if the changes in locomotor activity are driven by the SCN. A second limitation of our study is the caveat induced by evaluating locomotor activity using running wheels. Although wheel running is a standard measure of circadian locomotor activity, it does possess limitations, such as its rewarding properties and the potential difficulty for a late-pregnant mouse to climb onto the elevated wheel, due to the significant weight gain and change in body proportions. Thus, it is possible that wheel running decreases, but overall activity may not. To determine if this is the case, in house activity could be evaluated.

Aside from the SCN's role in driving locomotor activity, recent work has implicated kisspeptin neurons from the arcuate nucleus in modulating behavioral rhythms in addition to the timing of food intake, sleep, and body temperature in female mice [151]. Given the considerable metabolic changes occurring in the mother during pregnancy to support the developing fetus[184]

and the strong ties to circadian rhythmicity and metabolic state[101,102], is likely that such metabolic changes play into the circadian time-keeping system. This made us examine how PER2::LUC rhythms in the arcuate nucleus adapted to pregnancy. Our data did not reveal changes to PER2::LUC period during late pregnancy, nor was there a positive correlation between PER2::LUC period in the arcuate nucleus and activity onset. Despite these negative results, to our knowledge, this is the first record of PER2::LUC rhythms evaluated in the arcuate nucleus, and shows this structure possess a molecular clock, which can easily be studied using the PER2::LUC reporter mouse.

In conclusion, this work describes both behavioral and tissue-specific changes in circadian rhythms that occur during the estrous cycle and pregnancy. Our findings suggest that progesterone is involved in coordinating late pregnancy circadian rhythm function in the SCN, arcuate nucleus, and uterus. These studies are a first step towards understanding how the circadian time-keeping system adapts during pregnancy and will be instrumental in elucidating the molecular pathways involved in pregnancy loss and pregnancy associated complications.

CHAPTER 3 – LOW MATERNAL BLOOD LEVELS OF THE MOLECULAR CLOCK GENES CLOCK AND CRY2 ARE ASSOCIATED WITH INCREASED RISK OF SPONTANEOUS PRETERM BIRTH

This chapter was adapted from the following previously published manuscript:

Zhou, G, **Duong, TV**, Kasten, EP and Hoffmann, HM. *Low maternal blood levels of the molecular clock genes CLOCK and CRY2 are Associated with Increased Risk of Spontaneous Preterm Birth.* Biology of Reproduction. 2022 Jun; 105(4), 827–836. PMID: 34142702, PMCID: PMC8511660

ABSTRACT

Studies have observed an association between maternal circadian rhythm disruption and preterm birth (PTB). However, the underlying molecular mechanisms and the potential of circadian clock genes to serve as predictors of PTB remain unexplored. We examined the associations of 10 core circadian transcripts in maternal blood with spontaneous PTB (sPTB) versus term births using a nested case-control study design. We used a public gene expression dataset (GSE59491), which was nested within the All Our Babies (AOB) study cohort in Canada. Maternal blood was sampled in trimesters 2-3 from women with sPTB (n=51) and term births (n=106) matched for 5 demographic variables. Among the tested genes, only *CLOCK* and *CRY2* transcripts in the 2nd trimester maternal blood were significantly lower in sPTB versus term (p=0.02~0.03, FDR<0.20). In addition, the change of *PER3* mRNA from trimesters 2 to 3 was significantly different between sPTB and term (decline in sPTB but no change in term, p=0.02, FDR<0.20). When *CLOCK* and *CRY2* were modeled together in 2nd trimester blood, the odds of being in the low level of both circadian gene transcripts was greater in sPTB vs term (OR=4.86, 95%CI=(1.75,13.51), p<0.01). Using GSVA and Pearson correlation, we identified 98 common pathways which were negatively or positively correlated with *CLOCK* and *CRY2* expression (all p<0.05, FDR<0.10). Among the top three identified pathways were amyotrophic lateral sclerosis, degradation of extracellular matrix and inwardly rectifying potassium channels. These three processes have previously been shown to be involved with neuron death, parturition, and uterine excitability during pregnancy, respectively.

INTRODUCTION

Preterm birth (PTB) is the leading cause of perinatal morbidity and mortality in the United States[185,186], accounting for more than 50% of long-term morbidity and 60-80% of perinatal mortality[187]. PTB is defined as birth occurring between weeks 20 and 37 of gestation. PTB is associated with an increased risk of severe developmental delays and lifelong medical problems[188]. About 15 million babies are born preterm each year in the world[185,186]. The extensive medical cost associated with PTB puts a tremendous financial burden on the families and healthcare system, with an estimated annual cost of approximately $26 billion in 2005 in the US[189] and from 2005 to 2016, the average cost of a preterm birth increased by 25%[190]. Spontaneous preterm birth (sPTB), including spontaneous preterm labor (sPTL) and preterm premature rupture of membranes (PPROM), accounts for two-thirds of all preterm births in the US[191,192]. About 95% of sPTB cases are intractable to current interventions, and few predictors exist to identify women at risk for PTB[193,194]. However, recent findings suggest that circadian rhythms play a role in sPTB etiologies.

Circadian rhythms are 24-hour oscillations in behavior and physiology. Circadian rhythms exist across all types of organisms from bacteria and plants to mammals, including primates and humans[195–199]. Within cells, circadian rhythms are driven by endogenous biological clocks. The cellular “clock” is formed of a complex set of transcription factors and transcriptional regulators, which to a great extent have been conserved across species[200]. The mammalian core molecular clock consists of the transcription factors Brain and Muscle ARNT-like protein 1 (ARNTL, BMAL1 or MOP3), Cryptochromes 1 and 2 (CRY1, CRY2), Circadian Locomotor Output Cycles Kaput (CLOCK) and Period genes (PER1, PER2, and PER3)[201]. BMAL1 and CLOCK dimerize and initiate the transcription of CRY1/CRY2/CRY3 and PER1/PER2, which in turn dimerize and inhibit their own transcription in a ~24-hour oscillation[202]. To regulate the 24-hour transcript-translational feedback loop, a large number of additional transcription factors, kinases and DNA regulatory enzymes participate in this large regulatory network to fine tune the transcriptional activity of the

molecular clock[202,203]. Studies in both animal models and humans have demonstrated that circadian rhythms are involved in maintaining female reproductive health[204–208] and pregnancy success[169,208–210]. In pregnant women, numerous observational studies have shown an association between maternal circadian rhythm disruption (e.g., shift work-related chrono disruption) and spontaneous abortion, miscarriage, and preterm birth[208,211–216]. However, to date, the underlying molecular mechanism and the potential of clock genes being biomarkers to predict/classify these adverse reproductive outcomes in humans are still unclear.

In this study, we examined the associations of 10 core circadian transcripts (*ARNTL*, *ARNTL2*, *CLOCK*, *CRY1*, *CRY2*, *NPAS2*, *PER1*, *PER2*, *PER3*, and *TIMELESS*) in maternal blood with sPTB vs. term births using a microarray gene expression dataset from a Canadian cohort (GSE59491) in the National Center for Biotechnology Information (NCBI) Gene Expression Omnibus (GEO) database. These core clock genes were selected based on their critical roles in circadian rhythms[217] and the detectability of their mRNAs in the available microarray data. We also analyzed the circadian genes-correlated and sPTB-associated biological pathways using the Gene Set Variation Analysis (GSVA), which has greater noise/dimension reduction and biological interpretability[218].

MATERIALS AND METHODS

Selection of Pregnant Women and Demographics

The samples were nested within the All Our Babies (AOB) study cohort, a community-based longitudinal pregnancy cohort (N=1878, May 2008 - December 2010) in Calgary, Alberta, Canada. The inclusion criteria included 18 years of age, gestation age <18 weeks at time of recruitment, and singleton pregnancy[219]. The pregnant women with multifetal pregnancy and pre-existing medical conditions including diabetes, high blood pressure, autoimmune disorders, kidney disease, cardiovascular disease or chronic infection were excluded[219].

Spontaneous PTB was defined as a delivery that occurred ⩾20 and <37 weeks of gestation including spontaneous preterm labor (sPTL) or preterm premature rupture of membranes (PPROM)[219]. Term birth was ⩾37 weeks' gestation[219]. Women who had PTB were confirmed by a manual review of the medical charts[219].

In the sPTB group, the included pregnant women consisted of 76.5% Caucasian with a mean maternal age of 31 years, a mean pre-pregnancy BMI of 25, 19.6% smoked during pregnancy, and 52.9% were nulliparous[219].

Description of Nested Case-Control Data

We used a nested case-control study design, in which we had 51 sPTB samples at 2nd trimester (17-23 weeks' gestation) and 47 sPTB samples at 3rd trimester (27-33 weeks' gestation) as well as 114 term samples from both trimesters. Spontaneous PTBs were matched to term births at ratios of 1:1 (n=2), 1:2 (n=135), and 1:3 (n=20) on five characteristics, i.e. maternal age (<35 years vs. ⩾35 years), pre-pregnancy body mass index (BMI) (<18.5, 18.5–24.9, 25–29.9, and ⩾30 kg/m2), race/ethnicity (Caucasian vs. non-Caucasian), smoking during pregnancy (yes vs. no), and parity (no previous birth vs. at least one previous birth). Eight women delivered at term without matched cases and were excluded. The final dataset was composed of 51 sPTBs for 2nd trimester (15 sPTLs and 36 preterm premature rupture of membranes), 47 sPTB for 3rd trimester (14 sPTLs and 33 preterm premature rupture of membranes) and matched 106 term births for both trimesters. Maternal blood total RNA from each pregnant woman in both trimesters 2 and 3 was extracted, respectively, and then hybridized to Affymetrix Human Gene 2.1 ST (Affymetrix, Santa Clara, CA) for microarray measurement[219]. The generated raw gene expression values were normalized using the Robust MultiArray Average (RMA) method with a log base 2 (log2) transformation (GSE59491)[219].

Bioinformatics and Statistical Analyses

Figure 3.1 summarizes the pipeline of our bioinformatics and statistical analyses. We retrieved 10 core circadian genes (*ARNTL, ARNTL2, CLOCK, CRY1, CRY2, NPAS2, PER1, PER2, PER3,* and *TIMELESS*) from the dataset GSE59491. The mRNA levels (log2-transformed) of all 10 core circadian genes in 2nd and 3rd trimester maternal blood were summarized as means with standard deviations (SDs). We examined the mean differences in gene mRNA levels between the sPTB and term groups by using a two-sample, two-tailed t-test. Probability values were adjusted for multiple comparisons using a false discovery rate of 20% (FDR = 0.20)[220]. To test if there were threshold associations between circadian gene mRNA levels and sPTB, we categorized mRNA values into two levels: ⩽median and >median. The level of >median for each circadian gene was set as reference. Odds ratios for the threshold associations of sPTB with the categorized circadian gene mRNA levels were calculated in binary logistic regression models.

Next, we compared the differences of the changes of 10 core clock genes' mRNA levels from the 2nd to 3rd trimester between sPTB and term births using t-tests. The corresponding false discovery rate (FDR) q values were calculated with the SAS proc multtest procedure to correct multiple comparisons. The cut-off values for statistical significance were set as $p<0.05$ and FDR $q<0.20$[220].

To examine if there was a combined effect of two significant circadian genes on the risk of sPTB, we combined the categorized two circadian gene mRNA levels into one three-level variable: Level 1 – both gene mRNA levels <median; Level 3 – both gene mRNA levels ⩾median; and Level 2 – all other combinations. The association between the combined two circadian genes variable (3 levels) and sPTB (yes/no) was assessed with a binary logistic regression model. The cv.glm function in the R boot package was used for conducting a 5-fold cross-validation to examine if the final model had a possible overfitting problem (Figure 3.1). Based on our previous method[221], the levels of the identified *CLOCK* and *CRY2* transcripts were linearly combined to

generate a continuous risk score. We assessed the performance of this risk score to classify sPTB vs. term births with the receiver operating characteristic (ROC) analysis. We applied leave-one-out validation to validate the final area under curve (AUC) curve of the risk score by using the SAS “predprobs=crossvalidate” option in the proc logistic procedure. Finally, we calculated the sensitivity, specificity, and the corresponding maximum Youden J index for the final AUC curve[222].

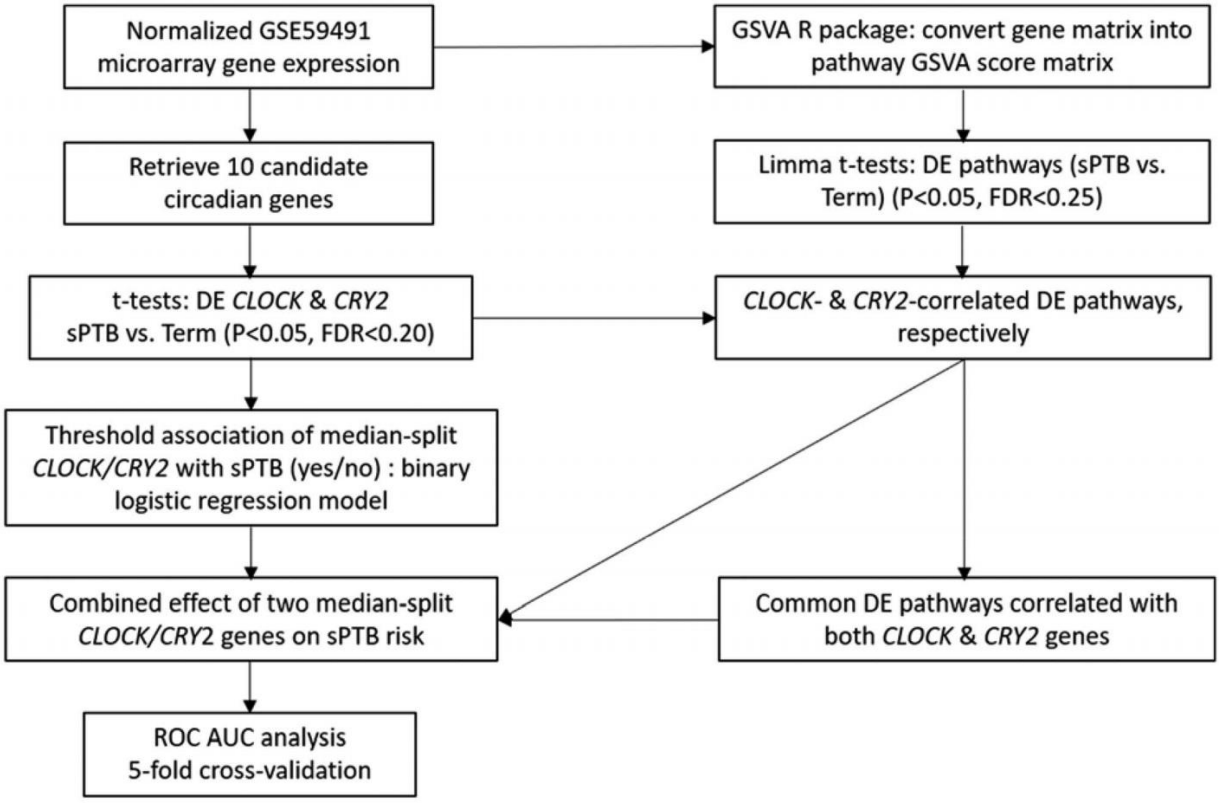

Figure 3.1. Flowchart summarizing the methodological steps of data analysis used in this study. Gene Set Variation Analysis (GSVA) was used to explore gene expression relationships between sPTB-clock gene changes and gene expression pathway changes. For details on statistical analysis see Bioinformatics and Statistical Analyses section. Abbreviations: DE, differentially expressed; ROC AUC, receiver operating characteristic area under the curve.

In order to explore the biological pathways that are involved in sPTB-clock gene relationship, the Gene Set Variation Analysis (GSVA), an unsupervised method to estimate the

variation of pathway activity over a sample population[223], was applied. The GSVA algorithm includes: the non-parametric kernel estimation of the cumulative density function (KCDF) for each gene expression profile; the rank-ordered expression-level statistic for each sample; and the calculation of the Kolmogorov-Smirnov-like rank statistic (i.e., GSVA enrichment score) for each gene set and each sample[223]. Compared to the classical gene set enrichment analysis (GSEA)[224], the GSVA method increases the statistical power to detect subtle changes of pathway activity over a sample population[223]. As shown in Figure 3.1, the cleaned and normalized microarray gene expression matrix (GSE59491) was converted into the sample-wise GSVA score matrix by using the pathway sub-collection - c2.cp.v7.1.symbols.gmt in the Molecular Signatures Database (MSigDB). A moderated t-statistic in limma R package[225] was applied to identify differentially expressed pathways between sPTB and term births (i.e., sPTB-associated pathways) with the cut-offs of $p < 0.05$ and Benjamini and Hochberg adjusted $p < 0.25$[226] (Figure 3.1). The Pearson Correlation statistic was used to examine the correlations of the identified DE clock gene mRNA levels with the sPTB-associated pathways ($p < 0.05$ and Benjamini and Hochberg adjusted $p < 0.10$)[227] (Figure 3.1). The subset of the pathways associated with both sPTB and clock genes was referred to as circadian gene-correlated sPTB-associated pathways. Finally, we overlapped the pools of sPTB-associated pathways correlated with individual circadian genes to get common up- or down-regulated pathways in sPTB that were shared by circadian genes (Figure 3.1).

All data management and statistical analyses were performed with SAS v9.4 (SAS Institute, Cary, North Carolina) and R (R Development Core Team).

According to the IRB guidelines and the HIPPA Privacy Rule, the analysis of de-identified, publicly available data does not constitute human subjects research as defined at 45 CFR 46.102 and thus, the present study does not require IRB review.

RESULTS

CLOCK and CRY2 are differentially expressed in maternal blood between sPTB and term births

Disrupted molecular clock function in transgenic mouse models has consistently been associated with poor pregnancy outcomes[228–233], and disrupted circadian rhythms, through mis-timed daily light exposure, such as during shift work, increases the risk of mis-timed birth[208], indicating that molecular clock function is important in pregnancy. To explore if changes in clock gene mRNA levels in maternal blood could predict sPTB, we analyzed transcript levels of the core circadian clock genes *ARNTL, ARNTL2, CLOCK, CRY1, CRY2, NPAS2, PER1, PER2, PER3,* and *TIMELESS* in maternal blood in women with sPTB and term birth. As shown in Tables 3.1 and 3.2, out of 10 core circadian gene transcripts measured in 2nd trimester maternal blood, *CLOCK* and *CRY2* were differentially expressed between sPTB and term births, where the means of *CLOCK* and *CRY2* transcripts were lower in sPTB than in term (Term birth mRNA expression mean±SD: *CLOCK* [7.58 ± 0.17] and *CRY2* [7.58 ± 0.12] versus mRNA levels in sPTB: *CLOCK* [7.51 ± 0.17] and *CRY2* [7.53 ± 0.13]; t-statistic: p=0.02~0.03 and FDR=0.15). It should be noted, however, that despite the statistical significance, the mean values of *CLOCK* and *CRY2 mRNA* expression between term and sPTB are numerically close. In contrast, the mean differences of all other studied genes were not statistically significant between the two groups (Table 3.1, p>0.05 and FDR>0.20). None of the circadian gene transcripts in 3rd trimester maternal blood were significantly associated with sPTB (p>0.05 and FDR>0.20) (Table 3.1).

Table 3.1. Descriptive statistics of 10 candidate circadian genes' expression levels in the 2nd and 3rd trimester maternal blood (sPTB vs. term).

	Term		sPTB			
Gene	**n**	**Mean[a] (SD)**	**n**	**Mean (SD)**	**p[b]**	**FDR[c]**
Trimester 2:						
ARNTL	106	9.25 (0.20)	51	9.26 (0.22)	0.6959	0.8699
ARNTL2	106	3.39 (0.20)	51	3.42 (0.20)	0.3417	0.5695
CLOCK	106	7.58 (0.17)	51	7.51 (0.17)	**0.0230**	**0.1500**
CRY1	106	5.98 (0.23)	51	5.97 (0.22)	0.8375	0.9306
CRY2	106	7.58 (0.12)	51	7.53 (0.13)	**0.0300**	**0.1500**
NPAS2	106	5.78 (0.41)	51	5.66 (0.35)	0.0789	0.2630
PER1	106	6.60 (0.25)	51	6.60 (0.28)	0.9457	0.9457
PER2	106	6.33 (0.17)	51	6.32 (0.20)	0.6333	0.8699
PER3	106	5.54 (0.27)	51	5.47 (0.26)	0.1343	0.3358
	106	4.61 (0.37)	51	4.54 (0.35)	0.2321	0.4642
TIMELESS						
Trimester 3:						
ARNTL	106	9.24 (0.18)	47	9.21 (0.22)	0.2689	0.3830
ARNTL2	106	3.42 (0.18)	47	3.45 (0.19)	0.3064	0.3830
CLOCK	106	7.53 (0.17)	47	7.46 (0.19)	0.0467	0.2335
CRY1	106	5.98 (0.19)	47	5.93 (0.20)	0.2275	0.3830
CRY2	106	7.55 (0.16)	47	7.51 (0.17)	0.1006	0.3353

Table 3.1. (cont'd)

NPAS2	106	5.79 (0.46)	47	5.61 (0.41)	0.0288	0.2335
PER1	106	6.62 (0.27)	47	6.68 (0.31)	0.2307	0.3830
PER2	106	6.30 (0.19)	47	6.34 (0.23)	0.2241	0.3830
PER3	106	5.52 (0.25)	47	5.55 (0.24)	0.6015	0.6683
	106	4.62 (0.33)	47	4.62 (0.34)	0.9394	0.9394
TIMELESS						

[a]Mean of gene expression values, expressed as normalized log2 (RMA signal intensity), where RMA robust multiarray average

[b]Two sample t test, $\alpha < 0.05$ as significant, two-tailed

[c]FDR values were calculated with the fdrtool package in R to correct comparisons.

Bold values denote statistical significance ($p < 0.05$ and FDR < 0.20)

Table 3.2. Associations of sPTB with the categorized mRNA levels of circadian genes (median split) in 2nd trimester maternal blood using logistic regressions.

	N (%)	Term, n (%)	sPTB, n (%)	$OR_{sPTB\ vs.\ term}$ (95% CI)	p	FDR
ARNTL						
≤median	78 (100.0)	53 (68.0)	25 (32.0)	0.96 (0.49, 1.88)	0.9084	0.9084
>median	79 (100.0)	53 (67.1)	26 (32.9)	Ref.		
ARNTL2						
≤median	78 (100.0)	54 (69.2)	24 (30.8)	0.86 (0.44, 1.67)	0.6486	0.8108

Table 3.2. (cont'd)

>median	79 (100.0)	52 (65.8)	27 (34.2)	Ref.		
CLOCK						
≤median	78 (100.0)	46 (59.0)	32 (41.0)	2.20 (1.11, 4.36)	**0.0244**	**0.1220**
>median	79 (100.0)	60 (76.0)	19 (24.0)	Ref.		
CRY1						
≤median	78 (100.0)	53 (68.0)	25 (32.0)	1.04 (0.53, 2.03)	0.9084	0.9084
>median	79 (100.0)	53 (67.1)	26 (32.9)	Ref.		
CRY2						
≤median	78 (100.0)	46 (59.0)	32 (41.0)	2.20 (1.11, 4.36)	**0.0244**	**0.1220**
>median	79 (100.0)	60 (76.0)	19 (24.0)	Ref.		
NPAS2						
≤median	78 (100.0)	50 (64.1)	28 (36.9)	1.36 (0.70, 2.67)	0.3648	0.7296
>median	79 (100.0)	56 (70.9)	23 (29.1)	Ref.		
PER1						

Table 3.2. (cont'd)

≤median	78 (100.0)	51 (65.4)	27 (34.6)	1.21 (0.62, 2.37)	0.5712	0.8108
>median	79 (100.0)	55 (69.6)	24 (30.4)	Ref.		
PER2						
≤median	78 (100.0)	51 (65.4)	27 (34.6)	1.21 (0.62, 2.37)	0.5712	0.8108
>median	79 (100.0)	55 (69.6)	24 (30.4)	Ref.		
PER3						
≤median	78 (100.0)	48 (61.5)	30 (38.5)	1.73 (0.88, 3.39)	0.1136	0.2840
>median	79 (100.0)	58 (73.1)	21 (26.6)	Ref.		
TIMELESS						
≤median	78 (100.0)	48 (61.5)	30 (38.5)	1.73 (0.88, 3.39)	0.1136	0.2840
>median	79 (100.0)	58 (73.1)	21 (26.6)	Ref.		

Bold values denote statistical significance ($p < 0.05$ and FDR < 0.20)

'Ref.' = 'reference'.

Lower transcript levels of CLOCK or CRY2 in the 2nd trimester maternal blood increased the risk of sPTB

To assess the threshold association between mRNA levels of each core circadian gene with sPTB, we divided each core circadian gene mRNA into two levels (median-split) (2-quantile) and determined the odds ratio of sPTB vs term births in each quantile. In the 2nd trimester maternal blood, odds of being in the lower quantile of both *CLOCK* and *CRY2* genes was greater in sPTB vs. term births than that of being in the higher quantile (odds-ratio (OR) (95% CI)= 2.20 (1.11, 4.36), p=0.02, FDR=0.12) (Table 3.2). All other studied genes had no threshold associations with the risk of sPTB (p>0.05 and FDR>0.20) (Table 3.2). In the 3rd trimester maternal blood, none of the 10 circadian genes studied had threshold associations with sPTB (p>0.05 and FDR>0.02) (Table S1: https://academic.oup.com/biolreprod/article/105/4/827/6302545#supplementary-data).

Specific decline of PER3 transcript from 2nd to 3rd trimester in sPTB

Table 3.3 demonstrated that the change in *PER3* mRNA levels from the 2nd to 3rd trimester was significantly different between sPTB and term births (p = 0.0153 and FDR q=0.1530). The *PER*3 mRNA levels had a slight increase over time ($Delta_{(T2-T3)}$=0.0182, SD=0.2803, Table 3.3) without significance in term (p=0.5063, data not shown), but a significant decline in sPTB from trimesters 2 to 3 ($Delta_{(T2-T3)}$=–0.0979, SD=0.2446, Table 3.3) (p=0.0086, data not shown).

Table 3.3. **Comparisons of the changes of 10 clock genes' mRNA levels across two different trimesters between sPTB and term.** N = number of samples.

	Mean Difference$_{(T2-T3)}$[a] in Term		Mean Difference$_{(T2-T3)}$ in sPTB	

Table 3.3. (cont'd)

Gene Name	N	$Delta_{(T2-T3)}$ (SD)	N	$Delta_{(T2-T3)}$ (SD)	$t_{term-sPTB}$	p*	FDR*
ARNTL	106	0.0013 (0.1551)	47	0.0565 (0.1764)	-1.95	0.0536	0.2680
ARNTL2	106	-0.0307 (0.2521)	47	-0.0323 (0.2586)	0.04	0.9717	0.9717
CLOCK	106	0.0497 (0.1851)	47	0.0372 (0.1968)	1.13	0.5994	0.7493
CRY1	106	-0.0001 (0.2504)	47	0.0262 (0.2504)	-0.60	0.5495	0.7493
CRY2	106	0.0274 (0.1736)	47	0.0209 (0.956)	0.20	0.8391	0.9323
NPAS2	106	-0.0049 (0.3946)	47	0.0804 (0.3083)	-1.31	0.1910	0.5372
PER1	106	-0.0272 (0.3104)	47	-0.0914 (0.3816)	1.10	0.2738	0.5372
PER2	106	0.0348 (0.2197)	47	-0.0152 (0.2508)	1.24	0.2159	0.5372
PER3	106	0.0182 (0.2803)	47	-0.0979 (0.2446)	2.45	**0.0153**	**0.1530**
TIMELESS	106	-0.0129 (0.4546)	47	-0.0922 (0.4573)	0.99	0.3223	0.5372

Increased risk of sPTB in 2nd trimester maternal blood samples with low mRNA levels of both CLOCK and CRY2

To evaluate a combined effect of the two significant circadian genes (median split) on the risk of sPTB, we modeled the two categorized *CLOCK* and *CRY2* genes together. The results demonstrated that the odds of being in the high risk level of *two* circadian genes (i.e., lower quantile for both *CLOCK* and *CRY2*) was greater in sPTB vs term (reference: low risk level, i.e., higher quantile for both *CLOCK* and *CRY2*) (OR=4.86 (1.75, 13.51), p=0.0025) while the medium risk level (i.e., all other combinations of two genes) had a non-significant OR (OR=2.24 (0.87, 5.78), p=0.0946) (Table 3.4). Five-fold cross-validation analysis indicated that the above model (combining two clock gene transcripts into a single variable) had no significant overfitting; the 5-fold cross-validation estimation error, delta1, was 0.2097, which was very close to the bias-corrected estimation error (delta2=0.2092) (data not shown). The performance of the linearly combined transcripts to classify sPTB vs. term births was assessed with the ROC analysis (Figure 3.2). The resulted area under the ROC curve (AUC) was 0.66 (95% CI: 0.57 ~ 0.75, p=0.0005, reference: by chance) with a sensitivity for sPTB of 76% and a specificity of 51% (data not shown). The leave-one-out validation demonstrated that the cross-validated AUC was 0.64 (95% CI: 0.54-0.73), which was very close to the non-validated AUC (Figure 3.2).

Table 3.4. Combined effects of *CLOCK* and *CRY2* (median splits) on sPTB in 2nd trimester maternal blood (n = 51 sPTB, n = 106 term) with logistic regression model.

	N (%)	Term, n (%)	sPTB, n (%)	$OR_{sPTB\ vs.\ term}$ (95% CI)	p
High risk level*	40 (100.0)	20 (50.0)	20 (50.0)	4.86 (1.75, 13.51)	**0.0025**
Middle risk level***	76 (100.0)	52 (68.4)	24 (31.6)	2.24 (0.87, 5.78)	0.0946
Low risk level**	41 (100.0)	34 (32.1)	7 (13.7)	Ref.	

* Both CLOCK and CRY2 transcripts ≤ median

Table 3.4. (cont'd)

** Both CLOCK and CRY2 transcripts > median

*** All other combinations

Bold values denote statistical significance ($p < 0.05$)

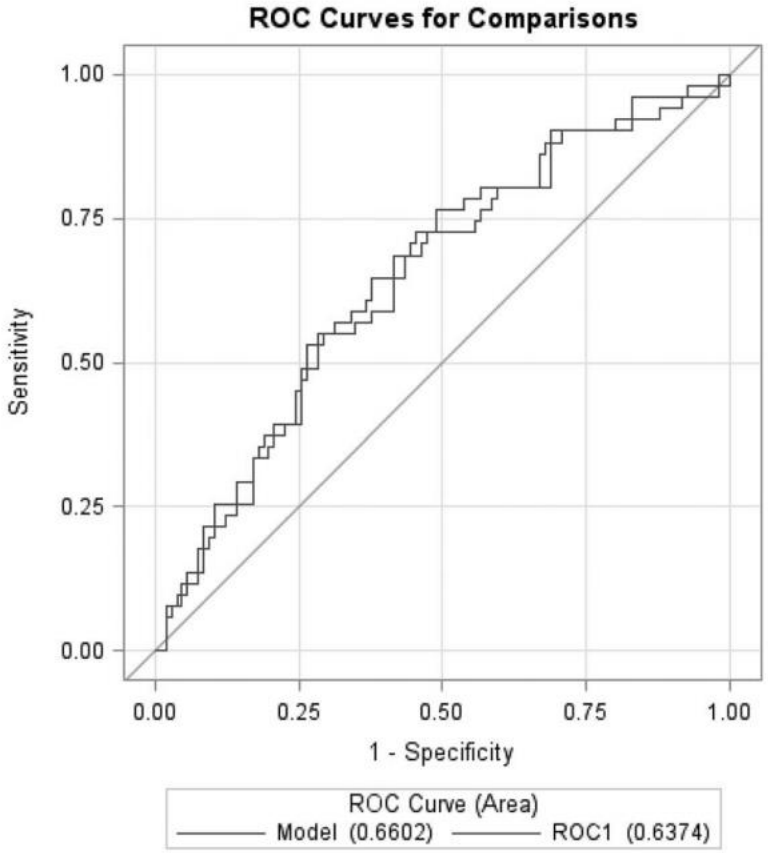

Figure 3.2. Visualization of the ROC analysis with the linearly combined CLOCK and CRY2 transcripts. The blue line represents the nonvalidated ROC curve (AUC=0.66, 95% CI=0.57–0.75, P = 0.0005, ref.: by chance) for the combined transcripts. The straight line represents the cross-validated ROC curve (AUC=0.64, 95% CI=0.54–0.73) for the combined transcripts.

sPTB-associated biological pathways commonly correlated with both CLOCK and CRY2 gene transcripts

Both CLOCK and CRY2 are transcriptional regulators[200,201], and changes in their expression would be expected to impact target gene expression patterns as well as molecular clock function. To determine if *CLOCK* and *CRY2* associated pathways were impacted in our term and sPTB groups, we used the GSVA and limma R packages. We identified 315 out of 1707 pathways significantly different between sPTB and term births, among which 199 and 116 pathways were down- and up-regulated, respectively ($p<0.05$ and adjusted $p<0.25$) (Table S2: https://academic.oup.com/biolreprod/article/105/4/827/6302545#supplementary-data). To further explore the sPTB-associated pathways that were commonly correlated with both circadian genes (*CLOCK* and *CRY2*), we used Pearson Correlation statistic to examine *CLOCK*/*CRY2* correlated sPTB-associated pathways. We found that 296 of 315 associated sPTB-pathways were significantly correlated with *CLOCK*, whereas 100 out of 315 were significantly correlated with *CRY2* (absolute correlation coefficient r = (0.1789~0.6470), $p\leq0.02$, and FDR≤0.03 for *CLOCK* gene; r = (0.1730~0.2952), $p\leq0.03$, and FDR<0.10 for *CRY2* gene) (Table S3: https://academic.oup.com/biolreprod/article/105/4/827/6302545#supplementary-data). The combination of both *CLOCK* and *CRY2* correlated sPTB-associated pathways resulted in 98 common pathways (30 up- and 68 down-regulated in sPTB) negatively or positively correlated with the two circadian genes (all $p<0.05$ and FDR<0.10) (Tables S4 and S5: https://academic.oup.com/biolreprod/article/105/4/827/6302545#supplementary-data). Based on the absolute correlation coefficient values of *CLOCK* in sPTB, the top three correlated and up-regulated pathways are AMYOTROPHIC LATERAL SCLEROSIS ALS, DEGRADATION OF THE EXTRACELLULAR MATRIX, and INWARDLY RECTIFYING K CHANNELS (r = –0.56 ~ –0.53) (Table 3.5) and the top three correlated and down-regulated pathways include TRNA PROCESSING, TRNA PROCESSING IN THE NUCLEUS, and TRANSPORT OF MATURE TRANSCRIPT TO CYTOPLASM (r = 0.58 ~ 0.65) (Table 3.5).

Table 3.5. Top 3 increased and decreased pathways in sPTB which were negatively and positively correlated with both *CLOCK* and *CRY2* gene mRNA levels in 2nd trimester maternal blood, respectively (all p<0.05 and FDR<0.10).

Pathway Name	Correlation Coefficient	
	CLOCK	***CRY2***
Increased Pathways in sPTB:		
KEGG_AMYOTROPHIC_LATERAL_SCLEROSIS_ALS	-0.56	-0.17
REACTOME_DEGRADATION_OF_THE_EXTRACELLULAR_MATRIX	-0.54	-0.21
REACTOME_INWARDLY_RECTIFYING_K_CHANNELS	-0.53	-0.22
Decreased Pathways in sPTB:		
REACTOME_TRNA_PROCESSING	0.65	0.18
REACTOME_TRNA_PROCESSING_IN_THE_NUCLEUS	0.62	0.20
REACTOME_TRANSPORT_OF_MATURE_TRANSCRIPT_TO_CYTOPLASM	0.58	0.18

DISCUSSION

Numerous studies in rodents have demonstrated the role of circadian rhythms, through the action of clock genes in pregnancy success[228–233]. In humans, although observational studies documented an association between maternal circadian rhythm disruption and preterm birth[213,234,235] and polymorphisms of *CLOCK* and *PER3* have been associated with adverse pregnancy outcome[236,237]; to date the systematic evaluation of core circadian gene transcripts in maternal blood in relation to sPTB has not yet been reported. Using a publicly available data set, we here show that reduced levels of both *CLOCK* and *CRY2* mRNAs in 2nd trimester maternal blood increased the odds ratio of sPTB about 5-fold, indicating that low mRNA levels of *CLOCK* and *CRY2* genes in maternal blood may be useful in detecting increased risk of sPTB as early as the 2nd trimester.

Limits of study

It is important to note the limits of the current study. The data set analyzed is a publicly available data set (NCBI GEO GSE59491), and we do not have information about time of day or time of year the samples were collected. In addition, our findings couldn't be validated in a second cohort as only one microarray maternal blood gene expression profiling dataset regarding sPTB (GSE59491) in the NCBI GEO database is currently available. The origins of maternal clock gene transcripts were unknown. In addition, the performance of the combined *CLOCK/CRY2* transcripts to classify sPTB vs. term births was modest, probably due to the relatively small number of sPTB cases (n = 51) and the heterogeneity of sPTB. Other biomarkers or clinical predictors may need to be included in the model for the improvement. These are all important caveats, as the body's circadian time keeping system adapts to the season of the year, and the key characteristic of molecular clock genes is their circadian expression. That said, we believe our findings remain relevant, and that low levels of *CLOCK* and *CRY2* mRNAs in maternal blood are novel biomarkers that can easily be screened for in 2nd trimester maternal blood. Indeed, we specifically found that a reduction in *CLOCK* and *CRY2* mRNA levels is associated with sPTB, whereas none of the other 8 molecular clock gene mRNA levels were associated with sPTB in 2nd trimester maternal blood. This indicates that independent of time of day, reduced *CLOCK* and *CRY2* transcript levels can predict, with a 5-fold increased chance, women at risk for sPTB during the 2nd trimester of pregnancy. To validate these genes as biomarkers for sPTB it will be important to repeat the study controlling for time of day of sample collection and season of year.

Disrupted molecular clock function is associated with increased risk of sPTB

Over the last decade, numerous studies have found an association between changed molecular clock gene expression and adverse pregnancy outcomes. This is particularly true for CLOCK. Lower CLOCK gene expression at both mRNA and protein levels was detected in fetal tissue and placental chorionic villi of spontaneous abortion (miscarriage), whose etiologies may

overlap with that of preterm birth[238–240], as compared to those of induced abortion in a Chinese population[241]. Using a publicly available maternal blood mRNA data set, we found that the odds ratio of either low *CLOCK* or *CRY2* transcript levels (⩽median) in the 2nd trimester maternal blood had a 2-fold increase in sPTB group compared to that in the term birth group. When both *CLOCK* and *CRY2* levels were low, the risk of sPTB was almost ~5-fold higher. To our knowledge, our results show for the first time that low mRNA levels of *CLOCK* and *CRY2* transcripts in maternal blood in the 2nd trimester of pregnancy is a potential new biomarker allowing to predict or classify the risk of sPTB in mid-pregnancy. Importantly, the additional 8 core circadian genes we analyzed neither were differentially expressed in maternal blood between sPTB and term births in the 2nd or 3rd trimester of pregnancy nor were they significantly associated with an increased risk of sPTB, making *CLOCK* and *CRY2* promising biomarkers allowing predicting women at increased risk of sPTB as early as the 2nd trimester of pregnancy. We are not the first to report that circadian rhythm changes in mid pregnancy are a potential predictor of pregnancy outcomes. A small cohort study in pregnant women found that women who had preterm labor did not have increased uterine contractions during the night period in the late 2nd trimester/early 3rd trimester of pregnancy[234] whereas another study revealed that uterine contraction frequency was significantly greater in women who had preterm birth[242]. Such controversy may be related to the use of the different definitions for the outcome and/or the different measuring time of the participants. More work is required to further our understanding and classification of what is considered normal circadian rhythm function in pregnancy, and how changes in circadian function adapts throughout pregnancy.

PER3 mRNA change from trimesters 2 to 3 and sPTB risk

We also found that the change of *PER3* mRNA from trimesters 2 to 3 was significantly different between sPTB and term (decline in sPTB but no change in term). In humans, a PER3

single-nucleotide polymorphism (SNP) has been documented to be associated with PTB[237]. In mice, the variation of *Per3* transcript was evidenced to be causally associated with and also responsive to stress and alcohol[243]. Maternal stress during pregnancy has been evidenced to increase the risk of preterm birth in a case-control study[244]. In addition, studies also indicated that maternal stress may be involved in the regulation of parturition in different domestic animal species[245]. However, whether the dynamic change of *PER3* transcript across trimesters 2 and 3 in sPTB is related to progressive maternal stress during pregnancy and/or parturition is unknown. More rigorous studies are needed for further clarification.

CLOCK and CRY2 associated pathways and their potential role in sPTB

To further explore the molecular mechanism(s) underlying the relationship between the mRNA levels of *CLOCK* and *CRY2* genes with sPTB, we examined the pathways enriched by both circadian genes and sPTB. The results revealed 30 up- and 68 down-regulated pathways in sPTB. The top three *CLOCK/CRY2* correlated and up-regulated pathways in sPTB are Amyotrophic Lateral Sclerosis (ALS), Degradation of the Extracellular Matrix (ECM), and Inwardly Rectifying K Channels.

ALS is a pathway related to neuron death[246]. Circadian rhythm dysfunction has been documented to induce neuron death via neuroinflammation and oxidative stress[247]. Evidence also showed that the neuronal activity of cervix-related sensory neurons increases during pregnancy in mice and plays a role in cervical ripening and parturition[248]. It will be of interest in future studies to determine if there is a causative link between lower clock gene expression and increased ALS pathway activity in maternal blood in sPTB in regard to cervix-related sensory neuron death and premature cervical ripening.

A second pathway we found to be associated with *CLOCK* and *CRY2* involved the extracellular matrix (ECM), the non-cellular component in tissues that constantly undergoes a remodeling process[249,250]. ECM remodeling is essential for tissue morphogenesis and cell

differentiation[250,251]. Studies have demonstrated that the protein levels of amniotic fluid matrix metalloproteinase-2 (MMP-2) and MMP-9, two enzymes regulating ECM remodeling and degradation [252], were increased in preterm premature rupture of membranes[253,254]. Particular, studies indicate that ECM degradation and remodeling is required for parturition and its abnormal alteration may result in preterm birth[255]. However, the exact mechanism underlying the relationship between an increase in ECM pathways and lower clock gene expression and sPTB is unclear.

Inwardly rectifying K channels (Kir channels) are integral membrane proteins responsible for transporting potassium (K^+) with a greater tendency for K^+ uptake than K^+ export[256,257]. The Kir channels exist in a variety of cell types (e.g., cardiac myocytes, neurons, blood cells, epithelial cells, etc.)[258]. In rat glial cells, the increased Kir channels were associated with the arrest of the cell cycle[259,260]. In myometrial cells, the Kir channel 7.1 (Kir7.1) plays an important role in myometrium excitability and allows to maintain uterine quiescence throughout pregnancy in mice[261]. However, *in vitro* results in animal cells appears to be controversial with our findings, where we found that lower clock gene expression correlated with increased Kir7.1 pathway activity. This could be related to different species, tissues, sampling time, or pathway interaction that might cause a functional downregulation of Kir7.1, relieving Kir7.1-promoted relaxation of the myometrium. More rigorous studies are needed to further clarify these associations.

In contrast, the top three *CLOCK/CRY2* correlated and down-regulated pathways in sPTB that we found in the present study include tRNA Processing, tRNA Processing in the Nucleus, and Transport of Mature Transcript to Cytoplasm. These down-regulated pathways in sPTB are consistent with the findings in our previous study, in which several tRNA-related pathways (e.g., cytosolic tRNA aminoacylation, tRNA charging, tRNA aminoacylation, and aminoacyl-tRNA biosynthesis) or RNA metabolism pathway (including RNA intracellular transport) that correlated with two lncRNAs were significantly decreased in sPTB[262,263]. This consistency suggests that

these circadian clock genes-correlated and down-regulated pathways in sPTB may also be related to epigenetic regulation.

Conclusions

We here describe that low transcript levels of both *CLOCK* and *CRY2* genes in 2nd trimester maternal blood may be informative in predicting the increased risk of sPTB. The underlying mechanism might be partially linked to the abnormal circadian clock regulation of the pathways such as increased neuron death, abnormal tissue/organ morphogenesis, and cell cycle arrest/altered uterine excitability, as well as decreased RNA processing and RNA transport. Additional pregnancy cohorts' studies are needed to examine the robustness and generalizability of our findings

CHAPTER 4 – BMAL1 REGULATES SPONTANEOUS UTERINE CONTRACTIONS AND TIME OF DAY EFFICACY OF OXYTOCIN IN THE MOUSE IN LATE PREGNANCY

This chapter was adapted from the following manuscript:

Duong, TV, Zhou, G, Cherukuri, A and Hoffmann, HM. *Bmal1 regulates spontaneous uterine contractions and time of day efficacy of oxytocin in the mouse in late pregnancy.* Journal of the Endocrine Society. In revision.

ABSTRACT

Labor induction achieved by the oxytocin receptor agonist Pitocin has a modest efficacy leading to a higher than necessary C-section rate. To determine if time of day impacts the efficacy of oxytocin and to understand the role of circadian rhythms in myometrium function, we deleted the molecular clock gene Brain and muscle ARNTL-like 1 (*Bmal1*) in the mouse myometrium using the *Telokin*^{Cre} allele (cKO). To determine if BMAL1 regulated uterine contractions, we used a myograph to measure *ex vivo* uterine contractions every 6 h over a 24 h period at gestation day 18 (GD18). Although spontaneous uterine contractions in the GD18 control group did not significantly change depending on the time of day, the sensitivity of the uterus to oxytocin was higher during the mouse active phase (night) than during the rest phase (day). The uterus of GD18 cKO had a significant increase in spontaneous contractile force as compared to controls at 3 of the 6 studied time points. However, the cKO uterus was less sensitive to oxytocin. Interestingly, even though we found oxytocin receptor to be under transcriptional control of BMAL1, the reduced uterine sensitivity to oxytocin in the cKO was not driven by a down-regulation of OXTR. Together, our findings identify increased uterine contractions in cKO, and show that the daily changes in uterine sensitivity to oxytocin were not associated with oxytocin receptor protein expression. More work is needed to elucidate how time of day changes the efficacy of oxytocin to promote uterine contractions in late gestation.

INTRODUCTION

Induction of labor (IOL) is one of the most common clinical procedures in modern obstetrics and is recommended when mother's or fetus' health is at risk. IOL is defined as an initiation of uterine contractions by medical and/or surgical means before their spontaneous onset, with the purpose of accomplishing vaginal birth. The overall IOL rate in the United States has risen from 9.6% in 1990[264] to 29.4% in 2019[265]. Failed IOL can be defined as the inability to achieve the active phase of vaginal labor and occurs in about 20% of induced pregnancies[266]. IOL failure may be related to multiple maternal characteristics and conditions including nulliparity, gestational duration less than 41 weeks, maternal age higher than 30 years, preeclampsia and gestational diabetes[267]. Additionally, an IOL procedure may increase the risk of caesarean section (C-section)[268].

The oxytocin receptor (OXTR) synthetic ligand Pitocin is one of the most commonly used drugs for IOL in the US[269]. The predictors of successful response to oxytocin for IOL include lower body mass index, greater cervical dilation, parity or gestational age[270]. Oxytocin is a neuropeptide produced in the hypothalamus and acts on oxytocin receptors, which are highly expressed in the uterine smooth muscle, the myometrium, promoting uterine contractions and labor onset[271]. The effects of oxytocin on uterine contractility in labor can be regulated by local levels of oxytocin and oxytocinase (an enzyme that degrades oxytocin) as well as the number and availability of oxytocin receptors[271,272]. It is well established that the level of oxytocin receptor mRNA increases during pregnancy in the uterus, and the density of myometrial oxytocin receptors reaches a peak at the onset of labor[273]. In mammals, the timing of peak *Oxtr* expression is generally aligned with the start of the inactive phase of the day[9], suggesting this receptor might be under circadian control. Additionally, mice that do not produce oxytocin do not restrict birth to the inactive phase of the day, suggesting oxytocin contributes to the timing of labor onset and birth[274]. However, it is still unknown if the loss of the circadian timing of birth in oxytocin deficient mice is also associated with daily changes in OXTR. In fact, most mammalian species experience labor and give birth

during their inactive phase of the day[9]. It is thought that this timing of labor and birth provides increased protection of the mother and newborn from predators due to the occupancy of a burrow and/or the presence of herd members, thus creating an evolutionary pressure to optimize physiological functions to prime labor and birth to the time of day with the highest chance of survival of the mother and offspring[9]. This evolutionary pressure remains evident in humans, where spontaneous uterine contractions in the 3rd trimester of pregnancy peak at ~2000 h, followed by the peak in birth at ~0430 h[10]. Supporting this theory is the increase in myometrial contractions during the night in the 3rd trimester of pregnancy in non-human primates and humans[17,275]. This increase in nocturnal contractions correlates with the time of day of maximal uterine sensitivity to oxytocin, as shown by a small cohort study of late-pregnant *Rhesus* monkeys that found that oxytocin was more efficient at inducing uterine contractions when given at night (rest phase of the day for *Rhesus* monkeys) than during the day[18]. The increased sensitivity of the uterus to oxytocin during the rest phase of the day could be one mechanism to explain why the uterus exhibits a nocturnal increase in contractions and why most human natural births occur at night[16,17]. The current clinical practice of labor induction, however, does not take this nocturnal aspect of a daily change in uterine sensitivity to oxytocin into account, and the majority of labor inductions are scheduled in the morning or early afternoon for the convenience of hospital staffing[13]. We speculate this timing difference between the time of labor induction and the time of day of increased uterine sensitivity to oxytocin might be a contributing factor to the high rate of unsuccessful labor inductions.

To generate daily 24 h rhythms within tissues, nearly all nucleated cells have an autonomous circadian time-keeping mechanism, referred to as “the molecular clock”. The molecular clock is highly conserved across species, including humans and rodents, and has been extensively studied in the mouse. Deletion of clock genes in mice results in irregular or ablation of circadian rhythms at the cellular and behavioral levels[21] and is frequently associated with reduced fertility, increased loss of pregnancy, increased embryo resorption and mistimed or

unproductive labor[44–46,276]. It is well established that the core molecular clock gene Brain and muscle ARNTL-like 1 (*Bmal1*) is essential to generate circadian rhythms at the cellular and behavioral levels in mice[21]. Particularly, *Bmal1* knock-out females are infertile[45], and close to 35% of female mice with conditional deletion of *Bmal1* in the myometrium have mistimed labor onset[58], suggesting an important role of *Bmal1* in pregnancy and defining the time of labor onset and birth.

Given the roles of *Bmal1* and oxytocin in timing labor onset as well as the time-of-day effects of oxytocin on uterine contractility in non-human primates, we hypothesized that *Bmal1* in the myometrium drives daily changes in contractile function and sensitivity to oxytocin in pregnancy.

MATERIALS AND METHODS

Mouse breeding

All animal procedures were performed according to the protocols approved by the Animal Use Committee and the Institutional Animal Care of Michigan State University and conducted in accordance with the Guide for the Care and Use of Laboratory Animals (National Research Council, 2011). Mice were maintained on a light/dark cycle of 12 h light, 12 h dark (LD12:12), with lights ON (150-300 lux in the cage) at Zeitgeber Time 0 (ZT0) and lights OFF at ZT12. Mice had food and water ad libitum. All mice were from a C57BL/6 genetic background 8-14 weeks-of-age at the start of experiments and 10-24 weeks-of-age at time of euthanasia. *PER2::LUC* [Tg(Per2-luc)1Jt, JAX #006852] and *Bmal1*^{flox} [B6.129S4(Cg)-*Arntl*^{tm1Weit}/J, JAX #007668] were crossed with *Telokin*^{Cre} mice[58]. All *Telokin*^{Cre} positive mice were heterozygous for Cre. Genotyping primer sequences were as follows: Per2F: CAAAGGCACCTCCAACATG, Per2R: AAAGTATTTGCTGGTGTGACTTG;

Bmal1F1: CTGGAAGTAACTTTATCAAACTG, Bmal1F2: CTGACCAACTTGCTAACAATTA Bmal1R: CTCCTAACTTGGTTTTTGTCTGT; CreF: ACCTGAAGATGTTCGCGATTATCT, CreR:

ACCGTCAGTACGTGAGATATCTT. Mice with germline recombination were excluded from the study.

Timed mating

Two females and one male were co-housed at ZT10-11 and vaginal plug formation was checked the next day at ZT 3-4 with a clean pipet tip for each female mouse. On the day of vaginal plug identification, the female was separated from the male. The morning of vaginal plug identification was considered gestational day 1 (GD1). Pregnancy was confirmed by a significant increase in body weight, where a weight gain of >2 g from GD1 to GD10 was considered indicative of pregnancy[277]. Final gestational stage confirmation was done on day of tissue collection by assessing embryo development using Theiler Stage[278].

PER2::LUCIFERASE bioluminescence recording

GD18 females were euthanized by cervical dislocation at ZT3-4. Following euthanasia, the uterus was removed and placed in semi-frozen 1× Hank's buffered salt solution (HBSS, 14065-056, Gibco). Under a dissecting scope (Laxco, T40-Z33) the uterus was opened with scissors in the longitudinal direction and gently spread out to a sheet on a dissection dish. For samples with endometrium removed, the endometrium was then gently scraped from the myometrium with a scalpel. Using a ruler, ~ 2×2 mm^2 uterine explants were collected midway between the cervix and the ovary near the placental attachment. Tissue explants were placed onto a MiliCell membrane (MilliCell, PICM0RG50, MilliporeSigma). Full-thickness uterine explants were placed with the inside of the uterus (endometrium side) facing the MilliCell membrane. MilliCell membranes were placed in 35-mm culture dishes (Nunc, Thermo Fisher Scientific) containing 1.5 ml of 35.5°C recording medium [(Neurobasal, 1964475, Gibco) supplemented with 20 mM HEPES (pH 7.2), B27 supplement (2%; 12349-015, Gibco), 1 mM luciferin (luciferin sodium salt; 1-360242-200, Regis, Grove, IL), and antibiotics (8 U/ml penicillin, 0.2 mg/ml

streptomycin, 4 mM l-glutamine; Sigma-Aldrich)]. Dishes were sealed using vacuum grease and placed into a LumiCycle (Actimetrics) inside a light-tight 35.5°C, 5% CO_2, non-humidified environmental chamber. The bioluminescence signal was counted every 10 min for 1.11 min for 6 days and analyzed on days 1–6 of recording time. Data were normalized by subtraction of the 24 h running average from the raw data and then smoothed with a 1 h running average (Luminometer Analysis, Actimetrics) and analyzed blind to experimental group. The initial 12 h (day 0) data from the LumiCycle recording was not analyzed to allow the tissue to adapt to the culture conditions, and to achieve a stable PER2::LUCIFERASE (PER2::LUC) waveform. Incomplete data sets were excluded from analysis. This included data sets with missing data points, technical problems, or explants failing to show two distinguishable PER2::LUC peaks, which were deemed arrhythmic[279]. Tissues with *Bmal1* deleted are known to not present rhythmic PER2::LUC expression[280] and were included in our analysis regardless of their rhythmicity. PER2::LUC recordings were analyzed by the Luminometer Analysis software (Actimetrics) with LM fit (damped sin) as the mathematical model. PER2::LUC period was defined as the time difference in hours between two peaks. PER2::LUC amplitude was defined as the value of the second peak in the time window of analysis as given by the Luminometer Analysis software. PER2::LUC time of first peak was defined as the time of day of the first peak (h) in the time window of analysis as given by the Luminometer Analysis software.

Uterine contractions

GD18 females were euthanized by cervical dislocation at ZT3, 7, 11, 15, 19 and 23. The uterus was removed, cleaned of placentas and membranes, and dissected along the longitudinal axis into full-thickness uterine strips (endometrium + myometrium) of ~ 2x5 mm^2 in ice cold oxygenated physiological saline solution (PSS) [154 mM NaCl, 5.6 mM KCl, 1.2 mM $MgSO_4$, 10.2 mM HEPES, 2 mM $CaCl_2$ and 8 mM glucose]. The uterine strips were mounted in tissue organ baths (DMT Muscle Strip Myograph System- 820MS) containing 6 mL oxygenated PSS at

36.0±0.5^{o}C to mimic physiological conditions. Each strip was stretched to a final tension of 6 mN to obtain optimal contraction recordings in our settings (Table 4.1). Uterine strips were allowed to equilibrate for ~2 h until 15 min of spontaneous contractions (regular, frequent and equal amplitude, to visual inspection) occurred. The tissues were then treated with vehicle (Milli Q water, at 1/2000 dilution), 500 nM atosiban (A3480-10MG, Sigma Life Science) or 1 nM oxytocin (O3251-1000IU, Sigma Life Science). At the end of all recordings, uterine strips were washed 3x with 6 mL PSS, 10 min between washes, and then treated with 100 mM KCl. Treatment with 100 mM KCl was used to confirm uterine viability. Analysis of contractions was done in LabChart software (ADInstruments) by evaluating area under the curve (AUC), amplitude and frequency of contractions over a period of 10 min during baseline or drug application periods. To compare spontaneous contractions between different time points and between groups (control versus *Bmal1*$^{fl/fl}$*:Telokin*^{Cre}, referred to as cKO), AUC and amplitude of each uterine strip were normalized to the peak of contraction in response to 100 mM KCl. To compare oxytocin-induced contractions, AUC, amplitude and frequency of oxytocin-treated contractions were normalized to vehicle-treated contractions prior to oxytocin application, which will be elaborated more in the results section.

Table 4.1. Tension optimization for *ex vivo* uterine contraction measured on a myograph. Each uterine strip from a GD18 control mouse euthanized at ZT3 was stretched at an increment of 2mN. After each stretch, the tissue was treated with 100mM KCl and the value of maximal contraction was recorded. The tissue was then washed 3x with PSS before being stretched for another 2mN. The process was repeated until the final total tension of 14mN. 6mN was chosen as the final tension to stretch each uterine strip since the value of contractile response to 100mM KCl (Mean of KCl peak in mN) started plateauing at 6mN.

Total tension	2mN	4mN	6mN	8mN	10mN	12mN	14mN
Mean	4.447	5.095	5.986	6.133	5.798	6.663	7.119
Standard Deviation	1.092	1.291	2.319	2.622	2.47	2.451	1.638
Standard Error of Mean	0.4883	0.5773	1.037	1.172	1.104	1.226	0.9455

Western Blot

Uterine tissues from GD18 females at ZT3, 7, 11, 15, 19 and 23 were collected in semi-frozen 1xHBSS. To obtain a myometrium enriched sample, the endometrium was removed by gently scraping the inside of the uterus with a scalpel. Myometrium samples (~10x10 mm^2) were rapidly frozen on dry ice before storage at -80^oC until use. Myometrium samples were minced with scissors and incubated in ice-cold lysis buffer [20 mM Tris-HCl (pH 7.4), 10 mM NaCl, 1 mM $MgCl_2$ and 1% protease and phosphatase inhibitor cocktail] for 15-30 min on ice before 2x 10 sec sonication at 20% (Sonifier, Branson). Lysates were centrifuged for 10 min at 4 ^oC at 2000 g. Supernatant was recovered and protein concentration determination by Bradford Assay (Bio-Rad). Protein samples were then denatured by boiling in Laemmli buffer at 95°C for 5 min. Fifteen µg of protein extract was run on a 10% SDS-polyacrylamide gel and transferred to a polyvinylidene difluoride (PVDF) membrane (Immun-Blot PVDF, pore size 0.2 µm, Bio-Rad, Hercules, CA) by electroblotting at 400 mA for 90 min. The PVDF membrane was washed in 1×

tris-buffered saline (TBS, pH 7.6)/0.3% Tween-20 (TBS-T), blocked with buffer containing 5% milk for 1 h at room temperature, and incubated with a rabbit anti–OXTR antibody (1:1000, Protein Tech*,* 23045-1-AP*,* RRID*: AB_2827425*) for 16 h at 4^{o}C. The blot was washed 3x5 min in TBS-T and incubated in goat anti-rabbit IgG-HRP antibody (1:2000, BioRad, 1706515, RRID: AB_11125142) in 5% milk for 1 h at room temperature. The blot was then washed 3x5 min in TBS-T, rinsed in TBS and HRP activity visualized in an iBright machine (ThermoFisher Scientific) using the ECL reagent (Amersham) according to the manufacturer's instructions. To control for equal loading, the blot was then washed 3x5 min in TBS, stripped with stripping buffer for 30 min at room temperature (Restore Western Blot Stripping Buffer, 21059, Thermo Scientific), washed 3x5 min in TBS and 1x5 min in TBS-T, blocked with buffer containing 5% milk for 1 h at room temperature, and incubated with a rabbit anti-Lamin B1 antibody (1:500, Invitrogen, PA5-19468, RRID: AB_10985414) for 16 h at 4^{o}C. Secondary antibody and visualization with ECL were similar to those for the OXTR antibody. Antibodies used have been validated in previous publications[281–286]. We identified the correct band by verifying the proteins by their molecular weight using a protein marker (Precision Plus Protein Standards, Bio-Rad, 161-0374).

Sequence alignment and conserved region analysis

DNA sequence alignment was done with Clustal Omega[287] and the UCSC Genome Browser[288]. Alignment with Clustal Omega was done on sequences from -1000bp to +200bp from the beginning of the *Oxtr* genes of mouse, rat, human and *Rhesus* monkey obtained from NCBI (August 2021).

Cell culture conditions, transient transfections and luciferase assays

Mouse embryonic fibroblast NIH-3T3 (American Type Culture Collection, VA, #CRL-1658) cells were cultured in DMEM (Mediatech), containing 10% fetal bovine serum (Gemini Bio), and 1x penicillin-streptomycin (Life Technologies/Invitrogen) in a humidified 5% CO_2 incubator at

37˚C. For luciferase assays, NIH-3T3 cells were seeded into 24-well plates (Nunc) at 50,000 cells per well. Transient transfections for luciferase assays were performed using PolyJet™ (SignaGen Laboratories), following manufacturer's recommendations. NIH-3T3 cells were co-transfected as indicated in the figure legends with 200 ng/well luciferase reporter plasmids, as well as 100 ng/well thymidine kinase-β-galactosidase reporter plasmid, which served as an internal control[289]. The plasmids used were human Oxtr overexpression plasmid (200 ng/uL, Addgene, #67848), mouse -1000 to +200bp Oxtr-luciferase (200 ng/uL, VectorBuilder), mouse Bmal1 overexpression plasmid (200 ng/uL (Addgene, #31367), mouse Bmal1-luciferase (200 ng/uL, Addgene, #46824), pGL3-luciferase (200 ng/uL), pcDNA 3.1 (between 0 ng/uL and 200 ng/uL), and pGL4-luciferase (200 ng/uL). Site directed mutagenesis of the Oxtr-luciferase reporter was performed using the NEB Q5 Site-Directed Mutagenesis Protocol (New England Biolabs Inc.), following manufacturer's instructions, to mutate each E'-box to TGACGA. Primers for NEB Q5 site-directed mutagenesis were designed using NEBaseChanger[290] (Table 2). To equalize the amount of DNA transfected into cells, we systematically equalized plasmid concentrations by adding the corresponding inactive plasmid backbone. Cells were given their respective ligands 24 h after transfection and were then harvested 48 h after transfection in lysis buffer [100 mM potassium phosphate (pH 7.8) and 0.2% Triton X-100]. Luciferase values were normalized to β-galactosidase values to control for transfection efficiency. Values were further normalized by expression as fold change compared to pGL3 control plasmid, as indicated in the figure legends.

Table 4.2. E'-box sequences (5'-CANNTG-3') and primers for site-directed mutagenesis.

E'-box	Original sequence	Actual mutated sequence	Forward primer (Uppercase = target-specific primer)	Reverse primer
E1	CATGTG	TGACGA	CTTAGGCTGTtgacgaTGTGACAGATACTAATG	GTTACAAAACACTCAGGTC
E2	CACGTT	GACG-A	TGCATCTAATtgacgaAGAGAGCCCTG	TGTTTTATCCTGACATGTTATTTC
E3	CATATG	TCGTCA	CCCTAGCGGAtgacgaTGGTGCCGCAGCTCAGGGTTC	GGCAGAGCAAACCGGCCG
E4	CAAATG	TCGTCA	CAGGGAAAAAtgacgaTCACTTTCCAAGGTTCCTATATCTCTG	AGTAAATTGTAATAAAGACGC

Statistical analysis

PER2::LUC expression comparisons between control and cKO were done with Student's t-test. For *ex vivo* uterine contraction data, the raw measurements were divided by the measured KCl peak value to normalize the contraction AUC and amplitude data. *Ex vivo* uterine contractions of both control and cKO mice were analyzed with One or Two-way ANOVA. To compare *ex vivo* oxytocin-treated uterine contractions over ZTs between control and cKO mice, we used (piecewise) linear mixed-effects models for three measured outcomes (normalized AUC/amplitude or raw frequency), respectively. The net effect of the oxytocin treatment was defined as the difference in the measurements (normalized AUC/amplitude or raw frequency) between oxytocin and vehicle treatments. Next, we plotted the net effect of the oxytocin treatment versus ZT using loess regression to visualize whether the trend of the outcome over ZT was linear

or non-linear. The non-linear trend was modeled using a piecewise linear mixed-effects model with the defined ZT breakpoints based on the above-mentioned visualization[291]. No treatment measurement was considered as a covariate in the models to remove its possible effect to the trend. Covariate 'Group' (coded as control vs. cKO) and its interactions with ZT periods separated by breakpoints were also included in the models to evaluate whether the different groups had different effects on baseline outcomes and/or outcome changes over ZT.

All data management and statistical analyses were done using Prism 9 (GraphPad Software, San Diego, CA, USA), R (R Development Core Team) or SAS v9.4 (SAS Institute, Cary, NC, USA).

RESULTS

Deleting Bmal1 in the myometrium abolishes myometrial circadian rhythms

To further understand the role of the molecular clock and circadian rhythms in the myometrium during pregnancy, we generated mice with *Bmal1* conditionally deleted in the myometrium by crossing *Bmal1*$^{flox/flox}$ and *Telokin*$^{Cre/WT}$ mice, here referred to as cKO. The *Telokin*^{Cre}-allele has previously been shown to target the myometrium and the bladder smooth muscle[58]. To confirm that *Telokin*^{Cre} recombines the *Bmal1*$^{flox/flox}$ allele in smooth muscle, we evaluated *Bmal1*$^{flox/flox}$ recombination in cKO females by PCR. The *Telokin*^{Cre}-allele recombined the *Bmal1*$^{flox/flox}$-allele in the myometrium, bladder, cervix, aorta, trachea and intestine, but not in the liver, spleen, kidney, heart, skeletal muscle and stomach (Figure 4.1A). To validate that the deletion of *Bmal1* in the myometrium disrupted myometrium circadian rhythms, we crossed controls and cKO mice with the validated circadian reporter mouse, PER2::LUC, here referred to as *cKO:PER2::LUC*. The rhythmicity of PER2::LUC was verified by comparing the goodness-of-fit (GOF) to the mathematical LM Fit (Damped Sin) model. A GOF of 100 means the data fit the mathematical model perfectly. We found that uterine explants from GD18 *Telokin*$^{Cre/WT}$*:PER2::LUC* and *Bmal1*$^{flox/flox}$*:PER2::LUC* had comparable PER2::LUC GOF, amplitude of second peak, time of first peak, and period, thus these data were pooled into one

group, referred to as *PER2::LUC*. GD18 *PER2::LUC* and *cKO:PER2::LUC* presented with a circadian expression of PER2::LUC from full-thickness, endometrium-intact uterine explants (endometrium + myometrium, Figure 1B) as supported by the GOF (Figure 4.1C). As expected, the GOF in the *cKO:PER2::LUC* was significantly decreased compared to the control (Figure 4.1C, Student's t-test, $p<0.01$, $n\geq8$ per group). Despite the significant difference in GOF, the amplitude of the second peak, time of day of the first peak (phase) and PER2::LUC period were comparable between control and *cKO:PER2::LUC* (Figures 4.1D-F, Student's t-test, $p>0.05$, $n\geq8$ per group). As the endometrium is known to have a functional molecular clock[292,293], we next evaluated how removing the endometrium would impact the PER2::LUC recordings in myometrium explants. We found that the GD18 control myometrium maintained circadian rhythms (myometrium, Figure 4.1G) and had a high GOF (Figure 4.1H), together confirming the viability of this tissue explant for up to 6 days in the LumiCycle. In contrast, the PER2::LUC rhythms were greatly diminished in the *cKO:PER2::LUC* myometrium explant (Figure 4.1G), and the GOF was below 60 for all the explants (Figure 4.1H, Student's t-test, $p<0.0001$, $n\geq6$ per group). In the myometrium explants, the amplitude of the second peak and phase were not statistically different between control and *cKO:PER2::*LUC, though the p-values were trending towards statistical significance (Figure 4.1I, J, Student's t-test, $p=0.13$ and 0.07, respectively, $n\geq6$ per group), and PER2::LUC period was significantly shorter in *cKO:PER2::LUC* than control (Figure 4.1K, Student's t-test, $p<0.01$, $n\geq5$ per group). Values of amplitude of second peak, phase and PER2::LUC period of *cKO:PER2::LUC* myometrium were also significantly more varied compared to control (F test. Full-thickness uterine explants: amplitude of second peak $p=0.88$, phase $p=0.64$, PER2::LUC period $p=0.047$. Myometrium-enriched uterine explants: amplitude of second peak $p=0.17$, phase $p=0.0001$, PER2::LUC period $p=0.06$), suggesting that myometrial circadian rhythms in *cKO:PER2::LUC* were deregulated.

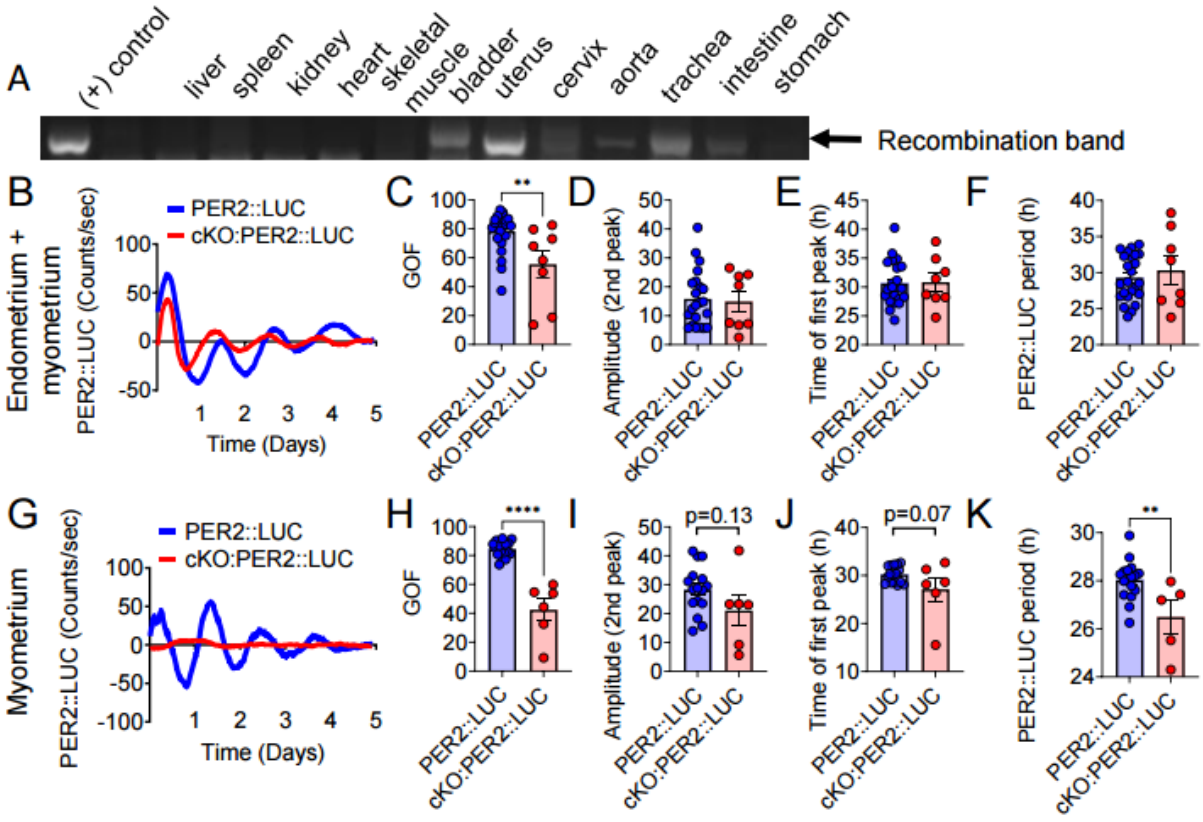

Figure 4.1. The myometrium from GD18 female mice exhibit circadian rhythms that are diminished in the absence of BMAL1. (A) Indicated tissues were collected from adult female cKO mice and analyzed for *Bmal1*$^{flox/flox}$-allele recombination using PCR. The presence of a white band indicates Cre-induced recombination. (B) Full-thickness uterine explants from PER2::LUCIFERASE reporter mice (PER2::LUC, blue) and triple transgenic cKO:PER2::LUC mice (red) at GD18 displayed cyclic PER2::LUCIFERASE (PER2::LUC) recordings over 6 days. Comparing (B-F) full-thickness uterine explants and (G-K) endometrium removed uterine explants between control (PER2::LUC, blue) and cKO (cKO:PER2::LUC, red) in terms of (C, H) the goodness-of-fit (GOF) of PER2::LUC rhythms to the mathematical model [LM Fit (Damped Sin)], (D, I) amplitude of the second peak of PER2::LUC rhythms, (E, J) time of day of the first peak of PER2::LUC rhythms and (F,K) PER2::LUC periods. Statistical analysis (C-F and H-K) Student's t-test, n≥5 per group, **p<0.01, ****p<0.0001. Outliers are excluded.

Loss of BMAL1 in the myometrium increases spontaneous contractions in GD18 uterine explants

To determine how loss of myometrial circadian rhythms impacts uterine contractile function, we performed *ex vivo* contraction studies on uterine strips obtained from control and cKO mice every 4 h over a 24 h period at GD18 (Figure 4.2A). We verified that *PER2::LUC, Bmal1*$^{flox/flox}$ and *Telokin*^{Cre} had comparable spontaneous uterine contractions and therefore pooled together these mice into the control group (Table 4.3). We found that control uterine strips displayed no significant change in *ex vivo* spontaneous contractions over a 24 h period with regards to AUC, amplitude and frequency (Control, blue, Figure 4.2B-G). To compare spontaneous uterine contractions between control and cKO, we carried out Two-way ANOVA on AUC, amplitude, and frequency. Our analyses reveal that contraction force (AUC) was significantly impacted by genotype [$F(1,96)=49.67$, $p<0.0001$] but not time of day [$F(5,96)=2.183$, $p=0.0624$], with no interaction of genotype and time of day [$F(5,96)=1.713$, $p=0.1389$]. Post hoc analysis showed that the cKO had significantly higher AUC at ZT3, 7, and 19 (Figure 4.2E, Sidak's multiple comparison test, *$p<0.05$, ***$p<0.001$, **** $p<0.0001$). Two-way ANOVA analysis showed that amplitude was significantly impacted by both genotype [$F(1,96)=33.97$, $p<0.0001$] and time of day [$F(5.96)=2.483$, $p=0.0362$], where an interaction between the two trended towards significance [$F(5,96)=2.307$, $p=0.0502$]. The post hoc analysis of the contraction amplitude data found that uterine strips from the cKO had significantly higher amplitude at ZT3 and ZT7 as compared to controls (Figure 4.2F, Sidak's multiple comparison test, ***$p<0.001$), whereas contraction frequency was comparable between genotype [$F(1,96)=3.249$, $p=0.0746$], time of day [$F(5,96)=2.277$, $p=0.0529$], and no interaction between genotype and time of day existed [$F(5,96)=0.3576$, $p=0.8762$] (Figure 4.2G).

Table 4.3. **Parameters for spontaneous baseline uterine contractions of control mice.** Spontaneous uterine contractions from *PER2::LUC, Bmal1*$^{flox/flox}$ and *Telokin*^{Cre} mice at GD18 were analyzed in terms of AUC, frequency and amplitude. Statistical analysis: One-way ANOVA, n=6 per group.

Group	AUC		Frequency		Amplitude	
	Mean ± SEM	P-value	Mean ± SEM	P-value	Mean ± SEM	P-value
PER2::LUC	296.30 ± 58.01	0.15	7.083 ± 0.597	0.70	1.582 ± 0.210	0.91
Telokin^{Cre}	182.80 ± 43.67		5.833 ± 1.358		1.263 ± 0.183	
Bmal1$^{flox/flox}$	338.60 ± 62.58		7.083 ± 1.440		1.852 ± 0.177	

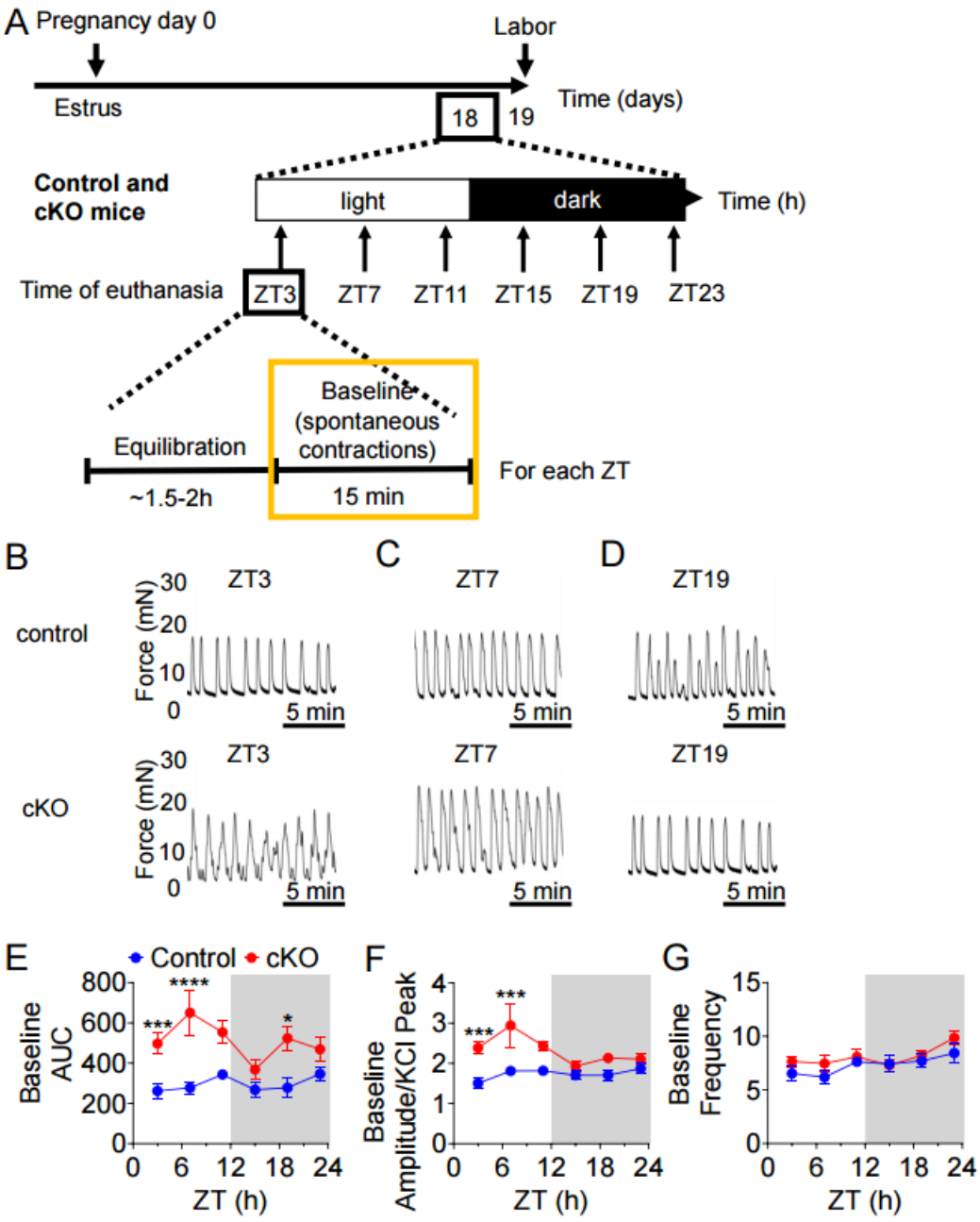

Figure 4.2. Depletion of *Bmal1* in the myometrium (cKO) increases *ex vivo* spontaneous contractions in the GD18 mouse uterus. (A) Timeline of uterine tissue collection and contraction recordings. Pregnant mice at GD18 were euthanized every 4 h over 24 h. At every time point, each uterine strip was mounted in a tissue organ bath of a DMT 820MS myograph, stretched to a final tension of 6 mN and allowed to equilibrate for ~2 h, until the tissue exhibited consistent, spontaneous baseline contractions for 15min. Data are *ex vivo* uterine spontaneous

Figure 4.2. (cont'd)

contractions analyzed during the time point indicated with the orange box. Representative tracings of *ex vivo* spontaneous uterine contractions between control (top) and cKO (bottom) at (B) ZT3, (C) ZT7 and (D) ZT19. *Ex vivo* spontaneous uterine contractions in cKO (red) and control (blue) at ZT3, 7, 11, 15, 19 and 23 with regards to (E) area under the curve (AUC), (F) amplitude and (G) frequency. Statistical analysis for (E-G) Two-way ANOVA, ***p<0.001, ****p<0.0001. n⩾6 per time point.

GD18 uterine explant contractile response to oxytocin in control mice is lowest at ZT11 and greatest at ZT15

To determine if time of day impacted the efficacy of oxytocin to promote uterine contractions in explants from GD18 control mice, we placed uterine strips on a myograph and recorded their contractile response to 1nM oxytocin every 4 h over a 24 h period (Figure 4.3A). We first verified OXTR specificity by blocking oxytocin-induced contractions with the OXTR antagonist atosiban (Figure 4.3B, C). Vehicle (water) did not induce significant changes in uterine contractions (Figure 4.3D-F), where a Two-way ANOVA showed that the contraction force (AUC), amplitude and frequency were not significantly affected by treatment (vehicle vs baseline, AUC: treatment [$F(1,34)=1.260$, $p>0.05$)], time of day [$F(3.129,48.82)=0.9839$, $p>0.05$)], interaction between treatment and time of day [$F(5,78)=0.1455$, $p>0.05$)]. Amplitude: treatment [$F(1,34)=0.1697$, $p>0.05$)], time of day [$F(3.160,49.29)=1.544$, $p>0.05$)] or an interaction between treatment and time of day [$F(5,78)=0.1066$, $p>0.05$)]. Frequency: treatment [$F(1,112)=1.225$, $p>0.05$)], time of day [$F(3.290,73.70)=1.802$, $p>0.05$)] or the interaction between treatment and time of day [$F(5,112)=0.1379$, $p>0.05$)]). In contrast, 1nM oxytocin significantly increased uterine contractions, where oxytocin promoted uterine contraction force (AUC) at all the studied time-points in the control mice (Figure 4.3G), and the Two-way ANOVA showed that AUC was

significantly affected by treatment [$F(1,34)=18.93$, $p=0.0001$)], but not time of day [$F(3.147,49.10)=0.4019$, $p>0.05$)] or the interaction between treatment and time of day [$F(5,78)=0.7363$, $p>0.05$)]. Oxytocin did not significantly increase contraction amplitude (Figure 4.3H, $p>0.05$), but did significantly increase contraction frequency at ZT7 and 19 (Figure 4.3I), where the Two-way ANOVA showed a significant effect of treatment [$F(1,112)=33.90$, $p<0.0001$)]. To determine if the efficacy of oxytocin changed depending on the time of day, we normalized the oxytocin data to the vehicle data at each ZT time point and expressed the normalized data as fold change from vehicle data. The fold change data revealed a time of day change in the capacity of oxytocin to promote uterine contractions (Figure 4.3J-L). One-way ANOVA with a Tukey's post hoc showed that oxytocin significantly increased contraction amplitude [Figure 4.3K, $F(5,56)=2.761$, $p=0.0268$] between ZT11 and ZT15, but did not significantly increase contraction force (AUC, Figure 4.3J, [$F(5,56)=1.75$, $p=0.1382$]) or frequency (Figure 4.3L, [$F(5,56)=0.9123$, $p=0.4798$]).

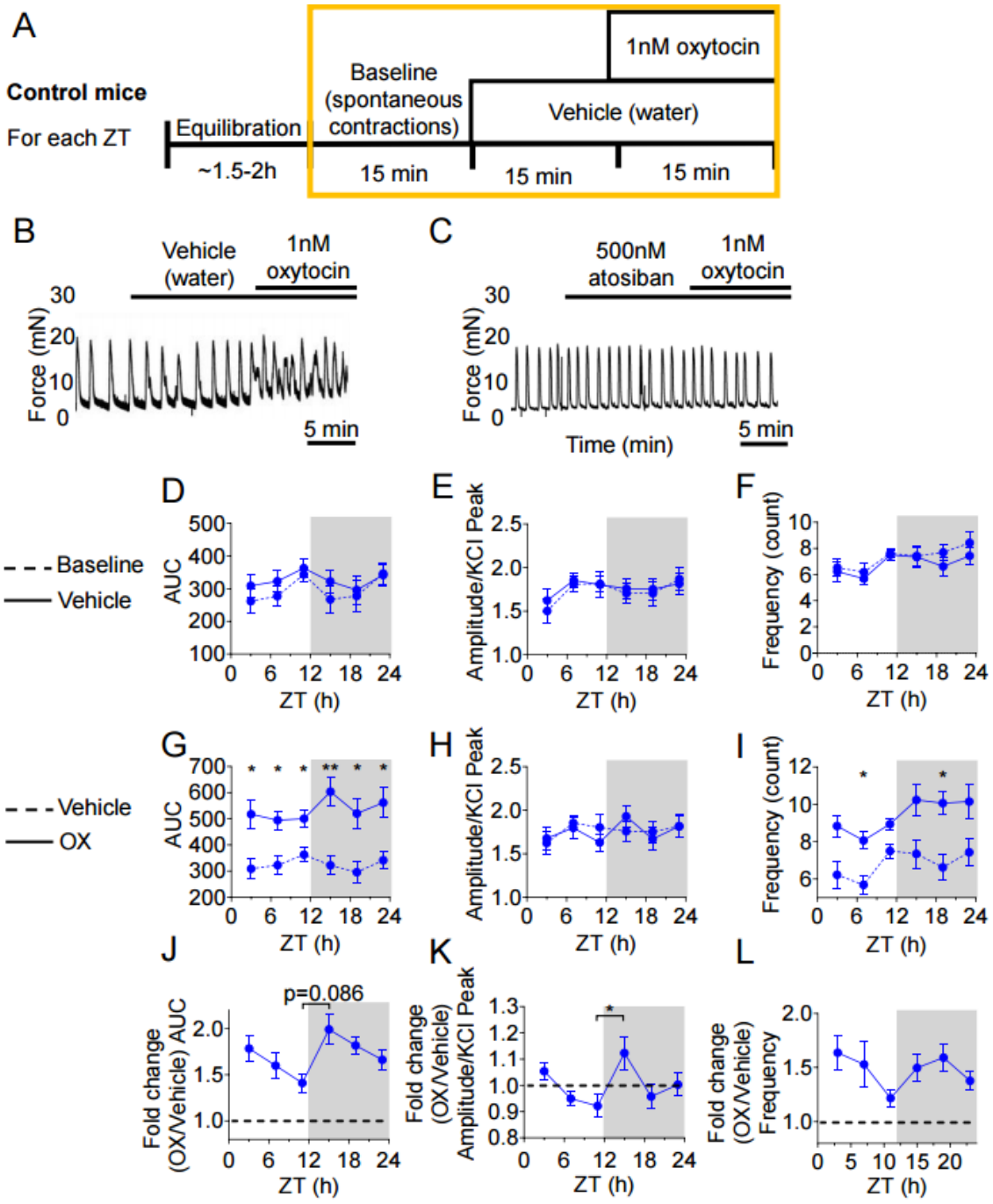

Figure 4.3. Time of day effect of oxytocin-induced uterine contractions in control GD18 mouse uterus. (A) Timeline for tissue treatment at each time point. After about 2 h of equilibration, baseline consistent, spontaneous contractions occurred for 15min. Each uterine strip was then treated with vehicle (water) for 15 min and then 1 nM oxytocin for 15 min. Data shown are *ex vivo* uterine spontaneous contractions, vehicle-treated contractions and oxytocin-

Figure 4.3. (cont'd)

treated contractions (orange box). (B, C) In uterine strips from GD18 control mice, oxytocin-induced contractions are inhibited by 500 nM atosiban, an OXTR antagonist (vehicle = water) (tracings representative of n≥3). (D-F) Vehicle did not induce significant change in contractions at any time over a 24 h period (dash line: baseline contraction, solid line: vehicle-treated contraction). (G-L) The capacity of 1 nM oxytocin to promote contractions in GD18 control uterine strips was assessed every 4 h over a 24 h time period. (G-I) Raw data of 1nM oxytocin induced uterine contractions with regards to (G) area under the curve (AUC), (H) amplitude and (I) frequency at multiple times over 24 h (dash line: vehicle-treated contraction, solid line: oxytocin-treated contraction). (J-K) Oxytocin-treated data were normalized to vehicle-treated data for better visualization of time of day effects of oxytocin on uterine contractions. This is the same data set as G-I except that oxytocin is divided by vehicle. A value of 1 (dash line) means no difference from vehicle. Statistical analysis for (D-I) by Two-way ANOVA with mixed effects and (J-L) One-way ANOVA, *$p<0.05$, **$p<0.01$. $n \geqslant 6$ per time point. Abbreviations: OX: oxytocin.

Loss of BMAL1 in the myometrium reduces GD18 uterine explant contractile response to oxytocin during the dark phase

To determine how the loss of myometrial circadian rhythms impacted the daily change in uterine contractile response to oxytocin, we treated control and cKO GD18 uterine strips with 1 nM oxytocin every 4 h over a 24 h period (Figure 4.4A). We first verified that vehicle did not induce significant changes in uterine contractions in control and cKO at all time points (Figure 4.4B-G, Two-way ANOVA with mixed effects, $p>0.05$, $n \geq 6$ per group). To determine how loss of BMAL1 in the myometrium impacted the daily change in uterine contractile response to oxytocin, we then evaluated the efficacy of oxytocin to promote contractions in control and cKO. Note that the control data in Figure 4.4 is replotted from Figure 4.3 to allow comparison to cKO. In contrast to controls,

where oxytocin induced significantly stronger force (AUC) and more frequent uterine contractions than vehicle at 2-6 of the 6 time points studied (blue, Figure 4.4H, J), in the cKO, oxytocin only increased uterine contraction force (AUC) and amplitude at ZT15 and did not significantly change contraction frequency (red, Figure 4.4H-J). When comparing controls to cKO, there was a significant effect of genotype on contraction force (AUC) [$F(3,192)=51.42$, $p<0.0001$] and frequency [$F(3,192)=21.33$, $p<0.0001$]. To determine if the efficacy of oxytocin changed depending on the time of day in the cKO, we normalized the oxytocin data to the vehicle data, allowing us to express it as fold change and compare the efficacy of oxytocin to induce contractions between controls and cKO (Figure 4.4K-L). The Two-way ANOVA mixed effect model showed that contraction force (AUC, Figure 4.4K) was significantly impacted by time of day [$F(5,96)=2.923$, $p=0.0169$] and genotype [$F(1,96)=10.61$, $p=0.0016$], although no interaction between time of day and genotype was identified [$F(5,96)=0.4497$, $p=0.8126$]. Contraction frequency (Figure 4.4M) was significantly impacted by genotype alone [$F(1,96)=5.849$, $p=0.0175$]. To confirm this statistical analysis, we reanalyzed our data by creating an overall mean profile of the AUC, amplitude, and frequency over ZT. Figures 4.4K-M indicate the existence of three breakpoints (ZT11, ZT15, ZT19) at which oxytocin-induced contractions with regards to AUC, amplitude and frequency changed directions. Thus, we fitted a 4-piecewise linear mixed-effects model in which we specified intercept as the random term with an unstructured covariance-structure (Table 4.4). AUC was comparable between control and cKO at all time points, but frequency and amplitude were different between control and cKO from ZT11 to ZT23 (Table 4.4). Specifically, from ZT11 to ZT15, cKO displayed a reduced increase in oxytocin-induced changes in amplitude than controls (Table 4.4, $\beta_{(\text{control vs cKO})}=0.111$, $SE=0.048$, $p=0.0238$). From ZT15 to ZT19, the cKO uterus displayed a reduced decrease in amplitude in response to oxytocin than control as compared to controls, but not frequency (Table 4.4, amplitude: $\beta_{(\text{control vs cKO})}=-0.163$, $SE=0.060$, $p=0.0075$; frequency: $\beta_{(\text{control vs cKO})}=1.036$, $SE=0.552$, $p=0.0635$). From ZT19 to ZT23, cKO uterine strips displayed an increased contraction frequency in response to oxytocin than

control (Table 4.4, $\beta_{(control\ cvs\ KO)}$=-1.522, SE=0.616, p=0.0152), confirming our findings using the Two-way ANOVA mixed effect model in Figure 4.4K-M.

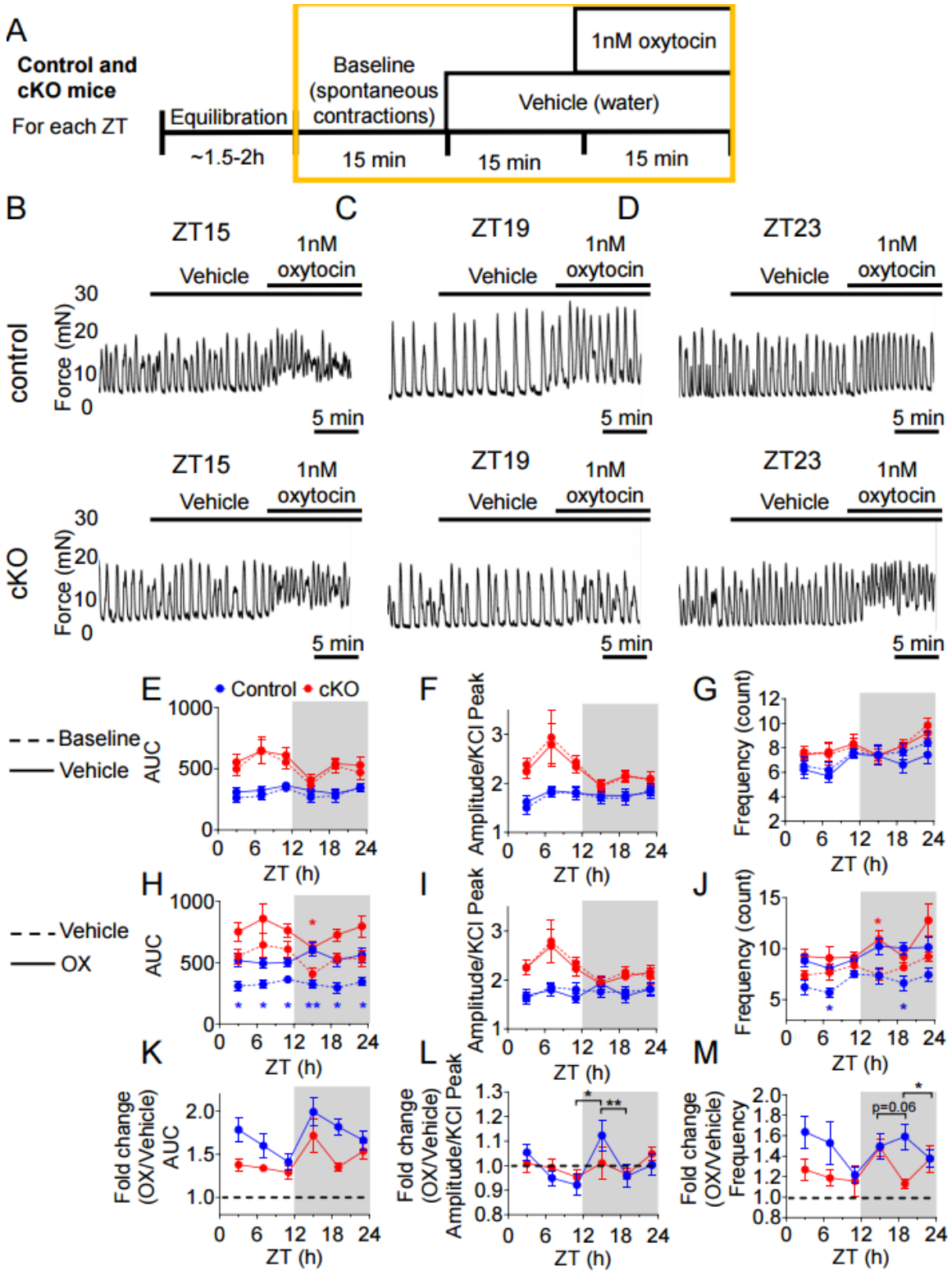

Figure 4.4. Depletion of *Bmal1* in the myometrium (cKO) alters the *ex vivo* contractile response to oxytocin in the GD18 mouse uterus. (A) Timeline for tissue treatment at each time

Figure 4.4. (cont'd)

point (same timeline as Figure 3A). (B-D) Representative tracings of *ex vivo* spontaneous, vehicle-treated and oxytocin-treated uterine contractions between control (top) and cKO (bottom) at indicated time points (ZT15, ZT19 and ZT23). (E-G) Vehicle did not induce significant changes in uterine contractions in both control and cKO at ZT3, 7, 11, 15, 19 and 23. (H-J) Raw data for oxytocin-induced uterine contractions in cKO (red) and control (blue) at ZT3, 7, 11, 15, 19 and 23 with regards to (H) area under the curve (AUC), (I) amplitude and (J) frequency. (K-M) Oxytocin-treated data were normalized to vehicle-treated data for better visualization of time of day effects of oxytocin on uterine contractions between control and cKO. This is the same data set as H-J except that oxytocin is divided by vehicle. A value of 1 (dash line) means no difference from vehicle. Control data (E-M) are the same as those in Figure 3D-L. Statistical analysis for (E-J) Two-way ANOVA with mixed effects, (K-M) piecewise linear mixed-effects models for three measured outcomes (AUC, amplitude, frequency) (analysis done on oxytocin-treated data subtracted by vehicle-treated data), *p<0.05, **p<0.01. n⩾6 per time point. Abbreviations: OX: oxytocin.

Table 4.4. Summary of the piecewise linear mixed-effects models for measured 3 outcomes (AUC/Amplitude/Frequency).

	$\Delta_{(\text{Contraction AUC})}$[a]			**$\Delta_{(\text{Contraction Amplitude})}$[b]**			**$\Delta_{(\text{Contraction Frequency})}$[c]**		
	β	**SE**	**p**	**β**	**SE**	**p**	**β**	**SE**	**p**
Intercept	178.150	65.952	**0.0082**	0.564	0.165	**0.0009**	3.309	1.666	**0.0499**
ZT3-11	-5.797	6.786	0.3951	-0.012	0.014	0.3869	-0.119	0.127	0.3523
ZT11-15	22.837	18.813	0.2278	-0.005	0.037	0.8975	0.756	0.338	**0.0275**
ZT15-19	-27.403	23.418	0.2448	0.017	0.045	0.7152	-1.211	0.416	**0.0044**
ZT19-23	31.552	24.221	0.1958	0.041	0.048	0.3937	1.258	0.449	**0.0062**
Baseline[d]	0.088	0.092	0.3397	-0.212	0.055	**0.0002**	-0.143	0.189	0.4489

Table 4.4. (cont'd)

Group:									
Control vs. cKO	38.258	79.475	0.6313	-0.250	0.203	0.2203	2.561	1.919	0.1852
Baseline*Group:									
Baseline* Control vs. Baseline* cKO	-0.005	0.142	0.9747	0.085	0.086	0.3258	-0.318	0.218	0.1471
ZT3-11*Group:									
ZT3-11* Control vs. ZT3-11*cKO	-3.926	8.784	0.6559	-0.012	0.018	0.5061	0.034	0.164	0.8361
ZT11-15*Group:									
ZT11-15* Control vs. ZT11-15*cKO	24.363	24.366	0.3199	0.111	0.048	**0.0238**	-0.327	0.443	0.4624
ZT15-19*Group:									
ZT15-19* Control vs. ZT15-19*cKO	-24.565	30.380	0.4207	-0.163	0.060	**0.0075**	1.036	0.552	0.0635
ZT19-23*Group:									
ZT19-23* Control vs. ZT19-23*KO	-19.601	32.975	0.5536	0.049	0.066	0.4605	-1.522	0.616	**0.0152**

BMAL1 drives Oxtr expression in vitro

Due to the daily changes in uterine contractile response to oxytocin in GD18 control mice (Figure 4.3) and the reduced sensitivity to oxytocin in GD18 cKO uterine strips (Figure 4.4), we asked if BMAL1 might regulate *Oxtr* expression. We used UCSC Genome Browser to identify highly conserved regions of the mouse, rat, human, and monkey *Oxtr* regulatory regions (Figure 4.5A). Within the conserved regions, we identified four semi-conserved BMAL1 binding sites (E'-boxes) in the promoter region of the *Oxtr* regulatory region (Figure 4.5B). To determine if BMAL1 regulated *Oxtr* expression through these E'-boxes, we carried out an *in vitro* reporter gene assay where NIH-3T3 cells were transiently transfected with a Bmal1-overexpressing plasmid and the *Oxtr* regulatory region driving-luciferase expression (Oxtr-luciferase). *Bmal1* overexpression increased Oxtr-luciferase expression in a dose-specific manner (Figure 4.5C, One-way ANOVA followed by a Tukey post hoc, [$F(3,12)=8.492$, $p=0.0027$]). To determine if the enhancing effect of BMAL1 on Oxtr-luciferase expression was through a direct action of BMAL1 binding to E'-boxes in the *Oxtr* regulatory region, we mutated the identified E'-boxes using site-directed mutagenesis (Table 4.2, Figure 4.5D). We found that 200 ng of Bmal1 significantly enhanced expression of the Oxtr-luciferase plasmid with μE1 and μE3 but did not significantly enhance Oxtr-luciferase expression with μE2 and μE4 (Figure 4.5D). Specifically, Two-way ANOVA showed Oxtr-luciferase expression was significantly impacted by the E'-boxes [$F(4,36)=3.178$, $p=0.0246$] and Bmal1 [$F(1,36)=32.25$, $p<0.0001$] but not an interaction between E'-boxes and Bmal1 [$F(2,36)=2.274$, $p=0.0803$]. Post-hoc analysis with Sidak's multiple comparison test showed that the original E'box (WT), and the mutated E'boxes μE1 and μE3 significantly enhanced Oxtr-luciferase expressions (WT: $p=0.0280$; μE1: $p=0.0010$; μE3: $p=0.0039$). To determine if OXTR in return regulates BMAL1, we repeated the transient transfection studies but with Oxtr overexpression plasmids and Bmal1-luciferase plasmid. We found that overexpressing OXTR did not significantly enhance Bmal1-luciferase (Figure 4.5E, Two-way ANOVA, $p>0.05$). To determine if the regulatory effect of BMAL1 on the Oxtr-luciferase plasmid resulted in daily changes in OXTR

protein levels in the GD18 myometrium, we performed Western Blot for OXTR and Lamin B1 (Figure 4.5F). We chose Lamin B1 as our housekeeping protein as its expression did not significantly change between the studied time points in GD18 myometrium samples (not shown). That said, when we normalized OXTR to Lamin B1 (Figure 4.5G), the cKO OXTR levels appeared to be higher than control, which is not what the Western Blot images showed (Figure 4.5F). Even though Two-way ANOVA with mixed effects on the normalized OXTR levels showed no significant difference in terms of time of day [$F(5,42)=1.258$, $p=0.3000$], genotype [$F(1,14)=1.251$, $p=0.2823$], or an interaction between time of day and genotype [$F(5,42)=0.7986$, $p=0.5570$], we also presented the data as raw OXTR levels (Figure 4.5H). The raw OXTR levels in controls and cKO were very comparable, and no significant difference in OXTR was detected by Two-way ANOVA with mixed effects (time of day: [$F(5,50)=0.6825$, $p=0.6388$]; genotype: [$F(1,14)=0.4288$, $p=0.5232$]; interaction between time of day and genotype: [$F(5,50)=1.424$, $p=0.2320$]) (Figure 4.5H). Independently of how we presented the OXTR data, we did not see a significant impact of time of day or genotype on OXTR protein levels in the GD18 myometrium.

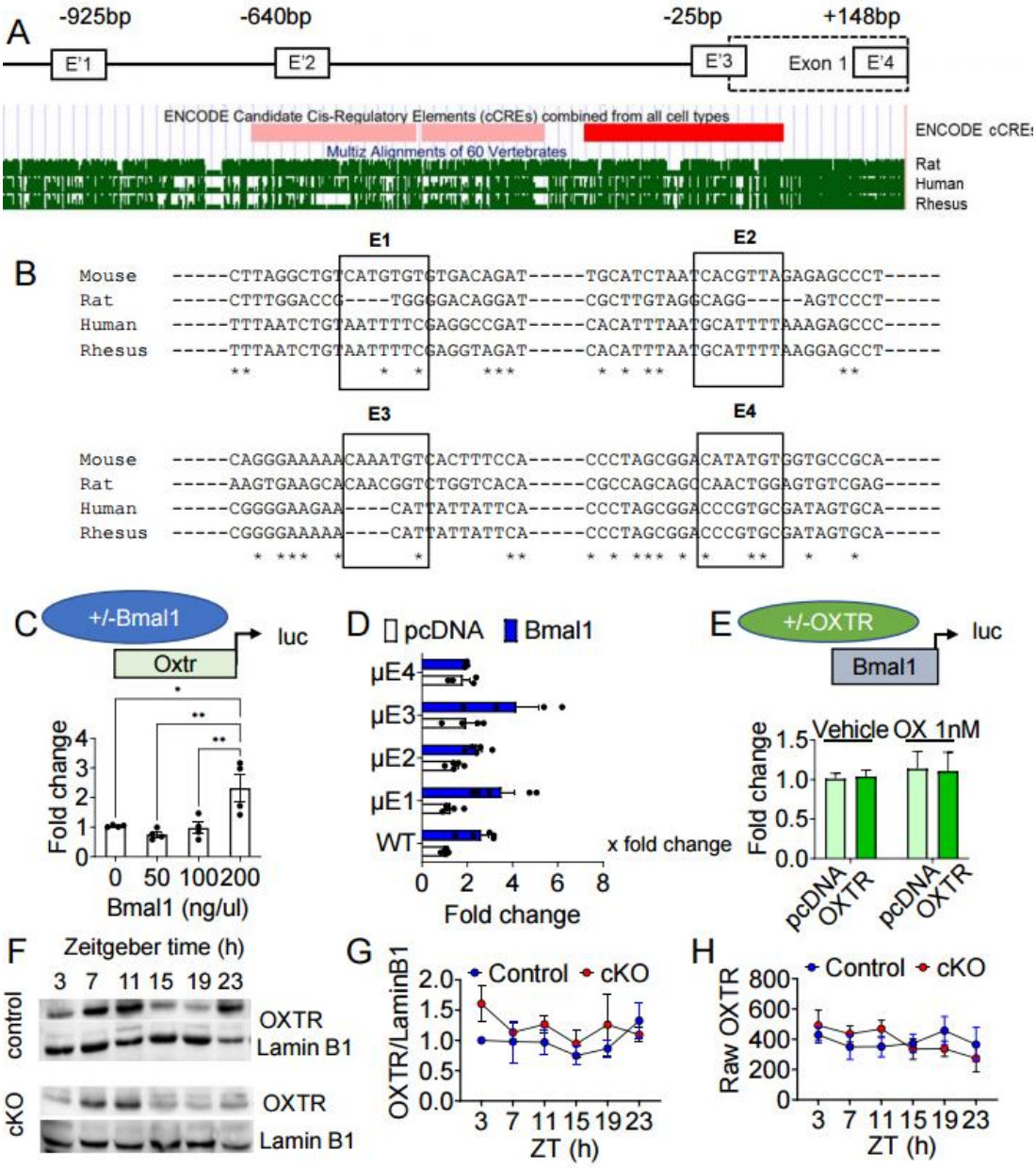

Figure 4.5. BMAL1 enhances expression of *Oxtr* through E'-boxes (5'-CANNTG-3') in the *Oxtr* regulatory region. (A) Using UCSC Genome Browser and (B) Clustal Omega, we identified four semi-conserved BMAL1 binding sites (E'-boxes) in the *Oxtr* regulatory region (E1, E2, E3, E4). ENCODE Candidate Cis-Regulatory Elements (cCREs) show sites of histone modifications (H3K4me3, pink) and promoter-like region (red). The * indicates perfectly conserved nucleotides. To determine if BMAL1 regulated *Oxtr* expression *in vitro*, NIH-3T3 cells were transiently

Figure 4.5. (cont'd)

transfected with Bmal1 overexpressing plasmid and Oxtr-luciferase plasmids (C) without or (D) with mutated E'-boxes (μE1, μE2, μE3, μE4). (E) To determine if a feedback mechanism existed, and establish if OXTR regulated Bmal1 expression, NIH-3T3 cells were transiently transfected with Oxtr overexpressing plasmid and Bmal1-luciferase plasmid and then treated with vehicle or 1nM oxytocin. (F) Representative Western Blot of GD18 myometrium for OXTR and Lamin B1. (G) OXTR levels were normalized to Lamin B1, and all the data were normalized to ZT3. (H) Histogram of OXTR protein levels without normalization (Raw OXTR) in the mouse myometrium at GD18 at indicated time points. Statistical analysis for (C) One-way ANOVA, n=4 per group, and (D, E) Two-way ANOVA, n=4-5 (B, C) and n≥5 (G, H) per group, ns: non-significant, * $p<0.05$, ** $p<0.05$, *** $p<0.005$.

DISCUSSION

Here we show that daily changes in uterine contractions in late pregnancy are regulated by the myometrium molecular clock. Specifically, we show that loss of the clock transcription factor BMAL1 in the myometrium increases spontaneous uterine contractions and reduces the contractile response to oxytocin in a time-of-day dependent manner. Although we identified BMAL1 as a direct regulator of *Oxtr in vitro*, we did not see a significant change in OXTR protein expression, suggesting the time of day effects of oxytocin are regulated by intracellular changes impacting OXTR signaling.

Daily changes of uterine contractions in the uterus and the role of oxytocin and its receptor herein

In humans and non-human primates, the myometrium increases contractions during the night in the 3rd trimester of pregnancy[17,275]. Unexpectedly, we did not find that *ex vivo* mouse GD18 uterine strips presented with a significant daily change in spontaneous contractions over a 24 h period. One limit of this study is that, in contrast to established daily changes in uterine

contractions during late pregnancy in humans and non-human primates, it remains unknown if this is also the case in mice. That said, indirect evidence suggests uterine contractions likely are circadian in mice, as this species, just like non-human primates and humans, display a circadian pattern of birth timing, which peaks during the rest phase of the day[9]. In non-human primates and humans, the increase in nocturnal uterine contractions appears to be at least partially driven by a nocturnal increase in the uterotonic efficacy of oxytocin[18], combined with the potentiating effect of the nocturnally released hormone melatonin on uterine contractions[16,294,295]. In addition to a daily change in hormone release that allows for increased nocturnal contractions in late gestation, the molecular clock transcription factor BMAL1 regulates daily changes in melatonin receptor expression, a receptor that is upregulated in the myometrium in late pregnancy in women[296,297]. To understand the molecular mechanisms allowing the development of the daily change in oxytocin efficacy, we asked if BMAL1 regulated OXTR expression. Using transient transfections of cells, we show for the first time that BMAL1 is a direct activator of *Oxtr*. Surprisingly, in GD18 mouse myometrium, we did not see a daily change in OXTR protein in the control or cKO, nor did cKO of *Bmal1* significantly reduce OXTR levels in the myometrium. This suggests that the level of OXTR (as evaluated by Western Blot) does not directly correlate with the efficacy of oxytocin to induce uterine contractions and indicates a more complex mechanism underlying the time of day changes in uterine contractile response to oxytocin. One possible explanation for the lack of correlation between OXTR levels and the uterus' contractile response to oxytocin is a potential change in the capacity of OXTR to modulate intracellular signaling cascades, especially calcium release from the sarcoplasmic reticulum, which might change depending on the time of day[298]. Moreover, the change in basal contractile function of the cKO myometrium (discussed in detail in section "*Deletion of Bmal1 in the myometrium strengthens spontaneous uterine contractions*") indicates that BMAL1 regulates myometrium excitability and might alter OXTR signaling through changes in expression and function of calcium channels on the membrane which are regulated by OXTR[298–300]. Taken together, we propose the daily changes in uterine contractions *in vivo* are

driven by daily changes in hormonal input to the uterus, combined with daily changes in target receptor expression and/or signaling efficacy.

Time of day impacts the efficacy of oxytocin to promote contractions in the GD18 mouse myometrium

C-section is often a result of failed IOL and much remains to be explored about uterine sensitivity to oxytocin, the hormone whose synthetic version, Pitocin, is commonly used in IOL[268,269]. While there is evidence that spontaneous uterine contractions and uterine sensitivity to oxytocin *in vivo* change depending on the time of day[17,18], little is known about what regulates this daily change in uterine function. In agreement with this prior work, we show here that the mouse myometrium has defined daily time windows of increased and decreased contractile response to oxytocin, with the greatest sensitivity to oxytocin at ZT15 and the lowest sensitivity to oxytocin at ZT11. Interestingly, ZT11 and ZT15 encompass the time points of transition between the light phase and the dark phase, when mice generally give birth[274]. This supports the idea that the daily change in uterine contractile response to oxytocin plays a role in timing labor onset. This finding could also be clinically relevant for the development of strategies to improve IOL success, as it is well established that chronopharmacological studies can improve drug efficacy while reducing drug dose[301]. To our knowledge, our study is the first to report a time of day effect of oxytocin in the mouse myometrium. These findings highlight the value of chronopharmacological studies to increase drug efficacy and indicate that Pitocin efficacy for IOL might be improved by identifying the daily time windows of increased capacity to promote uterine contractions in pregnant women.

Deletion of Bmal1 in the myometrium strengthens spontaneous uterine contractions

Spontaneous uterine contractions are significantly increased prior to labor onset in women having preterm birth[302]. Interestingly, our cKO mice, whose molecular clock function was disrupted, had a similar phenotype where their spontaneous uterine contractions were about two-

three times stronger than those of control mice during the light phase (rest phase of the mice), while control mice displayed no time of day change in spontaneous contractions. As BMAL1 is circadian in the pregnant uterus[72], these unexpected results might be caused by a deregulation of the balance between inhibitory and activating pathways regulated by BMAL1. The increases in spontaneous contraction force (AUC) in the cKO were primarily driven by an increase in the amplitude of the contractions, and not their frequency. Among the primary ion channels regulating contraction amplitude is the large-conductance voltage- and calcium-dependent potassium channel (BKCa), which belongs to a family of channels that we previously found to be among the top deregulated pathways downstream of the clock genes CRY2 and CLOCK[303]. Remarkably, in neurons of the brain's circadian pacemaker, the suprachiasmatic nucleus, BKCa channels drive the daily changes in neuron firing, which are higher during the day than night period[304,305]. BKCa channels in the suprachiasmatic nucleus have a circadian expression driven by the molecular clock[304,305]. In the myometrium, BKCa channels are the most abundant potassium channels responsible for membrane repolarization and muscle relaxation[306–308]. Membrane potential determines intracellular ion levels and ultimately determines the amplitude of contractions[309,310], where activation of BKCa drives myometrial relaxation while inhibition of BKCa leads to myometrial contraction[309,311]. It will be of interest in future work to determine how BKCa expression is impacted in the cKO uterus and to determine what other molecular mechanisms are driving the increase in basal contractions of this mouse model.

Bmal1 in the myometrium generates circadian rhythms

It is well established that BMAL1 is required for circadian rhythm generation[21]. In agreement with this, we find that deleting *Bmal1* in the myometrium significantly reduces the quality of the circadian rhythm, as evaluated through the GOF to the cosinor mathematical model. While the GOF is an indicator of reduced rhythmicity within the myometrium, the fact that we see a GOF of ~10-50 suggests our myometrium-enriched explants are not fully depleted of rhythms,

probably due to the presence of glands within the myometrium, which still have a functioning molecular clock, in addition to incomplete removal of the endometrium. Indeed, previous work has shown the *Telokin*^{Cre} allows deletion of BMAL1 in the myometrium but not the endometrium[58]. Further analysis of the PER2::LUC rhythms revealed a significant shortening in PER2::LUC period in myometrium-enriched explants, which translated into a non-significant (p=0.07) difference in phase. However, it is important to consider the limits of placing a high value on the cKO myometrial PER2::LUC period and phase data that do not fit the circadian rhythms of the cosinor mathematical model. Despite these limits, our data support the known circadian expression of clock genes in the endometrium[292,293], as our cKO full-thickness uterine explants (endometrium + myometrium), had no change in PER2::LUC period or phase as compared to control. This indicates that the endometrium significantly contributes to the circadian rhythm of the uterus. Taken together, these data validate the cKO model, by showing a functional loss/reduction of circadian rhythms in the myometrium depleted of *Bmal1.*

Conclusions

We here identify BMAL1 as a significant contributor to spontaneous uterine contractions in pregnancy. Using *ex vivo* uterine contraction studies we show that the GD18 mouse uterus exhibits a time of day sensitivity to oxytocin, validating previous findings in primates. Despite the approximately doubled spontaneous uterine contractions of the BMAL1 depleted myometrium (cKO), these mice had reduced contractile response to oxytocin. Together, these findings show that time of day of drug administration (chronopharmacology) is an import variable to be considered in pharmacological studies focused on uterine contractile function, and identify BMAL1 as a regulator of *Oxtr*, which might contribute to the changes in intracellular signaling cascades driving the daily change in oxytocin efficacy.

CONCLUDING REMARKS

This PhD dissertation explored the role of circadian rhythms in late pregnancy, with the primary goal of establishing how uterine circadian rhythms regulate uterine contractile function and the long-term goal of improving outcomes of mistimed labor. Mistimed labor onset leads to preterm labor or postterm labor. Each year, one in ten babies is born preterm and one in ten is born postterm. Preterm labor, if not halted, will result in preterm birth, which is associated with severe developmental delays including cerebral palsy and impairments in behavior, sensory, cardiovascular, and renal functions[312–314]. Postterm birth, on the other hand, is associated with neonatal encephalopathy and impaired social behavior in early childhood[315]. While there currently is no efficient treatment to halt preterm labor, labor in postterm women is often induced. However, labor induction efficacy is variable and often fails, leading to a high number of Caesarian sections, a procedure with associated surgical complications[5]. Ensuring that labor happens at term, between 37-40 weeks of pregnancy in women, will ensure better health outcomes for both mothers and their babies. By understanding the molecular mechanisms regulating labor onset, we can come up with novel pharmacological targets for preterm and postterm labors.

Labor onset is defined as a significant increase in uterine contractions, therefore the majority of this research focused on uterine contractile function in late pregnancy. While many factors regulate uterine contractions, little is known about what regulates the timing of labor onset. Interestingly, women that deliver at term exhibit a daily rhythm of uterine contractions, with significantly higher contractions at night than during the day in the third trimester of pregnancy[17]. This third-trimester nocturnal increase in uterine contractions is lost in some women with preterm birth[17], and significantly increased in others[242], suggesting daily rhythms within the uterus play a role in the timing of labor onset. One mechanism known to regulate daily changes in tissue function is the body's molecular clock. The molecular clock generates cellular endogenous 24h (circadian) rhythms through a complex feedback loop of molecular "clock" transcription factors, including the core transcription factors BMAL1, CLOCK, CRY1/2 and PER1/2/3[21]. The molecular clock exists in almost all cells and tissues in the body[21,71], aligning cell- and tissue-specific

functions to the appropriate time of day. The core molecular clock transcription factors are also associated with reproductive health and pregnancy outcomes[316–318]. Of particular interest is the involvement of these clock transcription factors in pregnancy outcome and labor progression/birth. Specifically, the dominant negative *ClockΔ19* mutant mice have non-productive labor (dystocia)[44], the myometrium-specific *Bmal1* knock-out mice have mistimed labor compared to wild-type mice[58], and *PER3* polymorphisms in humans are associated with sPTB[319]. Moreover, disruptions to circadian rhythms at the behavior level, particularly due to shiftwork, are associated with adverse pregnancy outcomes including an increased risk of miscarriage and sPTB in humans[317]. Despite these findings, little is known about how the molecular clock adapts to pregnancy and what roles it might lead in regulating uterine contractions in late pregnancy.

This thesis is separated into three topics with the overall goal of understanding how the molecular clock is involved in late pregnancy. My work looked at (1) how the molecular clock in reproductive tissues adapted to pregnancy in the mouse, (2) how the molecular clock is associated with sPTB in human, and (3) how the molecular clock regulates uterine contractions in late pregnancy.

Circadian rhythms in the body change as pregnancy progresses

Numerous studies have demonstrated that circadian rhythms and the molecular clock exist in different tissues in the non-pregnant state[71,72]. However, little is known about how the molecular clock adapts to pregnancy. Understanding changes in the molecular clock in normal pregnancy will allow us to figure out changes associated with pathologies of pregnancy complications, including mistimed labor onset, and identify potential targets for drug development for these complications. To answer this question, I looked at changes in the molecular clock in the reproductive axis (SCN, ovary, and uterus) as pregnancy progressed in mice. We found that circadian rhythms were present in the reproductive axis and the times of maximal clock gene expression changed from mid to late pregnancy in the mouse. As the molecular clock regulates

clock-controlled genes, this change in circadian rhythms of the reproductive axis in pregnancy would be expected to lead to changes in clock-controlled gene expression required for normal pregnancy progression. Evidence supporting a role of the molecular clock in normal pregnancy has been further demonstrated in mouse models with disrupted molecular clock function. Disruptions to the clock genes *Clock* (the negative dominant *ClockΔ19* mutant) and *Bmal1* (the myometrium-specific *Bmal1* knock-out) resulted in dystocia and mistiming of labor onset, respectively[44,45]. *Bmal1* null-mutants displayed an even more severe phenotype as they could not sustain pregnancy due to low serum progesterone levels[46], which could be one mechanism by which circadian rhythm disruption by shiftwork causes miscarriage in humans.

Though we do not know what regulates the change in the molecular clock in pregnancy, others have shown that steroid sex hormone levels, including estrogen and progesterone, have a daily change that also changes during pregnancy[320,321] and these hormones regulate circadian behavior[322–325]. Our study showed that progesterone regulated the molecular clock in the uterus and the SCN by decreasing time intervals between maximal clock gene expressions, thereby altering the timekeeping function in these tissues. However, even though the SCN controls locomotor activity onset and offset[326–328], we found no association between changes in SCN circadian rhythms and changes in circadian locomotor activity during pregnancy. Our findings show that progesterone regulates SCN circadian rhythms but does not regulate locomotor activity in the same manner during pregnancy compared to non-pregnancy. More work is needed to elucidate what regulates changes in locomotor behavior in pregnancy to understand the role of the molecular clock. In agreement with previously published findings[329], our study does show a decrease in murine locomotor activity as pregnancy progresses. However, our study revealed a daily delay in activity onset, whereas a previous study found a daily advance. This discrepancy could be due to the use of different mouse strains (C57BL6/J in our study versus C57BL6/N in the other study), different data analysis criteria for defining an activity bout, and different mouse housing facilities. Although mice are nocturnal (active at night) and humans are diurnal (active

during the day), during late pregnancy both species have a significant reduction in locomotor activity[329]. This supports the value of the mouse to further understand basic processes in normal pregnancy.

In conclusion, this work shows that circadian rhythms in the body change during normal pregnancy and identifies progesterone as a regulator of circadian rhythms at the tissue level. Future studies would involve identifying changes in circadian rhythms at the behavior level associated with adverse pregnancy outcomes such as preterm birth, to identify key behavioral changes as predictors for such pregnancy complications. Even though more work is also needed to understand what regulates circadian changes at the behavior level in pregnancy, the observed changes in circadian rhythms indicate that clock genes play a role in normal pregnancy.

Lower levels of the clock genes CLOCK and CRY2 put women at significantly increased risk of sPTB

While studies in humans and mice with environmental or genetic disruption to the circadian system have shown an association between disruptions of circadian rhythms and adverse pregnancy outcomes including miscarriage and sPTB[317], no work has focused on determining if changes in clock genes might be predictable of pregnancy outcome. To determine if clock gene levels in maternal blood change in women with sPTB, we analyzed publicly available gene expression data and found that low blood levels of *CLOCK* and *CRY2* in the second trimester of pregnancy significantly increased the risk of sPTB (Figure 5). This identified for the first time clock genes as potential biomarkers for sPTB. In addition, women with sPTB had deregulated *PER3* expression. As *PER3* polymorphisms have been associated with sPTB[319], this finding suggests that *PER3* may play a role in the pathology of sPTB and further supports that deregulation of clock genes and the circadian system negatively impact pregnancy outcome.[330]

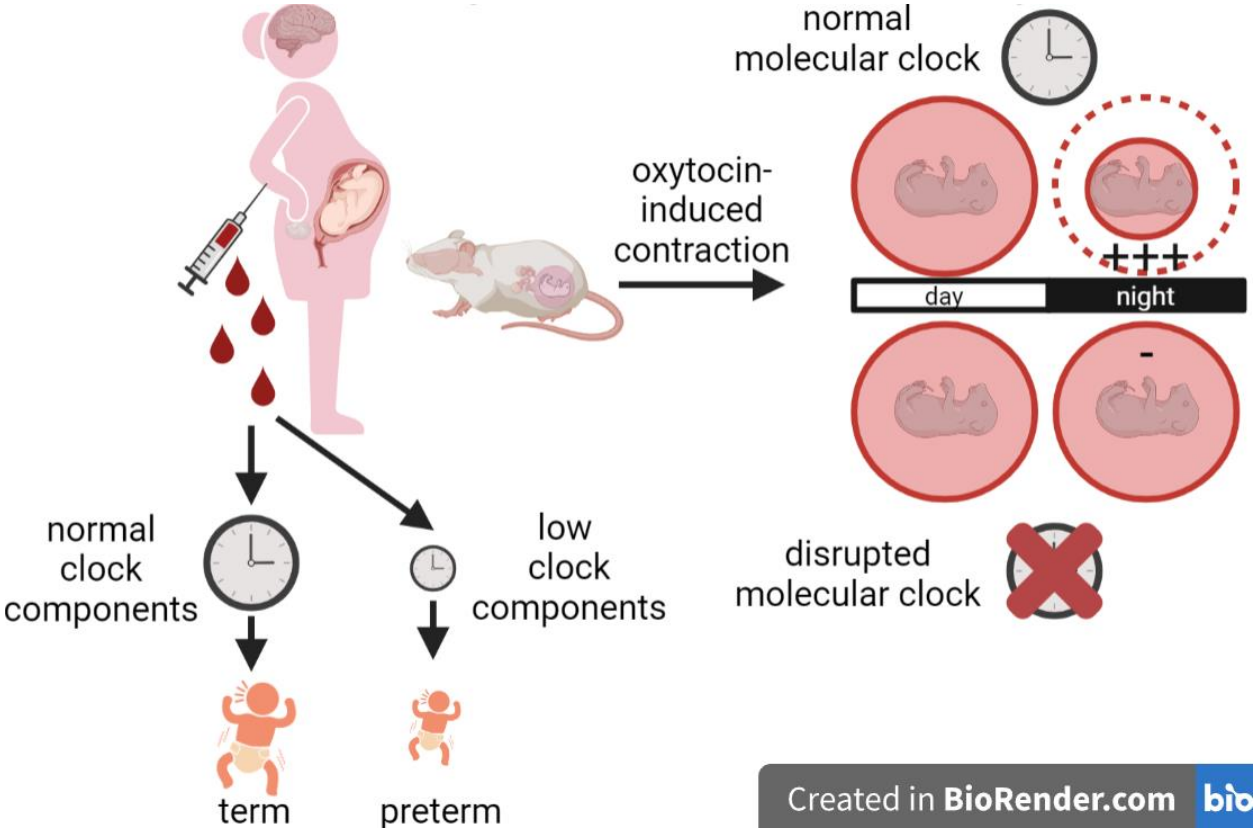

Figure 5.1. The molecular clock plays a role in normal pregnancy. The molecular clock exists in the reproductive axis, changes as pregnancy progresses, and adapts to changing levels of the core pregnancy hormone progesterone. The molecular clock is required for normal pregnancy progression as low serum levels of the clock genes *CLOCK, CRY2, and PER3* increased the risk of sPTB, showing a potential for the molecular clock to be used as biomarkers for sPTB. Lastly, the molecular clock regulates daily uterine contractile function, both spontaneous contractions and contractile response to oxytocin, indicating that time-of-day of oxytocin impacts the efficacy of oxytocin to promote contractions.

To further understand the potential role of the clock in sPTB, we performed a bioinformatics analysis to identify pathways predicted to be deregulated when *CRY2* and *CLOCK* were low. Among the identified pathways were those involved in cervical ripening[331] and maintaining uterine quiescence[261]. As labor can only happen when the cervix is ripe (sufficiently

thin and open to allow passage of the fetus) and uterine contractions are sufficient in strength, frequency and duration to push the fetus, these are undoubtedly two key factors involved in labor onset. These pathways might be under direct regulations of the molecular clock and play a role in the pathology of sPTB. However, more work is needed to establish a contribution of the identified pathways in sPTB and establish their value as potential targets for drug development.

In conclusion, in the second study, we identified *CLOCK, CRY2 and PER3* as associated with increased risk of sPTB. In addition, we found that *CLOCK* and *CRY2* are potential biomarkers for sPTB and their associated pathways might be involved in the pathology of sPTB. It is worth mentioning, however, that the dataset we used for our analysis did not consider time of day or time of year of serum collection. Because clock gene expression changes with the time of day and time of year (seasonality) and is associated with sPTB[330], future studies should take these two factors into consideration.

The myometrial molecular clock regulates uterine contractile function in late pregnancy

Given the lack of efficient treatments or biomarkers for sPTB, our finding that low *CRY2* and *CLOCK* are associated with sPTB led us to more closely examine the role of the molecular clock in uterine smooth muscle (myometrium) function in pregnancy. We generated a mouse model with low myometrial levels of clock genes by conditionally deleting the clock gene *Bmal1* and studied *ex vivo* uterine contractions in late pregnancy in these cKO mice. The cKO mice exhibited stronger *ex vivo* spontaneous uterine contractions than control mice, a phenomenon seen in women with sPTB[242,302]. The fact that cKO mice had stronger *ex vivo* spontaneous uterine contractions than control mice only during the light (inactive) phase shows a time-of-day effect on spontaneous uterine contractions, supporting the role of the molecular clock in regulating spontaneous uterine contractions. As the molecular clock regulates daily tissue function, this finding suggests that the molecular clock is also involved in daily uterine contractile function.

Since oxytocin is the most commonly used hormone in labor induction and many of its antagonists have been studied as treatments for preterm labor, we examined daily uterine contractile response to oxytocin. Indeed, the uterine strips from control mice exhibited a time-of-day contractile response to oxytocin, with the biggest difference between ZT11 and ZT15. Interestingly, this is the time encompassing the transition between the light phase and the dark phase, when mice generally give birth[274], suggesting that the daily uterine contractile response to oxytocin may play a role in the timing of labor onset. This finding is also the first chronopharmacological study done on the uterus in pregnancy, displaying its potential application in improving labor induction efficiency by scheduling labor induction at the time of day when the uterus is most responsive to oxytocin. To determine if the molecular clock regulates uterine contractile response to oxytocin, we compared uterine contractile response to oxytocin in cKO and control and found that cKO displayed a diminished response to oxytocin as compared to control. Even though *Oxtr* expression is regulated by BMAL1, OXTR levels did not correlate with time-of-day changes in uterine contractile response to oxytocin in control mice or explain the difference in contractile response to oxytocin seen between cKO and control. Based on the current literature, we propose that the complex mechanisms underlying the observed uterine contractile response to oxytocin could be generated downstream of OXTR, particularly by the capacity of OXTR to regulate calcium channel or potassium channel functions. However, such studies were out of scope for our studies and not explored in this dissertation, but they are interesting avenues for future research.

In conclusion, this work shows that the molecular clock regulates spontaneous uterine contractions and impacts the contractile response to oxytocin. Future work will involve identifying the key mechanisms underlying uterine contractile function differences between control and cKO and determining how the molecular clock can be used as a target for pharmacological development to treat preterm labor or enhance labor induction efficacy. Our finding that time of day impacts oxytocin capability to induce uterine contractions shows the potential for

chronopharmacology in enhancing labor induction, by scheduling labor induction when the uterus is most responsive to oxytocin. More work is needed to apply this concept in the clinical setting.

Overall conclusion

Preterm and postterm birth continue to cause serious neonatal morbidity and mortality and lack effective treatments. While strong evidence exists linking a role of circadian rhythms in maintaining normal pregnancy and the timing of labor onset, little is known about mechanisms underlying how circadian rhythms regulate these processes. This presented work begins to answer this gap of knowledge by investigating how the molecular clock is involved in regulating uterine contractile function in late pregnancy (Figure 5). Specifically, we established how the molecular clock in the reproductive axis changed in normal pregnancy in mice, identified the clock genes *CLOCK, CRY2* and *PER3* as associated with sPTB in women, and investigated the role of the clock gene *Bmal1* in *ex vivo* spontaneous uterine contractions and uterine contractile response to oxytocin in late pregnancy in the mouse. This work has shown that the molecular clock is a promising biomarker for sPTB and potential target for drug development for sPTB. Based on these results, chronopharmacolgy could be implemented to improve labor induction efficiency in the future. Even though more work is needed, the research done in this PhD dissertation provides a first step towards understanding and utilizing circadian rhythms in uterine functions to improve pregnancy outcomes.

REFERENCES

REFERENCES

1. Martin JA, Hamilton BE, Osterman MJK, Driscoll AK, Drake P. National Vital Statistics Reports Volume 67, Number 8, November 7, 2018. *National Vital Statistics Reports*. 2018;67(8):1-50. https://www.cdc.gov/nchs/data_access/Vitalstatsonline.htm

2. Martin JA, Hamilton BE, D P, et al. National Vital Statistics Reports Births : Final Data for 2018. *Statistics (Ber)*. 2019;68(13):1-47.

3. Truven Health Analytics Marketscan. The Cost of Having a Baby in the US. 2013;(January):1-85.

4. Truven Health Analytics Marketscan. The Cost of Having a Baby in the US. 2013;(January):1-85.

5. Caughey AB, Cahill AG, Guise JM, Rouse DJ. Safe prevention of the primary cesarean delivery This document was developed jointly by the with the assistance of. *American Journal of Obstetrics and Gynecology*. 2014;210(3):179-193. doi:10.1016/j.ajog.2014.01.026

6. Mayo Clinic. Labor induction. Published online 2019:2019.

7. Mathews TJ, Curtin S. When are babies born: morning, noon, or night? Birth certificate data for 2013. *NCHS Data Brief*. 2015;(200):200.

8. Cagnacci A, Soldani R, Melis GB, Volpe A. Diurnal rhythms of labor and delivery in women: modulation by parity and seasons. *Am J Obstet Gynecol*. 1998;178(1):140-145.

9. Olcese J. Circadian aspects of mammalian parturition : A review. *Molecular and Cellular Endocrinology*. 2012;349(1):62-67. doi:10.1016/j.mce.2011.06.041

10. Olcese J, Lozier S, Paradise C. Melatonin and the circadian timing of human parturition. *Reproductive Sciences*. 2013;20(2):168-174. doi:10.1177/1933719112442244

11. Moore J, Low LK. Factors that influence the practice of elective induction of labor: What does the evidence tell us? *Journal of Perinatal and Neonatal Nursing*. 2012;26(3):242-250. doi:10.1097/JPN.0b013e31826288a9

12. Bakker JJH, van der Goes BY, Pel M, Mol BWJ, van der Post JAM. Morning versus evening induction of labour for improving outcomes. *Cochrane Database of Systematic Reviews*. 2013;2013(2). doi:10.1002/14651858.CD007707.pub2

13. Mathews TJ, Curtin S. When are babies born: morning, noon, or night? Birth certificate data for 2013. *NCHS Data Brief*. 2015;(200):200.

14. McAllister-Williams RH, Bertrand D, Rollema H, et al. Pitocin. *Encyclopedia of Psychopharmacology*. Published online 2010:1030-1030. doi:10.1007/978-3-540-68706-1_4463

15. Otsuki Y, Yamaji K, Fujita M, Takagi T, Tanizawa O. Serial Plasma Oxytocin Levels during Pregnancy and Labor. *Acta Obstetricia et Gynecologica Scandinavica*. 1983;62:15-18.

16. Rahman SA, Bibbo C, Olcese J, Czeisler CA, Robinson JN, Klerman EB. Relationship between endogenous melatonin concentrations and uterine contractions in late third trimester of human pregnancy. *Journal of Pineal Research*. 2019;66(4):1-7. doi:10.1111/jpi.12566

17. Germain AM, Valenzuela GJ, Ivankovic M, Ducsay CA, Gabella C, Serón-Ferré M. Relationship of circadian rhythms of uterine activity with term and preterm delivery. *American Journal of Obstetrics and Gynecology*. 1993;168(4):1271-1277. doi:10.1016/0002-9378(93)90379-W

18. Honnebier MB, Myers T, Figueroa JP, Nathanielsz PW. Variation in myometrial response to intravenous oxytocin administration at different times of the day in the pregnant rhesus monkey. *Endocrinology*. 1989;125(3):1498-1503. doi:10.1210/endo-125-3-1498

19. Mohawk JA, Green CB, Takahashi JS. Central and Peripheral Circadian Clocks in Mammals. *Annual Review of Neuroscience*. Published online 2012. doi:10.1146/annurev-neuro-060909-153128

20. Ko CH, Takahashi JS. Molecular components of the mammalian circadian clock. *Hum Mol Genet*. 2006;15(suppl_2):R271-R277.

21. Lowrey PL, Takahashi JS. *Genetics of Circadian Rhythms in Mammalian Model Organisms*. Vol 74.; 2011. doi:10.1016/B978-0-12-387690-4.00006-4

22. Merrow M, Spoelstra K, Roenneberg T. The circadian cycle: Daily rhythms from behaviour to genes. *EMBO Reports*. 2005;6(10):930-935. doi:10.1038/sj.embor.7400541

23. Serin Y, Acar Tek N. Effect of Circadian Rhythm on Metabolic Processes and the Regulation of Energy Balance. *Annals of Nutrition and Metabolism*. 2019;74(4):322-330. doi:10.1159/000500071

24. Fustin JM, O'Neill JS, Hastings MH, Hazlerigg DG, Dardente H. Cry1 circadian phase in vitro: Wrapped up with an E-box. *Journal of Biological Rhythms*. 2009;24(1):16-24. doi:10.1177/0748730408329267

25. Yoo SH, Ko CH, Lowrey PL, et al. *A Noncanonical E-Box Enhancer Drives Mouse Period2 Circadian Oscillations in Vivo*.; 2005. www.pnas.orgcgidoi10.1073pnas.0409763102

26. Jin X, Shearman LP, Weaver DR, et al. *A Molecular Mechanism Regulating Rhythmic Output from the Suprachiasmatic Circadian Clock*. Vol 96.; 1999.

27. Hao H, Allen DL, Hardin PE. *A Circadian Enhancer Mediates PER-Dependent MRNA Cycling in Drosophila Melanogaster*. Vol 17.; 1997. https://journals.asm.org/journal/mcb

28. Kume K, Zylka MJ, Sriram S, et al. *MCRY1 and MCRY2 Are Essential Components of the Negative Limb of the Circadian Clock Feedback Loop to Coordinated Circadian*

Outputs from the Nucleus, Ulti-Mately Regulating Rhythms in Physiology and Behavior (Welsh et al Circadian Clocks Also Appear to Exist in Several Periph-Eral Tissues of Mammals That Are Synchronized by The. Vol 98.; 1999.

29. Kumaki Y, Ukai-Tadenuma M, Uno K ichiro D, et al. Analysis and synthesis of high-amplitude Cis-elements in the mammalian circadian clock. *Proceedings of the National Academy of Sciences*. 2008;105(39):14946-14951. doi:10.1073/pnas.0802636105

30. Chaudhary J, Skinner MK. Basic Helix-Loop-Helix Proteins Can Act at the E-Box within the Serum Response Element of the c- *fos* Promoter to Influence Hormone-Induced Promoter Activation in Sertoli Cells. *Molecular Endocrinology*. 1999;13(5):774-786. doi:10.1210/mend.13.5.0271

31. Desbarats L, Gaubatz S, Eilers M. Discrimination between different E-box-binding proteins at an endogenous target gene of c-myc. *Genes Dev*. 1996;10(4):447-460. doi:10.1101/gad.10.4.447

32. Gekakis N, Staknis D, Nguyen HB, et al. Role of the CLOCK protein in the mammalian circadian mechanism. *Science (1979)*. 1998;280(5369):1564-1569. doi:10.1126/science.280.5369.1564

33. Lee C, Etchegaray JP, Cagampang FR, Loudon AS, Reppert SM. Posttranslational mechanisms regulate the mammalian circadian clock. *Cell*. 2001;107(7):855-867. doi:10.1016/s0092-8674(01)00610-9

34. Sato TK, Panda S, Miraglia LJ, et al. A functional genomics strategy reveals rora as a component of the mammalian circadian clock. *Neuron*. 2004;43(4):527-537. doi:10.1016/j.neuron.2004.07.018

35. Guillaumond F, Dardente H, Giguère V, Cermakian N. Differential control of Bmal1 circadian transcription by REV-ERB and ROR nuclear receptors. *Journal of Biological Rhythms*. 2005;20(5):391-403. doi:10.1177/0748730405277232

36. Akashi M, Takumi T. The orphan nuclear receptor RORα regulates circadian transcription of the mammalian core-clock Bmal1. *Nature Structural and Molecular Biology*. 2005;12(5):441-448. doi:10.1038/nsmb925

37. Preitner N, Damiola F, Luis-Lopez-Molina, et al. The orphan nuclear receptor REV-ERBα controls circadian transcription within the positive limb of the mammalian circadian oscillator. *Cell*. 2002;110(2):251-260. doi:10.1016/S0092-8674(02)00825-5

38. Triqueneaux G, Thenot S, Kakizawa T, et al. The orphan receptor Rev-erbα gene is a target of the circadian clock pacemaker. *Journal of Molecular Endocrinology*. 2004;33(3):585-608. doi:10.1677/jme.1.01554

39. Yang X, Downes M, Yu RT, et al. Nuclear Receptor Expression Links the Circadian Clock to Metabolism. *Cell*. 2006;126(4):801-810. doi:10.1016/j.cell.2006.06.050

40. Bunger MK, Wilsbacher LD, Moran SM, et al. Mop3 is an essential component of the master circadian pacemaker in mammals. 2000;103(7):1009-1017.

41. Levi F, Schibler U. Circadian rhythms: Mechanisms and therapeutic implications. *Annual Review of Pharmacology and Toxicology*. 2007;47:593-628. doi:10.1146/annurev.pharmtox.47.120505.105208

42. Wharfe MD, Mark PJ, Wyrwoll CS, et al. Pregnancy-induced adaptations of the central circadian clock and maternal glucocorticoids. *Journal of Endocrinology*. 2016;228(3):135-147. doi:10.1530/JOE-15-0405

43. Wharfe MD, Wyrwoll CS, Waddell BJ, Mark PJ. Pregnancy suppresses the daily rhythmicity of core body temperature and adipose metabolic gene expression in the mouse. *Endocrinology*. 2016;157(9):3320-3331. doi:10.1210/en.2016-1177

44. Dolatshad H, Campbell EA, O'hara L, Maywood ES, Hastings MH, Johnson MH. Developmental and reproductive performance in circadian mutant mice. *Human reproduction*. 2005;21(1):68-79.

45. Ratajczak CK, Boehle KL, Muglia LJ. Impaired steroidogenesis and implantation failure in Bmal1 -/-mice. *Endocrinology*. 2009;150(4):1879-1885. doi:10.1210/en.2008-1021

46. Boden MJ, Varcoe TJ, Voultsios A, Kennaway DJ. Reproductive biology of female Bmal1 null mice. *Reproduction*. 2010;139(6):1077-1090. doi:10.1530/REP-09-0523

47. Zhai J, Li S, Hu J, et al. In Silico, In Vitro, and In Vivo Analysis Identifies Endometrial Circadian Clock Genes in Recurrent Implantation Failure. *J Clin Endocrinol Metab*. 2021;106(7):2077-2091. doi:10.1210/clinem/dgab119

48. Cui L, Xu F, Wang S, et al. Pharmacological activation of rev-erbα suppresses LPS-induced macrophage M1 polarization and prevents pregnancy loss. *BMC Immunol*. 2021;22(1):57. doi:10.1186/s12865-021-00438-4

49. Li Y, Li J, Hou Y, et al. Circadian clock gene Clock is involved in the pathogenesis of preeclampsia through hypoxia. *Life Sciences*. 2020;247. doi:10.1016/j.lfs.2020.117441

50. Hodžic A, Lavtar P, Ristanovic M, Novakovic I, Dotlic J, Peterlin B. Genetic variation in the clock gene is associated with idiopathic recurrent spontaneous abortion. *PLoS ONE*. 2018;13(5):8-13. doi:10.1371/journal.pone.0196345

51. Kovanen L, Saarikoski ST, Aromaa A, Lönnqvist J, Partonen T. ARNTL (BMAL1) and NPAS2 gene variants contribute to fertility and seasonality. *PLoS ONE*. 2010;5(4). doi:10.1371/journal.pone.0010007

52. McDearmon EL, Patel KN, Ko CH, et al. Dissecting the functions of the mammalian clock protein BMAL1 by tissue-specific rescue in mice. *Science (1979)*. 2006;314(5803):1304-1308. doi:10.1126/science.1132430

53. Liu AC, Tran HG, Zhang EE, Priest AA, Welsh DK, Kay SA. Redundant Function of REV-ERBα and β and Non-Essential Role for Bmal1 Cycling in Transcriptional Regulation of Intracellular Circadian Rhythms. Takahashi JS, ed. *PLoS Genetics*. 2008;4(2):e1000023. doi:10.1371/journal.pgen.1000023

54. Ko CH, Yamada YR, Welsh DK, et al. Emergence of Noise-Induced Oscillations in the Central Circadian Pacemaker. Mignot E, ed. *PLoS Biology*. 2010;8(10):e1000513. doi:10.1371/journal.pbio.1000513

55. DeBruyne JP, Weaver DR, Reppert SM. CLOCK and NPAS2 Have Overlapping Roles in the SCN Circadian Clock. *Nat Neurosci*. 2007;10(5):543-545. doi:doi: 10.1038/nn1884

56. Liu AC, Tran HG, Zhang EE, Priest AA, Welsh DK, Kay SA. Redundant function of REV-ERBα and β and non-essential role for Bmal1 cycling in transcriptional regulation of intracellular circadian rhythms. *PLoS Genetics*. 2008;4(2). doi:10.1371/journal.pgen.1000023

57. Takahashi JS, Ko CH, Yamada YR, et al. Emergence of noise-induced oscillations in the central circadian pacemaker. *PLoS Biology*. 2010;8(10). doi:10.1371/journal.pbio.1000513

58. Ratajczak CK, Asada M, Allen GC, et al. Generation of myometrium-specific Bmal1 knockout mice for parturition analysis. *Reproduction, Fertility and Development*. Published online 2012. doi:10.1071/RD11164

59. Yoo SH, Yamazaki S, Lowrey PL, et al. PERIOD2 :: LUCIFERASE real-time reporting of circadian dynamics reveals persistent circadian oscillations in mouse peripheral tissues. 2004;101(15):5339-5346.

60. Welsh DK, Imaizumi T, Kay SA. Real-time reporting of circadian-regulated gene expression by luciferase imaging in plants and mammalian cells. *Methods in Enzymology*. 2005;393:269-288. doi:10.1016/S0076-6879(05)93011-5

61. Yamazaki S, Numano R, Abe M, et al. Resetting Central and Peripheral Circadian Oscillators in Transgenic Rats. Published online 2000:682-685.

62. Hastings MH, Herzog ED. Clock genes, oscillators, and cellular networks in the suprachiasmatic nuclei. *Journal of Biological Rhythms*. 2004;19(5):400-413. doi:10.1177/0748730404268786

63. Wilsbacher LD, Yamazaki S, Herzog ED, et al. Photic and circadian expression of luciferase in mPeriod1-luc transgenic mice in vivo. *Proceedings of the National Academy of Sciences*. 2002;99(1):489-494. doi:10.1073/pnas.012248599

64. Feeney KA, Putker M, Brancaccio M, O'Neill JS. In-depth Characterization of Firefly Luciferase as a Reporter of Circadian Gene Expression in Mammalian Cells. *Journal of Biological Rhythms*. 2016;31(6):540-550. doi:10.1177/0748730416668898

65. Osaghae BE, Arrowsmith S, Wray S. Gestational and Hormonal Effects on Magnesium Sulfate's Ability to Inhibit Mouse Uterine Contractility. *Reproductive Sciences*. Published online 2019. doi:10.1177/1933719119828089

66. Kim SH, Riaposova L, Ahmed H, et al. Oxytocin Receptor Antagonists, Atosiban and Nolasiban, Inhibit Prostaglandin F 2α -induced Contractions and Inflammatory Responses in Human Myometrium. *Scientific Reports*. 2019;9(1):1-10. doi:10.1038/s41598-019-42181-2

67. Mackler AM, Ducsay CA, Veldhuis JD, Yellon SM. Maturation of spontaneous and agonist-induced uterine contractions in the peripartum mouse uterus. *Biology of Reproduction*. 1999;61(4):873-878. doi:10.1095/biolreprod61.4.873

68. McCarthy R, Martin-Fairey C, Sojka DK, et al. Mouse models of preterm birth: suggested assessment and reporting guidelines. *Biol Reprod*. 2018;99(5):922-937. doi:10.1093/biolre/ioy109

69. Kasahara T, Abe K, Mekada K, Yoshiki A, Kato T. Genetic variation of melatonin productivity in laboratory mice under domestication. *Proc Natl Acad Sci U S A*. 2010;107(14):6412-6417. doi:10.1073/pnas.0914399107

70. Kennaway DJ. Melatonin research in mice: a review. *Chronobiology International*. 2019;36(9):1167-1183. doi:10.1080/07420528.2019.1624373

71. Lowrey PL, Takahashi JS. MAMMALIAN CIRCADIAN BIOLOGY: Elucidating Genome-Wide Levels of Temporal Organization. *Annual Review of Genomics and Human Genetics*. 2004;5(1):407-441. doi:10.1146/annurev.genom.5.061903.175925

72. Ratajczak CK, Herzog ED, Muglia LJ. Clock Gene Expression in Gravid Uterus and Extra-Embryonic Tissues during Late Gestation in the Mouse. *Reproduction, Fertility and Development*. 2010;22(5). doi:10.1071/RD09243

73. Sellix MT, Menaker M. Circadian clocks in the ovary. *Trends in Endocrinology & Metabolism*. 2010;21(10):628-636.

74. Hellier V, Brock O, Candlish M, et al. Female sexual behavior in mice is controlled by kisspeptin neurons. *Nature Communications*. 2018;9(1):400. doi:10.1038/s41467-017-02797-2

75. Simonneaux V, Bahougne T, Angelopoulou E. Daily rhythms count for female fertility. *Best Practice & Research Clinical Endocrinology & Metabolism*. 2017;31(5):505-519.

76. Boden MJ, Varcoe TJ, Kennaway DJ. Circadian regulation of reproduction: From gamete to offspring. *Progress in Biophysics and Molecular Biology*. Published online 2013. doi:10.1016/j.pbiomolbio.2013.01.003

77. Sen A, Hoffmann HM. Role of core circadian clock genes in hormone release and target tissue sensitivity in the reproductive axis. *Molecular and Cellular Endocrinology*. Published online February 2020. doi:10.1016/j.mce.2019.110655

78. Ko CH, Takahashi JS. Molecular components of the mammalian circadian clock. *Hum Mol Genet*. 2006;15(suppl_2):R271-R277.

79. Zhang WX, Chen SY, Liu C. Regulation of reproduction by the circadian rhythms. *Sheng li xue bao:[Acta physiologica Sinica]*. 2016;68(6):799-808.

80. Paul S, Brown T. Direct effects of the light environment on daily neuroendocrine control. *Journal of Endocrinology*. 2019;1(aop).

81. Robinson JE, Karsch FJ. Refractoriness to inductive day lengths terminates the breeding season of the Suffolk ewe. *Biol Reprod*. 1984;31(4):656-663.

82. Robinson JE, Follett BK. Photoperiodism in Japanese quail: the termination of seasonal breeding by photorefractoriness. *Proceedings of the Royal Society of London Series B Biological Sciences*. 1982;215(1198):95-116.

83. Wang D, Li N, Tian L, et al. Dynamic expressions of hypothalamic genes regulate seasonal breeding in a natural rodent population. *Mol Ecol*. Published online 2019.

84. Dardente H, Wood S, Ebling F, Sáenz de Miera C. An integrative view of mammalian seasonal neuroendocrinology. *J Neuroendocrinol*. 2019;31(5):e12729.

85. Mosko SS, Moore RY. Neonatal ablation of the suprachiasmatic nucleus. Effects on the development of the pituitary-gonadal axis in the female rat. *Neuroendocrinology*. 1979;29(5):350-361.

86. Kriegsfeld LJ, Williams III WP. Circadian control of neuroendocrine circuits regulating female reproductive function. *Front Endocrinol (Lausanne)*. 2012;3:60.

87. Smarr BL, Gile JJ, De La Iglesia HO. Oestrogen-independent circadian clock gene expression in the anteroventral periventricular nucleus in female rats: Possible role as an integrator for circadian and ovarian signals timing the luteinising hormone surge. *J Neuroendocrinol*. 2013;25(12):1273-1279.

88. Williams III WP, Jarjisian SG, Mikkelsen JD, Kriegsfeld LJ. Circadian control of kisspeptin and a gated GnRH response mediate the preovulatory luteinizing hormone surge. *Endocrinology*. 2010;152(2):595-606.

89. Reppert SM. Time of birth in the rat is gated to the daily light cycle by a circadian mechanism. *Pediatr Res*. 1983;17:154A.

90. Olcese J. Circadian aspects of mammalian parturition: a review. *Molecular and Cellular Endocrinology*. 2012;349(1):62-67.

91. Backe B. A circadian variation in the observed duration of labor. *Acta Obstet Gynecol Scand*. 1991;70(6):465-468.

92. Cagnacci A, Soldani R, Melis GB, Volpe A. Diurnal rhythms of labor and delivery in women: modulation by parity and seasons. *Am J Obstet Gynecol*. 1998;178(1):140-145.

93. Martin-Fairey CA, McCarthy R, Ma X, England S, Herzog E. Chronotype changes during pregnancy. *Reproductive Sciences*. 2016;23(1 SUPPL. 1):291A.

94. Martin-Fairey CA, Zhao P, Wan L, et al. Pregnancy Induces an Earlier Chronotype in Both Mice and Women. *J Biol Rhythms*. 2019;34(3):323-331.

95. LeSauter J, Silver R. Localization of a suprachiasmatic nucleus subregion regulating locomotor rhythmicity. *Journal of Neuroscience*. 1999;19(13):5574-5585.

96. Stephan FK, Zucker I. Circadian rhythms in drinking behavior and locomotor activity of rats are eliminated by hypothalamic lesions. *Proceedings of the National Academy of Sciences*. 1972;69(6):1583-1586.

97. Schwartz WJ, Zimmerman P. Lesions of the suprachiasmatic nucleus disrupt circadian locomotor rhythms in the mouse. *Physiol Behav*. 1991;49(6):1283-1287.

98. Bell AW, Bauman DE. Adaptations of glucose metabolism during pregnancy and lactation. *J Mammary Gland Biol Neoplasia*. 1997;2(3):265-278.

99. Kumar P, Magon N. Hormones in pregnancy. *Nigerian medical journal: journal of the Nigeria Medical Association*. 2012;53(4):179.

100. Rutter J, Reick M, McKnight SL. Metabolism and the control of circadian rhythms. *Annu Rev Biochem*. 2002;71(1):307-331.

101. Froy O. Metabolism and circadian rhythms—implications for obesity. *Endocr Rev*. 2009;31(1):1-24.

102. Huang W, Ramsey KM, Marcheva B, Bass J. Circadian rhythms, sleep, and metabolism. *J Clin Invest*. 2011;121(6):2133-2141.

103. Albers EE, Gerall AA, Axelson JF. Effect of reproductive state on circadian periodicity in the rat. *Physiol Behav*. 1981;26(1):21-25.

104. Morin LP, Fitzgerald KM, Zucker I. Estradiol shortens the period of hamster circadian rhythms. *Science (1979)*. 1977;196(4287):305-307.

105. Takahashi JS, Menaker M. Interaction of estradiol and progesterone: effects on circadian locomotor rhythm of female golden hamsters. *American Journal of Physiology-Regulatory, Integrative and Comparative Physiology*. 1980;239(5):R497-R504.

106. Virgo BB, Bellward GD. Serum Progesterone Levels in the Pregnant and Postpartum Laboratory Mouse. *Endocrinology*. 1974;95(5):1486-1490. doi:10.1210/endo-95-5-1486

107. Barkley MS, Geschwind II. The Gestational and Progesterone Pattern Secretion of Estradiol , in Selected Testosterone Strains of Mice surges on. *Biology of Reproduction*. Published online 1979:733-738.

108. Barkley MS, Michael SD, Geschwind II, Bradford GE. Plasma testosterone during pregnancy in the mouse. *Endocrinology*. 1977;100(5):1472-1475. doi:10.1210/endo-100-5-1472

109. Bhurke AS, Bagchi IC, Bagchi MK. Progesterone-regulated endometrial factors controlling implantation. *American journal of reproductive immunology*. 2016;75(3):237-245.

110. Halasz M, Szekeres-Bartho J. The role of progesterone in implantation and trophoblast invasion. *J Reprod Immunol*. 2013;97(1):43-50.

111. Moriyama Ii, Sugawa T. Progesterone facilitates implantation of xenogenic cultured cells in hamster uterus. *Nature New Biology*. 1972;236(66):150-152.

112. Bindon BM. The role of progesterone in implantation in the sheep. *Australian Journal of Biological Sciences*. 1971;24(1):149-158.

113. Garg D, Ng SSM, Baig KM, Driggers P, Segars J. Progesterone-Mediated Non-Classical Signaling. *Trends in Endocrinology and Metabolism*. 2017;28(9):656-668. doi:10.1016/j.tem.2017.05.006

114. Karteris E, Zervou S, Pang Y, et al. Progesterone signaling in human myometrium through two novel membrane G protein-coupled receptors: Potential role in functional progesterone withdrawal at term. *Molecular Endocrinology*. 2006;20(7):1519-1534. doi:10.1210/me.2005-0243

115. Grimm SL, Hartig SM, Edwards DP. Progesterone Receptor Signaling Mechanisms. *Journal of Molecular Biology*. 2016;428(19):3831-3849. doi:10.1016/j.jmb.2016.06.020

116. Cabral R, Gutiérrez M, Fernández AI, Cantabrana B, Hidalgo A. Progesterone and pregnanolone derivatives relaxing effect on smooth muscle. *General Pharmacology*. 1994;25(1):173-178. doi:10.1016/0306-3623(94)90029-9

117. Wu SP, DeMayo FJ. Progesterone receptor signaling in uterine myometrial physiology and preterm birth. In: *Current Topics in Developmental Biology*. Vol 125. Elsevier; 2017:171-190.

118. Bhurke AS, Bagchi IC, Bagchi MK. Progesterone-regulated endometrial factors controlling implantation. *American journal of reproductive immunology*. 2016;75(3):237-245.

119. Hartmann PE, Trevethan P, Shelton JN. Progesterone and oestrogen and the initiation of lactation in ewes. *Journal of Endocrinology*. 1973;59(2):249-259.

120. Lyons WR. Hormonal synergism in mammary growth. *Proceedings of the Royal Society of London Series B-Biological Sciences*. 1958;149(936):303-325.

121. Cowie AT, Lyons WR. Mammogenesis and lactogenesis in hypophysectomized, ovariectomized, adrenalectomized rats. *Journal of Endocrinology*. 1959;19(1):29-NP.

122. Meites J. Recent studies on the mechanisms controlling the initiation of lactation. *Rev Can Biol*. 1954;13(4):359-370.

123. Bridges RS. A quantitative analysis of the roles of dosage, sequence, and duration of estradiol and progesterone exposure in the regulation of maternal behavior in the rat. *Endocrinology*. 1984;114(3):930-940.

124. Bridges RS, Rosenblatt JS, Feder HH. Serum progesterone concentrations and maternal behavior in rats after pregnancy termination: behavioral stimulation after progesterone withdrawal and inhibition by progesterone maintenance. *Endocrinology*. 1978;102(1):258-267.

125. Nielsen BW, Bonney EA, Pearce BD, Donahue LR, Sarkar IN, (PREBIC) PBIC. A cross-species analysis of animal models for the investigation of preterm birth mechanisms. *Reproductive Sciences*. 2016;23(4):482-491.

126. Kalkhoff RK. Metabolic effects of progesterone. *American Journal of Obstetrics and Gynecology*. 1982;142(6 II):735-738. doi:10.1016/S0002-9378(16)32480-2

127. Padilla SL, Perez JG, Ben-Hamo M, et al. Kisspeptin neurons in the arcuate nucleus of the hypothalamus orchestrate circadian rhythms and metabolism. *Current Biology*. 2019;29(4):592-604.

128. Marraudino M, Martini M, Trova S, et al. Kisspeptin system in ovariectomized mice: estradiol and progesterone regulation. *Brain Res*. 2018;1688:8-14.

129. Stephens SBZ, Tolson KP, Rouse Jr ML, et al. Absent progesterone signaling in kisspeptin neurons disrupts the LH surge and impairs fertility in female mice. *Endocrinology*. 2015;156(9):3091-3097.

130. Mahoney MM. Shift work, jet lag, and female reproduction. *Int J Endocrinol*. 2010;2010.

131. Dolatshad H, Campbell EA, O'hara L, Maywood ES, Hastings MH, Johnson MH. Developmental and reproductive performance in circadian mutant mice. *Human reproduction*. 2005;21(1):68-79.

132. Goldberg RJ, Ye C, Sermer M, et al. Circadian variation in the response to the glucose challenge test in pregnancy: implications for screening for gestational diabetes mellitus. *Diabetes Care*. 2012;35(7):1578-1584.

133. Nisa H, Qi KHT, Leng J, et al. The Circadian Rhythm–Related MTNR1B Genotype, Gestational Weight Gain, and Postpartum Glycemic Changes. *The Journal of Clinical Endocrinology & Metabolism*. 2018;103(6):2284-2290.

134. Pappa KI, Gazouli M, Anastasiou E, Iliodromiti Z, Antsaklis A, Anagnou NP. Circadian clock gene expression is impaired in gestational diabetes mellitus. *Gynecological Endocrinology*. 2013;29(4):331-335.

135. Zornoza-Moreno M, Fuentes-Hernández S, Prieto-Sánchez MT, et al. Influence of gestational diabetes on circadian rhythms of children and their association with fetal adiposity. *Diabetes Metab Res Rev*. 2013;29(6):483-491.

136. Rugh R. The mouse. Its reproduction and development. *The mouse Its reproduction and development*. Published online 1968.

137. Hoffmann HM. Determination of Reproductive Competence by Confirming Pubertal Onset and Performing a Fertility Assay in Mice and Rats. *JoVE (Journal of Visualized Experiments)*. 2018;(140):e58352.

138. Franklin KBJ, Paxinos G. *The Mouse Brain in Stereotaxic Coordinates*. Vol 3. Academic press New York:; 2008.

139. Landgraf D, Long JE, Welsh DK. Depression-like behaviour in mice is associated with disrupted circadian rhythms in nucleus accumbens and periaqueductal grey. *European Journal of Neuroscience*. 2016;43(10):1309-1320. doi:10.1111/ejn.13085

140. Welsh DK, Noguchi T. Cellular bioluminescence imaging. *Cold Spring Harbor Protocols*. 2012;7(8):852-866. doi:10.1101/pdb.top070607

141. Landgraf D, Long JE, Welsh DK. Depression-like behaviour in mice is associated with disrupted circadian rhythms in nucleus accumbens and periaqueductal grey. *European Journal of Neuroscience*. 2016;43(10):1309-1320. doi:10.1111/ejn.13085

142. Jacobs DC, Veitch RE, Chappell PE. Evaluation of immortalized AVPV- And Arcuate-Specific neuronal kisspeptin cell lines to elucidate potential mechanisms of estrogen responsiveness and temporal gene expression in females. *Endocrinology*. 2016;157(9):3410-3419. doi:10.1210/en.2016-1294

143. Earnest DJ, Liang FQ, DiGiorgio S, et al. Establishment and characterization of adenoviral E1A immortalized cell lines derived from the rat suprachiasmatic nucleus. *Journal of Neurobiology*. 1999;39(1):1-13. doi:10.1002/(SICI)1097-4695(199904)39:1<1::AID-NEU1>3.0.CO;2-F

144. Hoffmann HM, Gong P, Tamrazian A, Mellon PL. Transcriptional interaction between cFOS and the homeodomain-binding transcription factor VAX1 on the GnRH promoter controls Gnrh1 expression levels in a GnRH neuron maturation specific manner. *Molecular and Cellular Endocrinology*. 2018;461:143-154. doi:10.1016/j.mce.2017.09.004

145. Hoffmann HM, Trang C, Gong P, Kimura I, Pandolfi EC, Mellon PL. Deletion of Vax1 from Gonadotropin-Releasing Hormone (GnRH) Neurons Abolishes GnRH Expression and Leads to Hypogonadism and Infertility. *Journal of Neuroscience*. 2016;36(12):3506-3518. doi:10.1523/JNEUROSCI.2723-15.2016

146. Yoo SH, Yamazaki S, Lowrey PL, et al. PERIOD2:: LUCIFERASE real-time reporting of circadian dynamics reveals persistent circadian oscillations in mouse peripheral tissues. *Proceedings of the National Academy of Sciences*. 2004;101(15):5339-5346.

147. Lee JH, Kim TH, Oh SJ, et al. Signal transducer and activator of transcription-3 (Stat3) plays a critical role in implantation via progesterone receptor in uterus. *FASEB Journal*. 2013;27(7):2553-2563. doi:10.1096/fj.12-225664

148. Faul F, Erdfelder E, Lang AG, Buchner A. G*Power 3: A flexible statistical power analysis program for the social, behavioral, and biomedical sciences. In: *Behavior Research Methods*. ; 2007. doi:10.3758/BF03193146

149. School TO, Hediger ML, Schall JI, Ances IG, Smith WK. Gestational weight gain, pregnancy outcome, and postpartum weight retention. *Obstetrics & gynecology*. 1995;86(3):423-427.

150. Abrams B, Carmichael S, Selvin S. Factors associated with the pattern of maternal weight gain during pregnancy. *Obstetrics & Gynecology*. 1995;86(2):170-176.

151. Padilla SL, Perez JG, Ben-Hamo M, et al. Kisspeptin neurons in the arcuate nucleus of the hypothalamus orchestrate circadian rhythms and metabolism. *Current Biology*. 2019;29(4):592-604.

152. Zakar T, Hertelendy F. Progesterone withdrawal: key to parturition. *American Journal of Obstetrics and Gynecology*. 2007;196(4):289-296. doi:10.1016/j.ajog.2006.09.005

153. Brown AG, Leite RS, Strauss JF. Mechanisms underlying “functional” progesterone withdrawal at parturition. *Ann N Y Acad Sci*. 2004;1034(215):36-49. doi:10.1196/annals.1335.004

154. Murphy ZC, Pezuk P, Menaker M, Sellix MT, York N. Effects of Ovarian Hormones on Internal Circadian Organization in Rats 1. 2013;89(July):1-9. doi:10.1095/biolreprod.113.109322

155. Kruijver FPM, Swaab DF. Sex hormone receptors are present in the human suprachiasmatic nucleus. *Neuroendocrinology*. Published online 2002. doi:10.1159/000057339

156. Goodman RL, Holaskova I, Nestor CC, et al. Evidence that the arcuate nucleus is an important site of progesterone negative feedback in the ewe. *Endocrinology*. 2011;152(9):3451-3460.

157. Miller BH, Takahashi JS. Central circadian control of female reproductive function. *Front Endocrinol (Lausanne)*. 2014;4:195.

158. Sen A, Hoffmann HM. Role of core circadian clock genes in hormone release and target tissue sensitivity in the reproductive axis. *Molecular and Cellular Endocrinology*. Published online February 2020. doi:10.1016/j.mce.2019.110655

159. Loh DH, Kuljis DA, Azuma L, et al. Disrupted reproduction, estrous cycle, and circadian rhythms in female mice deficient in vasoactive intestinal peptide. *Journal of Biological Rhythms*. 2014;29(5):355-369. doi:10.1177/0748730414549767

160. Mereness AL, Murphy ZC, Forrestel AC, et al. Conditional deletion of Bmal1 in ovarian theca cells disrupts ovulation in female mice. *Endocrinology*. 2016;157(2):913-927. doi:10.1210/en.2015-1645

161. Ratajczak CK, Boehle KL, Muglia LJ. Impaired steroidogenesis and implantation failure in Bmal1 -/-mice. *Endocrinology*. 2009;150(4):1879-1885. doi:10.1210/en.2008-1021

162. Sellix MT. Clocks underneath : the role of peripheral clocks in the timing of female reproductive physiology. 2013;4(July):1-6. doi:10.3389/fendo.2013.00091

163. Liu Y, Johnson BP, Shen AL, et al. Loss of BMAL1 in ovarian steroidogenic cells results in implantation failure in female mice. *Proceedings of the National Academy of Sciences*. 2014;111(39). doi:10.1073/pnas.1209249111

164. Nakamura TJ, Sellix MT, Kudo T, et al. Influence of the estrous cycle on clock gene expression in reproductive tissues : Effects of fluctuating ovarian steroid hormone levels. 2010;75:203-212. doi:10.1016/j.steroids.2010.01.007

165. Karman BN, Tischkau SA. Circadian clock gene expression in the ovary: effects of luteinizing hormone. *Biol Reprod*. 2006;75(4):624-632.

166. Murphy ZC, Pezuk P, Menaker M, Sellix MT, York N. Effects of Ovarian Hormones on Internal Circadian Organization in Rats 1. 2013;89(July):1-9. doi:10.1095/biolreprod.113.109322

167. Nadeem L, Shynlova O, Matysiak-Zablocki E, Mesiano S, Dong X, Lye S. Molecular evidence of functional progesterone withdrawal in human myometrium. *Nat Commun*. Published online 2016. doi:10.1038/ncomms11565

168. Brown AG, Leite RS, Strauss JF. Mechanisms underlying “functional” progesterone withdrawal at parturition. *Ann N Y Acad Sci*. 2004;1034(215):36-49. doi:10.1196/annals.1335.004

169. Wharfe MD, Mark PJ, Wyrwoll CS, et al. Pregnancy-induced adaptations of the central circadian clock and maternal glucocorticoids. *Journal of Endocrinology*. 2016;228(3):135-147. doi:10.1530/JOE-15-0405

170. Karman BN, Tischkau SA. Circadian clock gene expression in the ovary: effects of luteinizing hormone. *Biol Reprod*. 2006;75(4):624-632.

171. Yoshikawa T, Sellix M, Pezuk P, Menaker M. Timing of the ovarian circadian clock is regulated by gonadotropins. *Endocrinology*. Published online 2009. doi:10.1210/en.2008-1280

172. He PJ, Hirata M, Yamauchi N, Hashimoto S, Hattori MA. Gonadotropic regulation of circadian clockwork in rat granulosa cells. *Molecular and Cellular Biochemistry*. Published online 2007. doi:10.1007/s11010-007-9432-7

173. Honnebier M, Nathanielsz PW. Primate parturition and the role of the maternal circadian system. *European Journal of Obstetrics & Gynecology and Reproductive Biology*. 1994;55(3):193-203.

174. Rosenwasser AM, Hollander SJ, Adler NT. Effects of pregnancy and parturition on free-running circadian activity rhythms in the rat. *Chronobiol Int*. 1987;4(2):183-187.

175. Albers EE, Gerall AA, Axelson JF. Effect of reproductive state on circadian periodicity in the rat. *Physiol Behav*. 1981;26(1):21-25.

176. Martin-Fairey CA, McCarthy R, Ma X, England S, Herzog E. Chronotype changes during pregnancy. *Reproductive Sciences*. 2016;23(1 SUPPL. 1):291A.

177. Welschen R, Osman P, Dullaart J, De Greef WJ, Uilenbroek JTJ, De Jong FH. Levels of follicle-stimulating hormone, luteinizing hormone, oestradiol-17β and progesterone, and follicular growth in the pseudopregnant rat. *Journal of Endocrinology*. 1975;64(1):37-47.

178. Capri KM, Maroni MJ, Deane H V, et al. Male C57BL6/N and C57BL6/J mice respond differently to constant light and running-wheel access. *Frontiers in Behavioral Neuroscience*. 2019;13:268.

179. Edgar DM, Kilduff TS, Martin CE, Dement WC. Influence of running wheel activity on free-running sleep/wake and drinking circadian rhythms in mice. *Physiol Behav*. 1991;50(2):373-378.

180. LeSauter J, Silver R. Localization of a suprachiasmatic nucleus subregion regulating locomotor rhythmicity. *Journal of Neuroscience*. 1999;19(13):5574-5585.

181. Stephan FK, Zucker I. Circadian rhythms in drinking behavior and locomotor activity of rats are eliminated by hypothalamic lesions. *Proceedings of the National Academy of Sciences*. 1972;69(6):1583-1586.

182. Schwartz WJ, Zimmerman P. Lesions of the suprachiasmatic nucleus disrupt circadian locomotor rhythms in the mouse. *Physiol Behav*. 1991;49(6):1283-1287.

183. Morin L, Studholme K. Millisecond light stimuli evoke cessation of locomotion followed by sleep-like behavior that persists in the absence of light. *J Biol Rhythms*. 2009;24(6):497. doi:10.1177/0748730409349059.Millisecond

184. Lain KY, Catalano PM. Metabolic changes in pregnancy. *Clin Obstet Gynecol*. 2007;50(4):938-948.

185. Kassebaum NJ, Barber RM, Dandona L, et al. Global, regional, and national levels of maternal mortality, 1990–2015: a systematic analysis for the Global Burden of Disease Study 2015. *The Lancet*. 2016;388(10053):1775-1812. doi:10.1016/S0140-6736(16)31470-2

186. Blencowe H, Cousens S, Oestergaard MZ, et al. National, regional, and worldwide estimates of preterm birth rates in the year 2010 with time trends since 1990 for selected countries: A systematic analysis and implications. *The Lancet*. 2012;379(9832):2162-2172. doi:10.1016/S0140-6736(12)60820-4

187. Wang W, Yen H, Chen CH, et al. Prevention of inflammation-associated preterm birth by knockdown of the endothelin-1-matrix metalloproteinase-1 pathway. *Molecular Medicine*. 2010;16(11-12):505-512. doi:10.2119/molmed.2010.00030

188. Mullan C. Management of preterm labour. *Obstetrics, Gynaecology and Reproductive Medicine*. 2018;28(7):208-214. doi:10.1016/j.ogrm.2018.06.005

189. Birth P, Behrman PRE, Butler AS, et al. *Preterm Birth: Causes, Consequences and Prevention*.; 2007.

190. Dimes M of. March of Dimes 2020 Report Card. Published online 2020.

191. Goldenberg RL, Culhane JF, Iams JD, Romero R. Epidemiology and Causes of Preterm Birth. *Lancet*. 2008;371:75-84.

192. Berkowitz GS, Blackmore-Prince C, Lapinski RH, Savitz DA. Risk Factors for PTB Subtypes. Published online 1998:279-285.

193. Birth P, Behrman PRE, Butler AS, et al. *Preterm Birth: Causes, Consequences and Prevention*.; 2007.

194. Di Renzo GC, Roura LC. Guidelines for the management of spontaneous preterm labor. *Journal of Perinatal Medicine*. 2006;34(5):359-366. doi:10.1515/JPM.2006.073

195. Ko CH, Takahashi JS. Molecular components of the mammalian circadian clock. *Human Molecular Genetics*. Published online 2006. doi:10.1093/hmg/ddl207

196. Leung JM, Martinez ME. Circadian Rhythms in Environmental Health Sciences. *Current Environmental Health Reports*. 2020;7(3):272-281. doi:10.1007/s40572-020-00285-2

197. Zee PC, Attarian H, Videnovic A. Circadian rhythm abnormalities. *CONTINUUM Lifelong Learning in Neurology*. 2013;19(1):132-147. doi:10.1212/01.CON.0000427209.21177.aa

198. Partch CL, Green CB, Takahashi JS. Molecular Architecture of the Mammalian Circadian Clock. *Trends Cell Biol*. 2014;24(2):90-99. doi:10.1016/j.tcb.2013.07.002

199. Sen A, Hoffmann HM. Role of core circadian clock genes in hormone release and target tissue sensitivity in the reproductive axis. *Molecular and Cellular Endocrinology*. 2020;501. doi:10.1016/j.mce.2019.110655

200. Lowrey PL, Takahashi JS. MAMMALIAN CIRCADIAN BIOLOGY: Elucidating Genome-Wide Levels of Temporal Organization. *Annual Review of Genomics and Human Genetics*. 2004;5(1):407-441. doi:10.1146/annurev.genom.5.061903.175925

201. Lowrey PL, Takahashi JS. *Genetics of Circadian Rhythms in Mammalian Model Organisms*. Vol 74. 1st ed. Elsevier Inc.; 2011. doi:10.1016/B978-0-12-387690-4.00006-4

202. Partch CL, Green CB, Takahashi JS. Molecular Architecture of the Mammalian Circadian Clock. *Trends Cell Biol*. 2014;24(2):90-99. doi:10.1016/j.tcb.2013.07.002

203. Leung JM, Martinez ME. Circadian Rhythms in Environmental Health Sciences. *Current Environmental Health Reports*. 2020;7(3):272-281. doi:10.1007/s40572-020-00285-2

204. Reiter RJ, Tan DX, Korkmaz A, Rosales-Corral SA. Melatonin and stable circadian rhythms optimize maternal, placental and fetal physiology. *Human Reproduction Update*. 2014;20(2):293-307. doi:10.1093/humupd/dmt054

205. Miller BH, Takahashi JS. Central circadian control of female reproductive function. *Frontiers in Endocrinology*. 2014;5(January):195. doi:10.3389/fendo.2013.00195

206. Sen A, Hoffmann HM. Role of core circadian clock genes in hormone release and target tissue sensitivity in the reproductive axis. *Molecular and Cellular Endocrinology*. Published online February 2020. doi:10.1016/j.mce.2019.110655

207. McCarthy RT, Jungheim ES, Fay JC, Bates K, Herzog ED, England SK. Riding the rhythm of melatonin through pregnancy to deliver on time. *Front Endocrinol (Lausanne)*. 2019;10:616.

208. Yaw A, McLane-Svoboda A, Hoffmann H. Shiftwork and Light at Night Negatively Impact Molecular and Endocrine Timekeeping in the Female Reproductive Axis in Humans and Rodents. *International Journal of Molecular Sciences*. Published online 2020. doi:10.3390/ijms22010324

209. Valenzuela FJ, Vera J, Venegas C, Pino F, Lagunas C. Circadian System and Melatonin Hormone: Risk Factors for Complications during Pregnancy. *Obstetrics and Gynecology International*. Published online 2015. doi:10.1155/2015/825802

210. Martin-fairey CA, Zhao P, Wan L, et al. Pregnancy Induces an Earlier Chronotype in Both Mice and Women. *Journal of Biological Rhythms*. Published online 2019:1-9. doi:10.1177/0748730419844650

211. Zhu JL, Hjollund NH, Andersen AMN, Olsen J. Shift work, job stress, and late fetal loss: The National Birth Cohort in Denmark. *J Occup Environ Med*. 2004;46(11):1144-1149.

212. Whelan EA, Lawson CC, Grajewski B, Hibert EN, Spiegelman D, Rich-Edwards JW. Work schedule during pregnancy and spontaneous abortion. *Epidemiology*. Published online 2007:350-355.

213. Lawson CC, Rocheleau CM, Whelan EA, et al. Occupational exposures among nurses and risk of spontaneous abortion. *Am J Obstet Gynecol*. 2012;206(4):327-e1.

214. Grajewski B, Whelan EA, Lawson CC, et al. Miscarriage among flight attendants. *Epidemiology*. 2015;26(2):192.

215. Begtrup LM, Specht IO, Hammer PEC, et al. Night work and miscarriage: a Danish nationwide register-based cohort study. *Occup Environ Med*. 2019;76(5):302-308.

216. Suzumori N, Ebara T, Matsuki T, et al. Effects of long working hours and shift work during pregnancy on obstetric and perinatal outcomes: A large prospective cohort study—Japan Environment and Children's Study. *Birth*. 2020;47(1):67-79. doi:10.1111/birt.12463

217. Albrecht U. Timing to Perfection: The Biology of Central and Peripheral Circadian Clocks. *Neuron*. 2012;74(2):246-260. doi:10.1016/j.neuron.2012.04.006

218. Hänzelmann S, Castelo R, Guinney J. GSVA: Gene set variation analysis for microarray and RNA-Seq data. *BMC Bioinformatics*. 2013;14. doi:10.1186/1471-2105-14-7

219. Heng YJ, Pennell CE, McDonald SW, et al. Maternal whole blood gene expression at 18 and 28 weeks of gestation associated with spontaneous preterm birth in asymptomatic women. *PLoS ONE*. 2016;11(6):1-17. doi:10.1371/journal.pone.0155191

220. Feng Y, Wang Y, Liu H, et al. Novel Genetic Variants in the P38MAPK Pathway Gene ZAK and Susceptibility to Lung Cancer. *Mol Carcinog*. 2018;57(2):216-224. doi:10.1002/mc.22748.Novel

221. Zhou G, Holzman C, Heng YJ, Kibschull M, Lye SJ. Maternal blood EBF1-based microRNA transcripts as biomarkers for detecting risk of spontaneous preterm birth: a nested case-control study. *Journal of Maternal-Fetal and Neonatal Medicine*. 2020;0(0):1-9. doi:10.1080/14767058.2020.1745178

222. Zhou G, Holzman C, Heng YJ, Kibschull M, Lye SJ. Maternal blood EBF1-based microRNA transcripts as biomarkers for detecting risk of spontaneous preterm birth: a nested case-control study. *Journal of Maternal-Fetal and Neonatal Medicine*. 2020;0(0):1-9. doi:10.1080/14767058.2020.1745178

223. Hänzelmann S, Castelo R, Guinney J. GSVA: Gene set variation analysis for microarray and RNA-Seq data. *BMC Bioinformatics*. 2013;14. doi:10.1186/1471-2105-14-7

224. Subramanian A, Tamayo P, Mootha VK, et al. Gene Set Enrichment Analysis: A Knowledge-Based Approach for Interpreting Genome-Wide Expression Profiles. *Proceedings of the National Academy of Sciences*. 2005;102(43):15545-15550. doi:/10.1073/pnas.0506580102

225. Ritchie ME, Phipson B, Wu D, et al. Limma powers differential expression analyses for RNA-sequencing and microarray studies. *Nucleic Acids Research*. 2015;43(7):e47. doi:10.1093/nar/gkv007

226. Zhou G, Holzman C, Chen B, et al. EBF1-Correlated Long Non-coding RNA Transcript Levels in 3rd Trimester Maternal Blood and Risk of Spontaneous Preterm Birth. *Reproductive Sciences*. 2021;28(2):541-549. doi:10.1007/s43032-020-00320-5

227. Zhou G, Holzman C, Heng YJ, Kibschull M, Lye SJ, Vazquez A. EBF1 Gene mRNA Levels in Maternal Blood and Spontaneous Preterm Birth. *Reproductive Sciences*. 2020;27(1):316-324. doi:10.1007/s43032-019-00027-2

228. Miller BH, Olson SL, Turek FW, Levine JE, Horton TH, Takahashi JS. Circadian Clock mutation disrupts estrous cyclicity and maintenance of pregnancy. *Current Biology*. Published online 2004. doi:10.1016/j.cub.2004.07.055

229. Chappell PE, White RS, Mellon PL. Circadian gene expression regulates pulsatile gonadotropin-releasing hormone (GnRH) secretory patterns in the hypothalamic GnRH-secreting GT1-7 cell line. *The Journal of neuroscience*. 2003;23(35):11202-11213. doi:10.1111/j.1600-6143.2008.02497.x.Plasma

230. Kennaway DJ, Boden MJ, Voultsios A. Reproductive performance in female ClockΔ19 mutant mice. *Reproduction, Fertility and Development*. Published online 2004. doi:10.1071/RD04023

231. Dolatshad H, Campbell EA, O'hara L, Maywood ES, Hastings MH, Johnson MH. Developmental and reproductive performance in circadian mutant mice. *Human reproduction*. 2005;21(1):68-79.

232. Pilorz V, Steinlechner S. Low reproductive success in Per1 and Per2 mutant mouse females due to accelerated ageing? *Reproduction*. Published online 2008. doi:10.1530/REP-07-0434

233. Boden MJ, Varcoe TJ, Voultsios A, Kennaway DJ. Reproductive biology of female Bmal1 null mice. *Reproduction*. Published online 2010. doi:10.1530/REP-09-0523

234. Germain AM, Valenzuela GJ, Ivankovic M, Ducsay CA, Gabella C, Serón-Ferré M. Relationship of circadian rhythms of uterine activity with term and preterm delivery. *American Journal of Obstetrics and Gynecology*. 1993;168(4):1271-1277. doi:10.1016/0002-9378(93)90379-W

235. Suzumori N, Ebara T, Matsuki T, et al. Effects of long working hours and shift work during pregnancy on obstetric and perinatal outcomes: A large prospective cohort study—Japan Environment and Children's Study. *Birth*. 2020;47(1):67-79. doi:10.1111/birt.12463

236. Hodžic A, Lavtar P, Ristanovic M, Novakovic I, Dotlic J, Peterlin B. Genetic variation in the clock gene is associated with idiopathic recurrent spontaneous abortion. *PLoS ONE*. 2018;13(5):8-13. doi:10.1371/journal.pone.0196345

237. Kovac U, Jasper EA, Smith CJ, et al. The association of polymorphisms in circadian clock and lipid metabolism genes with 2nd trimester lipid levels and preterm birth. *Frontiers in Genetics*. 2019;10(JUN):1-10. doi:10.3389/fgene.2019.00540

238. Hammoud E, Bujold E, Krapp M, Diamond M, Baumann P. Recurrent Miscarriages and Risks of PTB. *Fertility and Sterility*. 2004;82:S18.

239. Oliver-Williams C, Fleming M, Wood AM, Smith GCS. Previous miscarriage and the subsequent risk of preterm birth in Scotland, 1980-2008: A historical cohort study. *BJOG: An International Journal of Obstetrics and Gynaecology*. 2015;122(11):1525-1534. doi:10.1111/1471-0528.13276

240. Fukuta K, Yoneda S, Yoneda N, et al. Risk factors for spontaneous miscarriage above 12 weeks or premature delivery in patients undergoing cervical polypectomy during pregnancy. *BMC Pregnancy and Childbirth*. 2020;20(1):1-9. doi:10.1186/s12884-019-2710-z

241. Li R, Cheng S, Wang Z. Circadian clock gene plays a key role on ovarian cycle and spontaneous abortion. *Cellular Physiology and Biochemistry*. 2015;37(3):911-920. doi:10.1159/000430218

242. Iams JD. What have we learned about uterine contractions and preterm birth? The HUAM Prediction Study. *Seminars in Perinatology*. 2003;27(3):204-211. doi:10.1016/S0146-0005(03)00018-1

243. Wang X, Mozhui K, Li Z, et al. A promoter polymorphism in the Per3 gene is associated with alcohol and stress response. *Translational Psychiatry*. 2012;2(December 2011). doi:10.1038/tp.2011.71

244. Lilliecreutz C, Larén J, Sydsjö G, Josefsson A. Effect of maternal stress during pregnancy on the risk for preterm birth. *BMC Pregnancy and Childbirth*. 2016;16(1):1-8. doi:10.1186/s12884-015-0775-x

245. Nagel C, Aurich C, Aurich J. Stress effects on the regulation of parturition in different domestic animal species. *Animal Reproduction Science*. 2019;207(April):153-161. doi:10.1016/j.anireprosci.2019.04.011

246. Kanehisa M, Goto S. KEGG: Kyoto Encyclopedia or Genes and Genomes. *Nucleic Acids Research*. 2000;28(1):27-30.

247. Vallée A, Lecarpentier Y, Guillevin R, Vallée JN. Circadian rhythms, Neuroinflammation and Oxidative Stress in the Story of Parkinson's Disease. *Cells*. 2020;9(2):314. doi:10.3390/cells9020314

248. Mowa CN, Papka RE. The role of sensory neurons in cervical ripening: Effects of estogen and neuropeptides. *Journal of Histochemistry and Cytochemistry*. 2004;52(10):1249-1258. doi:10.1369/jhc.4R6383.2004

249. Lu P, Takai K, Weaver VM, Werb Z. Extracellular Matrix degradation and remodeling in development and disease. *Cold Spring Harbor Perspectives in Biology*. 2011;3(12):1-24. doi:10.1101/cshperspect.a005058

250. Frantz C, Stewart KM, Weaver VM. The extracellular matrix at a glance. *Journal of Cell Science*. 2010;123(24):4195-4200. doi:10.1242/jcs.023820

251. Lu P, Takai K, Weaver VM, Werb Z. Extracellular Matrix degradation and remodeling in development and disease. *Cold Spring Harbor Perspectives in Biology*. 2011;3(12):1-24. doi:10.1101/cshperspect.a005058

252. Visse R, Nagase H. Matrix metalloproteinases and tissue inhibitors of metalloproteinases: Structure, function, and biochemistry. *Circulation Research*. 2003;92(8):827-839. doi:10.1161/01.RES.0000070112.80711.3D

253. Athayde N, Edwin SS, Romero R, et al. A role for matrix metalloproteinase-9 in spontaneous rupture of the fetal membranes. *American Journal of Obstetrics and Gynecology*. 1998;179(5):1248-1253. doi:10.1016/S0002-9378(98)70141-3

254. Fortunato SJ, Menon R, Lombardi SJ. MMP/TIMP imbalance in amniotic fluid during PROM: An indirect support for endogenous pathway to membrane rupture. *Journal of Perinatal Medicine*. 1999;27(5):362-368. doi:10.1515/JPM.1999.049

255. Geng J, Huang C, Jiang S. Roles and regulation of the matrix metalloproteinase system in parturition. *Molecular Reproduction and Development*. 2016;83(4):276-286. doi:10.1002/mrd.22626

256. Minor DL, Masseling SJ, Yuh NJ, Lily YJ. Transmembrane structure of an inwardly rectifying potassium channel. *Cell*. 1999;96(6):879-891. doi:10.1016/S0092-8674(00)80597-8

257. Hibino H, Inanobe A, Furutani K, Murakami S, Findlay I, Kurachi Y. Inwardly rectifying potassium channels: Their structure, function, and physiological roles. *Physiological Reviews*. 2010;90(1):291-366. doi:10.1152/physrev.00021.2009

258. Fabregat A, Jupe S, Matthews L, et al. The Reactome Pathway Knowledgebase. *Nucleic Acids Research*. 2018;46(D1):D649-D655. doi:10.1093/nar/gkx1132

259. MacFarlane SN, Sontheimer H. Changes in ion channel expression accompany cell cycle progression of spinal cord astrocytes. *Glia*. 2000;30(1):39-48. doi:10.1002/(SICI)1098-1136(200003)30:1<39::AID-GLIA5>3.0.CO;2-S

260. Olsen ML, Sontheimer H. Functional implications for Kir4.1 channels in glial biology: From K + buffering to cell differentiation. *Journal of Neurochemistry*. 2008;107(3):589-601. doi:10.1111/j.1471-4159.2008.05615.x

261. McCloskey C, Rada C, Bailey E, et al. The inwardly rectifying K + channel KIR 7.1 controls uterine excitability throughout pregnancy . *EMBO Molecular Medicine*. 2014;6(9):1161-1174. doi:10.15252/emmm.201403944

262. Zhou G, Holzman C, Heng YJ, Kibschull M, Lye SJ, Vazquez A. EBF1 Gene mRNA Levels in Maternal Blood and Spontaneous Preterm Birth. *Reproductive Sciences*. 2020;27(1):316-324. doi:10.1007/s43032-019-00027-2

263. Zhang G, Feenstra B, Bacelis J, et al. Genetic Associations with Gestational Duration and Spontaneous Preterm Birth. *New England Journal of Medicine*. 2017;377(12):1156-1167. doi:10.1056/nejmoa1612665

264. Osterman MJK, Martin JA. Trends in low-risk cesarean delivery in the United States, 1990-2013. *Natl Vital Stat Rep*. 2014;63(6):1-16.

265. Martin JA, Hamilton BE, Osterman MJK, Driscoll AK. Births: Final Data for 2019. *National Vital Statistics Reports*. 2021;70(2).

266. Giugliano E, Cagnazzo E, Milillo V, et al. The risk factors for failure of labor induction: A cohort study. *Journal of Obstetrics and Gynecology of India*. 2014;64(2):111-115. doi:10.1007/s13224-013-0486-z

267. Giugliano E, Cagnazzo E, Milillo V, et al. The risk factors for failure of labor induction: A cohort study. *Journal of Obstetrics and Gynecology of India*. 2014;64(2):111-115. doi:10.1007/s13224-013-0486-z

268. Marconi AM. Recent advances in the induction of labor. *F1000Res*. 2019;8:1829. doi:10.12688/f1000research.17587.1

269. Bulletins AC on P. Induction of Labor. *Obstetrics & Gynecology*. 2009;114(2):386-397. doi:10.1097/AOG.0b013e3181b48ef5

270. Satin AJ, Leveno KJ, Sherman ML, McIntire DD. Factors Affecting the Dose Response to Oxytocin for Labor Stimulation. *Am J Obstet Gynecol*. 1992;166:1260-1261. doi:10.1016/s0002-9378(11)90619-x

271. Vrachnis N, Malamas FM, Sifakis S, Deligeoroglou E, Iliodromiti Z. The oxytocin-oxytocin receptor system and its antagonists as tocolytic agents. *International Journal of Endocrinology*. 2011;2011(May). doi:10.1155/2011/350546

272. Nunes AR, Gliksberg M, Varela SAM, et al. Developmental Effects of Oxytocin Neurons on Social Affiliation and Processing of Social Information. *J Neurosci*. 2021;41(42):8742-8760. doi:10.1523/JNEUROSCI.2939-20.2021

273. Blanks AM, Thornton S. The role of oxytocin in parturition. *BJOG: An International Journal of Obstetrics and Gynaecology*. 2003;110(SUPPL. 20):46-51. doi:10.1016/S1470-0328(03)00024-7

274. Roizen J, Luedke CE, Herzog ED, Muglia LJ. Oxytocin in the circadian timing of birth. *PLoS ONE*. 2007;2(9):10-13. doi:10.1371/journal.pone.0000922

275. Honnebier M, Nathanielsz PW. Primate parturition and the role of the maternal circadian system. *European Journal of Obstetrics & Gynecology and Reproductive Biology*. 1994;55(3):193-203.

276. Pilorz V, Steinlechner S. Low reproductive success in Per1 and Per2 mutant mouse females due to accelerated ageing? *Reproduction*. 2008;135(4):559-568. doi:10.1530/REP-07-0434

277. Rugh R. *The Mouse: Its Reproduction and Development*. Oxford University Press; 1968.

278. EMAP. Theiler Stage Definition. Published 2020. Accessed January 20, 2021. https://www.emouseatlas.org/emap/ema/theiler_stages/StageDefinition/stagedefinition.html

279. Landgraf D, Long JE, Welsh DK. Depression-like behaviour in mice is associated with disrupted circadian rhythms in nucleus accumbens and periaqueductal grey. *European Journal of Neuroscience*. 2016;43(10):1309-1320. doi:10.1111/ejn.13085

280. Ray S, Valekunja UK, Stangherlin A, et al. Circadian rhythms in the absence of the clock gene Bmal1. *Science (1979)*. 2020;367(6479):800-806. doi:10.1126/science.aaw7365

281. McKay EC, Beck JS, Khoo SK, et al. Peri-infarct upregulation of the oxytocin receptor in vascular dementia. *Journal of Neuropathology and Experimental Neurology*. 2019;78(5):436-452. doi:10.1093/jnen/nlz023

282. Denoix N, Merz T, Unmuth S, et al. Cerebral Immunohistochemical Characterization of the H2S and the Oxytocin Systems in a Porcine Model of Acute Subdural Hematoma. *Frontiers in Neurology*. 2020;11(July):1-12. doi:10.3389/fneur.2020.00649

283. Liu Y, Conboy I. Unexpected evolutionarily conserved rapid effects of viral infection on oxytocin receptor and TGF-β/pSmad3. *Skeletal Muscle*. 2017;7(1):1-10. doi:10.1186/s13395-017-0125-y

284. Czarnecka AM, Milewski K, Albrecht J, Zielińska M. The status of bile acids and farnesoid x receptor in brain and liver of rats with thioacetamide-induced acute liver failure. *International Journal of Molecular Sciences*. 2020;21(20):1-12. doi:10.3390/ijms21207750

285. Huang JW, Acharya A, Taglialatela A, et al. MCM8IP activates the MCM8-9 helicase to promote DNA synthesis and homologous recombination upon DNA damage. *Nature Communications*. 2020;11(1). doi:10.1038/s41467-020-16718-3

286. Bendiks L, Geiger F, Gudermann T, Feske S, Dietrich A. Store-operated Ca2+ entry in primary murine lung fibroblasts is independent of classical transient receptor potential

(TRPC) channels and contributes to cell migration. *Scientific Reports*. 2020;10(1):1-11. doi:10.1038/s41598-020-63677-2

287. Madeira F, Park YM, Lee J, et al. The EMBL-EBI search and sequence analysis tools APIs in 2019. *Nucleic Acids Research*. 2019;47(W1):W636-W641. doi:10.1093/nar/gkz268

288. Kent WJ, Sugnet CW, Furey TS, et al. The Human Genome Browser at UCSC. *Genome Research*. 2002;12(6):996-1006. doi:10.1101/gr.229102

289. Hoffmann HM, Gong P, Tamrazian A, Mellon PL. Transcriptional interaction between cFOS and the homeodomain-binding transcription factor VAX1 on the GnRH promoter controls Gnrh1 expression levels in a GnRH neuron maturation specific manner. *Molecular and Cellular Endocrinology*. 2018;461:143-154. doi:10.1016/j.mce.2017.09.004

290. NEBase Changer. https://nebasechanger.neb.com/

291. Chen J, Zhou G, Fu X, et al. The apheresis platelet donation was increased after a nationwide ban on family/replacement donation in China. *BMC Public Health*. 2021;21(1):1-11. doi:10.1186/s12889-021-10819-4

292. Tasaki H, Zhao L, Isayama K, et al. Profiling of circadian genes expressed in the uterus endometrial stromal cells of pregnant rats as revealed by DNA microarray coupled with RNA interference. *Frontiers in Endocrinology*. 2013;4(JUL):1-11. doi:10.3389/fendo.2013.00082

293. Lv S, Wang N, Ma J, Li WP, Chen ZJ, Zhang C. Impaired decidualization caused by downregulation of circadian clock gene BMAL1 contributes to human recurrent miscarriage†. *Biology of Reproduction*. 2019;101(1):138-147. doi:10.1093/biolre/ioz063

294. Sharkey JT, Puttaramu R, Word RA, Olcese J. Melatonin synergizes with oxytocin to enhance contractility of human myometrial smooth muscle cells. *Journal of Clinical Endocrinology and Metabolism*. 2009;94(2):421-427. doi:10.1210/jc.2008-1723

295. Olcese J, Beesley S. Clinical significance of melatonin receptors in the human myometrium. *Fertility and Sterility*. 2014;102(2):329-335. doi:10.1016/j.fertnstert.2014.06.020

296. Beesley S, Lee J, Olcese J. Circadian clock regulation of melatonin MTNR1B receptor expression in human myometrial smooth muscle cells. *Molecular Human Reproduction*. 2015;21(8):662-671. doi:10.1093/molehr/gav023

297. Schlabritz-Loutsevitch N, Hellner N, Middendorf R, Müller D, Olcese J. The human myometrium as a target for melatonin. *Journal of Clinical Endocrinology and Metabolism*. 2003;88(2):908-913. doi:10.1210/jc.2002-020449

298. Arrowsmith S, Wray S. Oxytocin : Its Mechanism of Action and Receptor Signalling in the Myometrium Neuroendocrinology. 2014;(8):356-369. doi:10.1111/jne.12154

299. Zatkova M, Reichova A, Bacova Z, Strbak V, Kiss A, Bakos J. Neurite Outgrowth Stimulated by Oxytocin Is Modulated by Inhibition of the Calcium Voltage-Gated

Channels. *Cellular and Molecular Neurobiology*. 2018;38(1):371-378. doi:10.1007/s10571-017-0503-3

300. Bakos J, Srancikova A, Havranek T, Bacova Z. Molecular Mechanisms of Oxytocin Signaling at the Synaptic Connection. *Neural Plasticity*. 2018;2018. doi:10.1155/2018/4864107

301. Kuo TT, Ladurner AG. Exploiting the Circadian Clock for Improved Cancer Therapy: Perspective From a Cell Biologist. *Frontiers in Genetics*. 2019;10(December):1-7. doi:10.3389/fgene.2019.01210

302. Iams JD, Newman RB, Thom EA, et al. Frequency of uterine contractions and the risk of spontaneous preterm delivery. *N Engl J Med*. 2002;346(4):250-255. doi:10.1056/NEJMoa002868

303. Zhou G, Duong T V, Kasten EP, Hoffmann HM. Low CLOCK and CRY2 in 2nd trimester human maternal blood and risk of preterm birth: a nested case-control study† . *Biology of Reproduction*. Published online 2021:1-10. doi:10.1093/biolre/ioab119

304. Ko GYP, Shi L, Ko ML. Circadian regulation of ion channels and their functions. *Journal of Neurochemistry*. 2009;110(4):1150-1169. doi:10.1111/j.1471-4159.2009.06223.x

305. Meredith AL, Wiler SW, Miller BH, et al. BK calcium-activated potassium channels regulate circadian behavioral rhythms and pacemaker output. *Nat Neurosci*. 2006;9(8):1041-1049. doi:10.1038/nn1740

306. Aaronson PI, Sarwar U, Gin S, et al. A role for voltage-gated, but not Ca 2+-activated, K + channels in regulating spontaneous contractile activity in myometrium from virgin and pregnant rats. *British Journal of Pharmacology*. 2006;147(7):815-824. doi:10.1038/sj.bjp.0706644

307. Berkefeld H, Fakler B, Schulte U. Ca2+-activated K+ channels: From protein complexes to function. *Physiological Reviews*. 2010;90(4):1437-1459. doi:10.1152/physrev.00049.2009

308. Noble K, Floyd R, Shmygol A, Shmygol A, Mobasheri A, Wray S. Distribution, expression and functional effects of small conductance Ca-activated potassium (SK) channels in rat myometrium. *Cell Calcium*. 2010;47(1):47-54. doi:10.1016/j.ceca.2009.11.004

309. Wray S, Prendergast C. *The Myometrium_ From Excitation to Contractions and Labour*. Vol 1124. (Hashitani H, Lang R, eds.). Springer Nature Singapore; 2019.

310. Malik M, Roh M, England SK. Uterine contractions in rodent models and humans. *Acta Physiologica*. 2021;231(4):1-17. doi:10.1111/apha.13607

311. Lorca RA, Prabagaran M, England SK. Functional insights into modulation of BKCa channel activity to alter myometrial contractility. *Frontiers in Physiology*. 2014;5 JUL(July):1-12. doi:10.3389/fphys.2014.00289

312. Chehade H, Simeoni U, Guignard JP, Boubred F. Preterm Birth: Long Term Cardiovascular and Renal Consequences. *Current Pediatric Reviews*. 2018;14(4):219-226. doi:10.2174/1573396314666180813121652

313. Platt MJ. Outcomes in preterm infants. *Public Health*. 2014;128(5):399-403. doi:10.1016/j.puhe.2014.03.010

314. Ream MA, Lehwald L. Neurologic Consequences of Preterm Birth. *Current Neurology and Neuroscience Reports*. 2017;18(8). doi:10.1007/s11910-018-0862-2

315. el marroun H, Zeegers M, Steegers EA, et al. Post-term birth and the risk of behavioural and emotional problems in early childhood. *International Journal of Epidemiology*. 2012;41(3):773-781. doi:10.1093/ije/dys043

316. Miller BH, Takahashi JS. Central circadian control of female reproductive function. *Frontiers in Endocrinology*. 2014;5(JAN):1-8. doi:10.3389/fendo.2013.00195

317. Yaw AM, McLane-Svoboda AK, Hoffmann HM. Shiftwork and light at night negatively impact molecular and endocrine timekeeping in the female reproductive axis in humans and rodents. *International Journal of Molecular Sciences*. 2021;22(1):1-28. doi:10.3390/ijms22010324

318. Sen A, Hoffmann HM. Role of core circadian clock genes in hormone release and target tissue sensitivity in the reproductive axis. *Mol Cell Endo*. 2020;501:1-27. doi:10.1016/j.mce.2019.110655

319. Kovac U, Jasper EA, Smith CJ, et al. The association of polymorphisms in circadian clock and lipid metabolism genes with 2nd trimester lipid levels and preterm birth. *Frontiers in Genetics*. 2019;10(JUN):1-10. doi:10.3389/fgene.2019.00540

320. Murr SM, Stabenfaldt GH, Bradford GE, Geschwind II. *Plasma Progesterone During Pregnancy in the Mouse*. Vol 246.; 1973. https://academic.oup.com/endo/article-abstract/94/4/1209/2622019

321. Barkley,' MS, Geschwind2 II, Bradford GE. *The Gestational Pattern of Estradiol, Testosterone and Progesterone Secretion in Selected Strains of Mice*. https://academic.oup.com/biolreprod/article-abstract/20/4/733/2767788

322. Omotola O, Legan S, Slade E, Adekunle A, Julie X, Pendergast S. Estradiol regulates daily rhythms underlying diet-induced obesity in female mice. *Am J Physiol Endocrinol Metab*. 2019;317:1172-1181. doi:10.1152/ajpendo.00365

323. Takahashi JS, Menaker M. Interaction of estradiol and progesterone: effects on circadian locomotor rhythm of female golden hamsters. *Am J Physiol*. 1980;239(5):R497-504. doi:10.1152/ajpregu.1980.239.5.R497

324. Leibenluft E. Do gonadal steroids regulate circadian rhythms in humans? *J Affect Disord*. 1993;29(2-3):175-181. doi:10.1016/0165-0327(93)90031-e

325. Blattner MS, Mahoney MM. Circadian parameters are altered in two strains of mice with transgenic modifications of estrogen receptor subtype 1. *Genes, Brain and Behavior*. 2012;11(7):828-836. doi:10.1111/j.1601-183X.2012.00831.x

326. Stephan FK, Zucker I. Circadian rhythms in drinking behavior and locomotor activity of rats are eliminated by hypothalamic lesions. *Proc Natl Acad Sci U S A*. 1972;69(6):1583-1586. doi:10.1073/pnas.69.6.1583

327. Schwartz WJ, Zimmerman P. Lesions of the suprachiasmatic nucleus disrupt circadian locomotor rhythms in the mouse. *Physiology & Behavior*. 1991;49(6):1283-1287. doi:10.1016/0031-9384(91)90364-T

328. LeSauter J, Silver R. Localization of a Suprachiasmatic Nucleus Subregion Regulating Locomotor Rhythmicity. *The Journal of Neuroscience*. 1999;19(13):5574-5585. doi:10.1523/JNEUROSCI.19-13-05574.1999

329. Martin-Fairey CA, Zhao P, Wan L, et al. Pregnancy Induces an Earlier Chronotype in Both Mice and Women. *J Biol Rhythms*. 2019;34(3):323-331.

330. Baroutis G, Mousiolis A, Hoffman D, Antsaklis A. Preterm birth seasonality in Greece: An epidemiological study. *Journal of Maternal-Fetal and Neonatal Medicine*. 2012;25(8):1406-1412. doi:10.3109/14767058.2011.636103

331. House M, Kaplan DL, Socrate S. Relationships Between Mechanical Properties and Extracellular Matrix Constituents of the Cervical Stroma During Pregnancy. *Seminars in Perinatology*. 2009;33(5):300-307. doi:10.1053/j.semperi.2009.06.002